A NOVEL APPROACH TO FORMULATION OF ANTICANCER DRUGS IN NANOPARTICLES

by

Xinyi Gu

A dissertation submitted in partial fulfillment
of the requirements for the degree of
Doctor of Philosophy
(Pharmaceutical Sciences)
in The University of Michigan
2008

Doctoral Committee:

Professor Steven P. Schwendeman, Chair
Professor Mark M. Meyerhoff
Professor Victor Yang
Associate Professor Gustavo Rosania

2008

Dedication

To my parents, Maojian Gu and Haijie Yan,
who have sacrificed so much for me and guided me in the right direction in life

And

To my fiancée, Tina, who I love dearly

Acknowledgements

I would like to express my sincerest gratitude to my advisor, Dr. Steven Schwendeman, for all of his help and support as well as challenging me to be more than I can be. I have learned a tremendous amount from him about how to be a better researcher as well as a better person and all these things will serve me well in my future endeavors.

I would also like to sincerely thank my committee members, Dr. Mark Meyerhoff, Dr. Victor Yang, and Dr. Gustavo (Gus) Rosania for their help and input in my research and giving me guidance and direction when I most needed it. They have helped me to expand my understanding of science and become not just a better scientist, but a better thinker. I would also like to recognize the late Dr. David Fleisher, who has been an inspiration to me not only in science, but in everyday life, where he courageously faced and conquered numerous adversities.

I am also thankful for my colleagues in the Department of Pharmaceutical Sciences and College of Pharmacy as well as the wonderful friends I have met here at the University of Michigan. Without their constantly encouragement, advice, and support, life during these six years would not have been so pleasant and enjoyable. I would like to especially thank the late Lynn Alexander, who has been a model and inspiration for all of us at the College of Pharmacy and the now-retired Terri Azar, who has kept me up to date on everything I've needed to accomplish to obtain this Ph.D.

I would like to recognize and thank my labmates over these six years, including Dr. Anna Schwendeman, Dr. Jichao Kang, Dr. Lei Li, Dr. Yanqiang Zhong, Dr. Mangesh

Despande, Dr. Kashappa-Goud Desai, Dr. Ying Zhang, Dr. Christian Wischke, Dr. Chengji Cui, Dr. Amy Ding, Andreas Sophocleous, Kiarri Kershaw, Sam Reinhold, and Li Zhang. Not only have they helped me to overcome many obstacles during this scientific journey, but they have provided understanding and companionship which has made this enjoyable. I would also like to thank Gavin Sy from Cerenis Corporation for his help with the Malvern Nanosizer for particle sizing and zeta potential analysis. I would like to recognize Dr. Zhengrong Zhou for helping me formulate PEG-PLA copolymers. I would also like to recognize Dr. Scott Woehler for his help with NMR training and analysis and Dr. Kai Sun and Dr. Haiping Sun for their help with scanning electron microscopy (SEM) and X-ray photoelectron spectroscopy (XPS).

Most of all, I would like to thank my parents and my fiancée for their unconditional love, support, and patience.

Finally, I am grateful for the financial support from College of Pharmacy, Fred Lyons Fellowship, grant number GM007767 from NIGMS, and American Foundation for Pharmaceutical Research (AFPE).

Table of Contents

List of Figures

Figures

List of Tables

Tables

ABSTRACT

A NOVEL APPROACH TO FORMULATION OF ANTICANCER DRUGS IN NANOPARTICLES

by

Xinyi Gu

Chair: Steven P. Schwendeman

Many anticancer drugs, due to their hydrophilicity, have poor drug loading in nanoparticles, which has limited efficient drug delivery. Charge-charge interactions may be effective for improving loading where charges in nanoparticles attract oppositely charged drug molecules. A new strategy, incorporation of charged hydrophobic excipients into nanoparticles followed by drug loading via incubation of nanoparticles in the presence of drug solution, may effectively increase drug loading.

First, hydrophobic alkyl sulfates were tested for improved loading of a model hydrophilic drug, doxorubicin hydrochloride (doxHCl). Ion pairing between alkyl sulfates and doxHCl yielded hydrophobic complexes based on solubility and partition coefficient determinations and indicated favorable incorporation into hydrophobic nanoparticle cores. However, encapsulation into nanoparticles failed due to poor complex solubility in organic solvents and no significant improvement in drug loading after incorporation.

A more hydrophobic series of borate-based anionic excipients was then studied. Solubility studies found ethyl acetate to be a suitable organic solvent for dissolving borate-based excipients at high concentrations. One of the excipients, potassium tetrakis(4-chlorophenyl) borate (KTpClPB), was the best candidate as it had characteristics suitable for nanoparticle incorporation and extraction of doxHCl into a hydrophobic phase. A new incubation loading strategy was utilized for drug uptake into nanoparticles. Optimization of this process found maximizing free acid number of polymers, amount of KTpClPB used, and drug:nanoparticle ratio increased drug loading. Increasing incubation temperature both increased polymer strand rearrangements and promoted drug uptake. PEGylation of nanoparticles, or adding PEG-PLA polymers into the formulation, reduced nanoparticle aggregation to promote drug uptake.

Using the optimized incubation loading procedure, a second model drug, vinblastine sulfate, also achieved high drug loading, demonstrating that this procedure may be more broadly applicable. Plasma drug uptake using optimized nanoparticles and incubation loading led to successful extraction of doxHCl at high plasma drug concentrations, suggesting potential application of these nanoparticles as drug detoxifiers.

Comparison of incubation loading with traditional drug loading procedures (O/W or W/O/W emulsions), found traditional drug loading produced half the loading relative to incubation loading due to limited drug extraction into organic phase of O/W emulsions and limited inner aqueous phase volume of W/O/W emulsions. *In vitro* drug release profiles were similar for all nanoparticles, and the presence of KTpClPB, despite charge attractions, failed to slow drug release. Further drug loading optimization found that changing incubation times did not change drug loading, while reducing polymer

concentration of nanoparticles improved drug loading due to smaller size and increased surface area-to-volume ratio.

Hence, the novel nanoparticles and encapsulation approach developed here may find broad application in drug delivery and drug detoxification.

Chapter 1

Introduction

1.1 Drug delivery overview

1.1.1 Introduction

Drug delivery has evolved over the last several decades to become more sophisticated and efficacious for treating diseases of interest. Since the early days, when simple dosage forms such as pills and topical creams were the norm, more sophisticated systems, such as injections, infusions, and implants, have been developed for treating the multitude of diseases with different sites and mechanisms of action.

A few notable achievements in drug delivery include 1) special coatings for drug tablets or pills, which have resulted in extended-release formulations where the active ingredient is slowly release (Cialis® and Ambien®) and site-specific coating that protect the active ingredient from degradation at a specific location (such as the acidic environment of the stomach); 2) development of drug patches (Nicoderm®) with extended release of active ingredient that can penetrate through the skin to reach the bloodstream (Fig. 1.1); and 3) development of nanoparticulate carriers to entrap and deliver anticancer drugs to disease sites (an example is Doxil®, a liposomal carrier of doxorubicin hydrochloride).

1.1.2 Drug delivery devices: goals

Even with the present accomplishments in drug delivery, more breakthroughs are still needed to further improve the efficacy of existing drugs. To achieve these breakthroughs, it is important to understand the goals for drug delivery. For the purposes of improving drug delivery, the goals are all similar and include: 1) protecting drugs from degradation during formulation or dosage preparation and after administration into the

body; 2) controllable release period to achieve desirable body residence time or increased dosing intervals; 3) enhanced targeting of drug molecules to disease sites; 4) reducing overall side effects; and 5) creating safer formulations that can work broadly to improve efficacy of many classes of drugs.

1.1.3 Extended release delivery systems

1.1.3.1 Microspheres

One of the goals scientists have targeted is controlled drug release. Many drugs, such as chemotherapeutics, require multiple injections or infusions, while others require taking many pills multiple times each day to maintain therapeutic level in patients. Because this can lead to patient discomfort, extended release drug delivery devices are desirable. An early device for this was microspheres, or envelopes containing drug-dissolved solution (Poznansky and Juliano 1984) and now defined as polymeric spheres between 1-999 micrometers that can be formulated using solvent evaporation or various polymerization methods (Kreuter 1996; Freiberg and Zhu 2004). These particles can entrap or encapsulate drug molecules to protect the integrity of drugs under physiological conditions, reduce potential side effects through localized release, as well as release drug slowly over an extended period of time (weeks to months) depending on formulation parameters.

Early studies used albumin, polyvinylpyrrolidone, and polyacrylamide to formulate microspheres (Fig. 1.2), but problems included poor release kinetics, inflammatory reactions, or restrictions in the types of drugs that can be delivered (Kramer 1974). A breakthrough in this field came when biodegradable and biocompatible polymers were used to formulate an implant that reduced immune responses and achieved sustained drug release over 100 days (Langer and Folkman 1976), drastically reducing the number of administrations needed while maintaining therapeutic concentrations in the body. In the 30+ years since this advancement, numerous classes of drugs, including proteins (antibody) and peptides (Langer 1996; Duncan, Jess et al. 2005; Li and Schwendeman 2005; Wang, Tabata et al. 2006), small molecules (Lamprecht, Yamamoto et al. 2003; Abdekhodaie and Wu 2006), and genetic material (Yun, Goetz et al. 2004;

Jang and Shea 2006) have been encapsulated into or adsorbed onto these biodegradable microspheres for improved efficacy or release.

1.1.3.2 Millicylinders

In addition to microspheres, another local extended release formulation is the millicylinder, which are cylinders in the millimeter range in length and micrometers in diameter with drugs dispersed throughout a polymer matrix. However, they are less extensively studied relative to microspheres because of the larger needle used or even surgery used to administer this dosage form, even though drug loading and release can be extensive. An example of a drug on the market using this technology is Norplant® and Norplant II®, where levonorgestrel, the active ingredient, is dispersed throughout the matrix of silicone rods (Fig. 1.3).

Even though microspheres and millicylinders are effective for extended and controlled drug delivery and preservation of drug integrity, they lack target specificity and their relatively large size only allows for local administration and drug release (Kohane 2006). Because of these inherent disadvantages, another class of controlled drug delivery vehicle with targeting and systemic administration properties, nanoparticles, has been studied extensively in recent years.

1.2 Nanoparticle drug delivery systems

1.2.1 Introduction/background

As the name suggests, nanoparticles are solid particles ranging from 10 nm to 1000 nm in size (Kreuter 1996). They have many of the characteristics and advantages of microspheres and they can be made from different materials depending on the type of nanoparticles and different types of drugs, including proteins, peptides, small molecules, and genetic material, that are loaded into the particles.

Even though most people know nanoparticles are effective for drug delivery, many do not realize that there are different types of nanoparticle formulations that vary depending on formulation procedure, materials used, type of drug encapsulated, drug

distribution in the particle, morphology and size of the particles. Thus, a thorough understanding of prevalent formulations is required to successfully prepare nanoparticle delivery vehicles. Below, brief overviews of popular nanoparticle formulations are presented.

1.2.2 Nanoparticle carriers

1.2.2.1 Liposomes

One of the earliest nano-scale formulations investigated were liposomes (Fig. 1.4A). Their discovery dates to the 1960s, when it was found that hydrated dry lipid films can form spherical vesicles resembling cellular organelles with lipid bilayers (Bangham 1993). After more than 40 years of extensive study, liposomes are now broadly defined as spherical lipid bilayers from 50-1000 nm in diameter with the lipid bilayer enclosing an inner aqueous phase (Banerjee 2001; Lian and Ho 2001). The lipid bilayer can be constructed from different phospholipids along with different amounts of cholesterol to increase particle stability. Different phospholipids impart different properties (e.g., charges) to liposomes. For example, phosphatidylserine and phosphatidylglycerol result in negative surface charge which can reduce particle aggregation and improve stability while dioleoyl phosphatidylethanolamine result in positive surface change valuable for loading and delivering DNA (Farhood, Serbina et al. 1995). In addition to constituent material, liposomes are also distinguished into unilamellar or multilamellar vesicles. As the names suggest, unilamellar vesicles have single lipid bilayer surrounding an aqueous core while multilamellar vesicles have multiple lipid bilayers surrounding the aqueous core. Because they have aqueous core surrounded by lipid bilayers, hydrophilic drugs may be encapsulated in the aqueous core while hydrophobic drugs can be entrapped in the lipid bilayer.

An important factor for the efficacy of liposomes, and perhaps nanoparticles in general, is particle size. Extensive investigations showed that liposome uptake by the reticuloendothelial system (RES), a system that clears particles from the bloodstream and thus reduces particle/drug circulation time, increases with particle size (Banerjee 2001; Lian and Ho 2001). In addition to size, another aspect of liposomes that will be discussed

in detail later is the targeting ability of these particles. Different molecules, such as antibodies, may be coated or conjugated onto the surface of liposomes to promote localization to a particular type of cell in the body that overexpress receptors for these molecules.

Extensive research for the last several decades have led to numerous successful marketed drugs using liposome technology (Dutta 2007).

1.2.2.2 Micelles

Micelles are another type of nanoparticles with enormous potential for the delivery of hydrophobic drugs. The basic unit of a micelle is a block copolymer with amphiphilic character where one segment is hydrophobic while the other is hydrophilic (Fig. 1.4B). In an aqueous environment, copolymers assemble to form polymeric micelles with a hydrophobic core and a hydrophilic shell. Copolymer association occurs when their solution concentration reach a threshold value, known as the critical micelle concentration (CMC). Unlike micelles formed from surfactants such as sodium dodecyl sulfate (SDS), polymeric micelles have a much lower CMC, improving their stability in body. Other advantages of micelles include relatively uniform small size, which normally varies between 10-100 nm; ease of preparation and drug loading; and innate stealth effect, the ability to repel body protein adsorption onto particle surface and removal by macrophages, due to a outer shell of hydrophilic polymer (Kataoka, Harada et al. 2001; Croy and Kwon 2006). However, one of the important limitations of a micelle is the type of drugs it can deliver. Because of the hydrophobic core of this carrier and passive nanoparticle formulation procedure, hydrophobic drugs are most suitable for loading although some researchers have also loaded genetic material (Katayose and Kataoka 1998) and enzymes (Harada and Kataoka 1998) into micelles formulated using ionic copolymers.

Even though no micelle-based drugs are currently marketed, micelle-based formulations of doxorubicin HCl (NK911) and taxol (NK105) have entered clinical trials and bring hope to this area of research (Matsumura, Hamaguchi et al. 2004).

1.2.2.3 Dendrimers

Dendrimers are another nanoparticle formulation extensively researched in recent years. This carrier was first illustrated in 1979 by Vogtle and pioneering work by Tomalia (Tomalia, Baker et al. 1985) and Newkome (Newkome, Yao et al. 1985) in the mid-1980s helped to establish this field of study. Dendrimers are essentially repeatedly branching units (dendrons) radiating from a central core with individual/identical branching units made from monomer units linked to each other through covalent bonds (Fig. 1.4C). The number of branching points tallied moving outward from the core to the periphery of the dendrimer defines its generation (G-1, G-2, G-3…). The most commonly used dendrimer scaffold is polyamidoamine (PAMAM), built from a core of ethylene diamine (EDA), and tested for applications in MRI and drug delivery (Lee, MacKay et al. 2005; Svenson and Tomalia 2005; Yang and Kao 2006).

There are currently two methods to produce dendrimers, divergent and convergent methods. The divergent method was first introduced by Tomalia and is where monomer units extend peripherally from the core in a radial fashion while the convergent method, pioneered by Frechet, proceeds from the surface to form identical branches or dendrons and then attachment of these to a multifunctional core to form the dendrimer (Svenson and Tomalia 2005).

Dendrimers have various characteristics advantageous for drug delivery. These include: 1) construction from almost any type of chemistry (polyamidoamines, polyamines, polyamides, polyesters, DNA, etc.) that is usefully for tailoring their solubility and degradability; 2) potential for controlled surface functionality or multivalency that allows multiple drug conjugation for drug loading and multiple antigen attachment for active drug targeting; and 3) and well-defined structure with very low polydispersity (uniform size) which can improve drug targeting and reduce therapeutic variability (Lee, MacKay et al. 2005).

Despite being around for a little more than 20 years, dendrimer-based technology has become very pervasive with commercial products such as Starburst™ by Dendritech, VivaGel™ by Starpharma as a topical microbicide to prevent STD transmission, Superfect® by Qiagen for gene transfection, Alert Ticket™ by US Army Research

Laboratory for anthrax detection and Stratus® CS for cardiac marker diagnostics (Yang and Kao 2006).

1.2.2.4 Solid lipid nanoparticles (SLN)

As the name suggests, solid lipid nanoparticles are made from solid lipids (lipids solid at room and body temperature) stabilized by surfactants with drug dissolved or dispersed in the particle matrix (Fig. 1.4D). This field was discovered in the 1960s when the first parenteral fat emulsion (Intralipid®) was used for nutrition delivery. However, previous formulations in this field used liquid oils with small size, making controlled drug release difficult (Mehnert and Mader 2001; Wissing, Kayser et al. 2004; Wong, Bendayan et al. 2007); thus, the concept of solid lipid usage was conceived.

The basic ingredients of SLN include solid lipids, including triglycerides, partial glycerides, fatty acids, steroids, and waxes, and emulsifiers and water. There are four general methods of SLN preparation. The first is high shear homogenization/ultrasonication where lipid pellets are reduced in size. The second is high pressure homogenization at hot or cold temperature, where the lipid suspension or emulsion is reduced in size using a high pressure homogenizer. The third is solvent emulsification/evaporation where like micelles, the lipids and drug are dissolved in water-immiscible organic solvent and emulsified in an aqueous phase. Lastly, one of the more recent methods is microemulsion-based SLN preparation where the components chosen and their ratios help to control particle formation and size (Mehnert and Mader 2001; Wissing, Kayser et al. 2004).

Drug can be loaded into the core or shell of solid lipid nanoparticles, and in many cases, may be dispersed in the lipid matrix. Because the lipid matrix is made from physiological lipids, SLN can also reduce toxicity although certain formulations require high concentrations of stabilizing surfactant/emulsifiers that may be toxic in itself. Nowadays, innovations in this area has led to hybrid polymer/lipid SLN that improve particle stability and drug loading and release (Wong, Bendayan et al. 2007).

1.2.2.5 Other carriers

Other nanoparticulate drug carriers include albumin nanoparticles, which can be prepared by emulsion formation, desolvation, or coacervation methods. However, a surfactant-free pH-coacervation method has become the standard with the introduction of the first albumin nanoparticle-based drug, Abraxane® (Langer, Balthasar et al. 2003). Another potential carrier are magnetic nanoparticles although to this day, they are used more as a diagnostic tool due to poor drug loading.

1.2.2.6 Polymeric nanoparticles

With the above nanoparticulate drug carriers in mind, we now focus on the most relevant and important nanoparticle formulation for this project, polymeric nanoparticles. As its name suggests, these nanoparticles can be thought of as solid particles composed of intertwining polymer strands. Although recently, distinctions between polymeric nanoparticles and other polymer-based nanoparticles such as dendrimers and micelles have been blurred.

Polymeric nanoparticles have been made from many types of polymers ranging from basic polymers such as poly(lactide-*co*-glycolide) (PLGA), poly(lactic acid) (PLA), chitosan, poly(alkylcyanoacrylate) (PACA) such as polybutylcyanoacrylate, poly(ε-caprolactone) (PCL), etc, to more complex diblock and triblock polymers such as poly(ethylene glycol)-poly(lactide acid) (PEG-PLA) (Soppimath, Aminabhavi et al. 2001; Galindo-Rodriguez, Allemann et al. 2004; Astete and Sabliov 2006).

PLGA (Fig. 1.5) is a polymer commonly used to formulate nanoparticles; it is synthesized through ring-opening polymerization of two monomer components, lactic acid and glycolic acid, linked through hydrolysable ester bonds. Due to its biodegradability and biocompatibility, PLGA is very often used in FDA-approved devices such as Lupron Depot®, which is prescribed for treatment of advanced prostate cancer (Sinha and Trehan 2005).

1.2.2.6.1 Formulation procedures

There are numerous reported procedures for formulating polymeric nanoparticles, and almost all of them fall under several categories. These methods for nanoparticle

formulation include: 1) emulsion/solvent evaporation; 2) nanoprecipitation; 3) monomer polymerization; 4) salting-out; and 5) spray-drying method (Govender, Stolnik et al. 1999).

In the emulsion/solvent evaporation method, polymer is dissolved in organic solvents such as dichloromethane and this is emulsified into an aqueous solution with a suitable surfactant for particle stability. Extraction of the oil phase into aqueous phase leads to hardening of the nanoparticles. This is the basic oil-in-water (O/W) emulsion (Fig. 1.6). Other variations include water-in-oil-in-water (W/O/W) where a small volume of aqueous solution is first emulsified into the oil phase to form a W/O emulsion, then this is emulsified into a larger volume aqueous solution to form the W/O/W particles; solid-in-oil-in-water (S/O/W) (Kumar, Ramakrishna et al. 2006) emulsion, where solid drug is suspended/emulsified into polymer-containing oil phase, then the S/O primary emulsion is emulsified into an outer aqueous phase to form the S/O/W nanoparticles; and less extensively used O/O emulsion, where two immiscible organic solvents, one containing the polymer and drug, are emulsified to form nanoparticles. In the above procedures, drug loading can be achieved through dissolution (in the inner aqueous or oil phase) or dispersion (as a solid in the oil phase) during nanoparticle formulation (Soppimath, Aminabhavi et al. 2001; Astete and Sabliov 2006).

In the nanoprecipitation method, nanoparticle hardening occurs spontaneously when a water-miscible organic solvent containing dissolved polymer and drug is slowly mixed with and displaced into a surfactant-containing aqueous phase (Govender, Stolnik et al. 1999). This technique is easy and reproducible; however, because only a small number of drugs are soluble in water-miscible organic solvents, this limits the applications of this procedure.

The salting-out method, researched sparingly, was patented by Doelker and colleagues (Bindschaedler, Gurny et al. 1988). In this procedure, a polymer-dissolved organic phase, which should be water-miscible, is emulsified in an aqueous phase under strong stress. The aqueous phase contains an emulsifier and a large amount of undissolved salt to prevent organic phase displacement. Then addition of pure water to this emulsion with careful mild stirring will gradually reduce the ionic strength and induce organic solvent displacement and particle formation (Astete and Sabliov 2006).

The monomer polymerization method, as the name suggests, uses monomeric units such as alkyl cyanoacrylates and mixes them mechanically in an acidic aqueous media, in the presence of surfactants at room temperature, to form nanoparticles containing polymers such as poly(alkylcyanoacrylate) (PACA). The drug is dissolved in the medium before or after polymerization for loading (Soppimath, Aminabhavi et al. 2001).

Lastly, in the spray-drying technique, dried nanoparticles are created in a one-step process. A feed solution containing polymer and drug is first added into a spray-drying instrument and then atomized into a spray. As the spray droplets contact air, they are dried and the solid nanoparticles sediment for collection (Raffin, Jornada et al. 2006; Tewa-Tagne, Briancon et al. 2006). The size of these particles is based on orifice size of the nozzle and atomizing pressure. Advantages of this technique include a one-step formulation process and ease of scale-up while disadvantages include variable yields, potentially low drug loading and dispersed size (Raffin, Jornada et al. 2006).

With all the different techniques listed above, it is no surprise that the polymeric nanoparticle approach is one of the most versatile for drug loading. While at this stage, it is difficult to proclaim any one of the techniques as better than others, the emulsion/solvent evaporation method has been extensively studied due to its simple procedure and broader drug applicability relative to the other methods. For this reason, this nanoparticle formulation strategy will be the focus of this project.

1.2.2.6.2 Distinguishing features of polymeric nanoparticles

Despite similarities to other nanoparticle carriers, polymer nanoparticles have many important advantages. For example, as solid polymers, their stability is excellent relative to nanoparticles such as micelles, which spontaneously form above the critical micelle concentration (CMC) of constituent copolymers and could collapse below this concentration, and liposomes, which are made of fragile lipid bilayers. In addition, polymeric nanoparticles can be tailor-made to promote simple entrapment of different types of drugs (hydrophilic or hydrophobic, small molecule or proteins/peptides), whereas carriers such as micelles are most suitable for loading hydrophobic small molecule drugs and carriers such as dendrimers, although suitable for loading

hydrophobic or hydrophilic drugs, require complicated chemical conjugation for drug loading (Yokoyama 2005). Also, compared to dendrimers, which are made through chemical synthesis, polymeric nanoparticles could be formulated more easily through emulsion-based methods with relatively less stress. Liposomes, although used for several marketed drugs, are relatively unstable compared to polymeric nanoparticles as mentioned above (Wissing, Kayser et al. 2004), and are not the best candidates for achieving long-term (weeks to months) controlled release due to their fragile outer shell that could collapse in two days or less. Solid lipid nanoparticles, although stable and suitable for long-term release, present challenges for drug loading due to their harsh formulation conditions.

1.2.2.6.3 Drug loading methods

Drug incorporation into polymeric nanoparticles can be categorized into entrapment during nanoparticle formulation, drug conjugation to polymer strands before or after nanoparticle formulation, and drug absorption in preformed nanoparticles.

Drug entrapment is by far the most commonly used strategy. Common examples of this involve water-in-oil-in-water (W/O/W) and oil-in-water (O/W) emulsion nanoparticles. With this traditional strategy, drug molecules are either dissolved or suspended in the inner aqueous or oil phase of emulsion-based nanoparticles; as nanoparticles form, drugs are entrapped in the polymer matrix or may even partition into the polymer matrix in the case of hydrophobic drugs to promote drug loading.

Conjugation drug loading is less common. This involves either chemical conjugation of drug and polymer and then use of these conjugates to form nanoparticles or chemical conjugation of drugs to pre-formulated blank nanoparticles. This method has not been widely adopted mainly because of the small number of reactive sites available on nanoparticles for drug loading as well as finding suitable conjugation reactions that will not degrade any components.

Absorption loading, or in certain cases, adsorption, is also less commonly used (Fig. 1.7). Here, pre-formulated nanoparticles are suspended in an aqueous drug solution (in rare cases, certain organic solvents may also be used for drug dissolution as long as nanoparticle integrity is not compromised), and incubation conditions may be

tailored/altered to produce desirable results. This strategy has been applied extensively to proteins/peptides, which lose efficacy under stressful nanoparticle formulation conditions. With the potential to alter incubation drug loading conditions, depending on the type of drug and nanoparticle used, this strategy may prove to be the most useful and will be explored further in this project.

1.2.2.6.4 Release mechanisms/stages

A very important consideration for polymeric nanoparticles is drug release rate. In a perfect world, drug release from polymeric nanoparticles, or any nanoparticle formulation for that matter, would be zero-order with continuous drug release over days, weeks, or months depending on the drug and indication of interest. Unfortunately, due to the small diameter of nanoparticles, surface area-to-volume ratio is very large and can lead to burst release of the majority of encapsulated drug over the first few hours and little release afterwards.

Through extensive studies over the years on microspheres and nanoparticles, scientists have elucidated the mechanism by which drug molecules are released from polymeric matrices of particles. During the initial stage, drugs loosely bound to or embedded on particle surfaces are released upon contact with bulk release media. Then, drugs in the surface layer of nanoparticles may be released from pores near the surface (hydrophilic drugs) or partition through the polymer phase to the bulk aqueous phase (hydrophobic drugs). Next, drugs in the core of nanoparticle matrix diffuse out, with hydrophilic drugs released through aqueous channels while hydrophobic drugs diffuse out through the hydrophobic polymeric matrix. Also during this stage, the polymer may become increasingly swollen due to water absorption, further facilitating drug diffusion through the polymer matrix. For larger particles such as microspheres, there is also a final stage when the polymer matrix erodes and bulk particle degradation occurs, leading to release of any remaining drug. For nanoparticles, however, their small size usually cause the majority of drug to be released long before this stage can take effect (Jalil and Nixon 1990; Soppimath, Aminabhavi et al. 2001).

In order to achieve zero-order release, the only proven ways scientists have slowed drug release from nanoparticles is either through the use of hydrolysable linkers

conjugating drug to the polymer (hydrolysis-limiting) or converting drugs to hydrophobic forms with poor water solubility (solubility-limiting) (Budhian, Siegel et al. 2008). In an example of hydrolysis-limiting release, Yoo et al. (Yoo, Oh et al. 1999) achieved one month, nearly zero-order release of doxorubicin from PLGA nanoparticles. However, formulation of these particles was complex as doxorubicin was first chemically conjugated to PLGA before formulation and drug loading was less than desirable (around 3.5% w/w). Coincidentally, doxorubicin hydrochloride is also a hydrophilic drug which can be converted to a hydrophobic form with the addition of materials such as triethylamine during nanoparticle formulation, and this improves drug loading and release. The above information illustrates that unless an additional layer of attraction, such as chemical linkage or phase attraction between drug molecules and the polymer matrix can be implemented, slow controlled release of the drug is very difficult to achieve.

1.2.2.6.5 Research obstacles

Having looked at various nanoparticle formulations as well as important properties of polymeric nanoparticles, we now focus our attention on the emulsion/solvent-evaporation formulations. Relative to other formulation strategies, emulsion/solvent-evaporation has been extensively studied due to broader applicability to numerous classes of drugs, the ability to tailor formulations according to different needs, and the availability of a large arsenal of polymers, each with their unique properties; however, there are still numerous obstacles for this strategy.

Some obstacles for emulsion/solvent-evaporation nanoparticles include large dispersity of particle sizes, which may lead to potentially different biodistribution and release rates; potential degradation of certain drugs due to stressful formulation procedure; burst release of drug, as mentioned above, where a large percentage of encapsulated drug is released from particles within a few hours of administration and may cause toxicity; poor targeting of drug-loaded particles to disease sites, leading to reduced efficacy and side effects; and relatively low drug loading for hydrophilic drugs, which could require increases in the total amount of drug and nanoparticles administered for each dose and increase of administration time.

As mentioned before, higher nanoparticle drug loading is desirable due to direct benefits such as reduced dosage amount (weight) and administration time and more extended release interval as well as indirect benefits such as reduced side effects and increased administration interval. However, for many categories of drugs, such as proteins, peptides, vaccines, genetic material, and small molecules, high drug loading into emulsion-based nanoparticles has been difficult to achieve. Drug loss could occur in different stages of the formulation process such as sonication-induced emulsification (where drugs may not be encapsulated or degraded) and nanoparticle hardening (where hydrophobic drugs escape out with organic solvents or hydrophilic drugs in the surface layer diffuse out into the hardening media). With this issue in mind, a superior alternative could be the absorption drug loading method mentioned earlier. Because loading conditions can be tailored depending on the type of drug and nanoparticle used and different variables may be optimized to produce the best results, this could provide a powerful tool for drug loading. Normally, absorption loading of drug into polymeric nanoparticles occurs via a passive concentration gradient driving drugs into the particles; however, the presence of an active or charge-based uptake mechanism, in addition to passive concentration gradient, could significantly improve drug loading. The uptake mechanism we will explore is ion complexation or ion-exchange.

1.3 Ion complexation/pairing

1.3.1 Background

Ion complexation strategies have been used to stabilize proteins/peptides in solution and involved pairing of oppositely charged small molecules (hydrophobic in many cases) to proteins/peptides to form new entities. Recently, because hydrophilic small molecule drugs have poor compatibility with the hydrophobic core of polymeric nanoparticles, leading to poor drug loading, ion complexation has been used to provide additional attraction between the nanoparticle and drug to improve loading (Eroglu, Kas et al. 2001; Ubrich, Bouillot et al. 2004; Wong, Bendayan et al. 2004; Wong, Rauth et al. 2006). An example of this is where the ionizable group of a drug, such as the positive amine group of doxorubicin, is electrostatically attracted to negative charges incorporated

into the nanoparticle, such as acid groups on polymer strands. Various studies have demonstrated the effectiveness of ion complexation strategy in nanoparticles for improving drug loading, release profile, and changes in biodistribution, using either specially-tailored polymers/copolymers (Cavalli, Gasco et al. 2002; Wong, Bendayan et al. 2004; Wong, Rauth et al. 2006; Chavanpatil, Khdair et al. 2007; Tian, Bromberg et al. 2007) or polymer building-blocks such as dextran sulfate (Janes, Fresneau et al. 2001) or alginate (Cafaggi, Russo et al. 2007) as counterions.

1.3.2 Specific applications for proteins

Despite the effectiveness of ion complexation for nanoparticle drug delivery, the majority of existing research has been applied to protein/peptide loading via drug absorption or adsorption, where blank nanoparticles are incubated with a concentrated protein or peptide solution and drug is taken up into the particles. In these cases, special anionic polymers or copolymers that have been synthesized to promote protein/peptide loading include sulfobutylated poly(vinyl alcohol)-graft-poly(lactide-*co*-glycolide) to incorporated tetanus toxoid (Jung, Breitenbach et al. 2000), poly(ε-caprolactone)-poly(ethylene glycol)-poly(ε-caprolactone) to enhance human basic fibroblast growth factor incorporation (Gou, Huang et al. 2007) and using poly(styrene-*co*-4-styrene-sulfonate) to enhance lysozyme loading (Cai, Bakowsky et al. 2008). These examples have demonstrated significantly improved drug loading while minimizing drug degradation during the loading process.

1.3.3 Lipophilic anion use in nanoparticles as ion complexing agents

Despite the ingenuity that has made ion complexation an effective tool for drug delivery, integration of this with polymeric nanoparticles have focused on specially synthesized polymers or copolymers which are complex in design and fabrication. An interesting alternative or addition to the use of anionic polymers would be incorporation of lipophilic anions that could be obtained cheaply and easily. The lipophilicity of these molecules could promote their incorporation into hydrophobic cores of polymeric nanoparticles while their anionic charges could enhance drug loading. Small molecule

lipophilic anions that could be studied for this purpose include sulfate-based compounds, such as sodium dodecyl sulfate, and borate-based compounds, such as sodium tetraphenyl borate. These compounds have either hydrophobic carbon chains or aromatic rings linked to either anionic sulfates or borates which would be ideal for entrapment in the hydrophobic core of nanoparticles while the anionic charge would be beneficial for improving uptake of cationic drugs, especially hydrophilic small molecules.

1.4 Applicable cationic drugs

There are numerous classes of hydrophilic, positively charged drugs which could benefit from ion complexation. Examples include anesthetics such as bupivacaine hydrochloride; tricyclic antidepressants such as amytriptyline and desipramine; antibiotics such as gentamycin sulfate and capreomycin sulfate; and hypertension drugs such as amiloride.

One of the most important classes which will be the focus of this study is chemotherapeutic drugs, which includes doxorubicin hydrochloride (doxHCl) and vinblastine sulfate (VS), two excellent candidates (model drugs) for incorporation into ion-complexing/pairing nanoparticles (Fig. 1.8). An important indicator of suitability of the drug is its pKa value; doxHCl has a pKa of around 8.2, meaning that at physiological pH of 7.4, more than 80% of doxHCl molecules have a net positive charge; vinblastine sulfate (VS) has a pKa of around 7.4, meaning that around 50% of VS molecules have a net positive charge at physiological pH. These pKa values demonstrate both drugs have the ability to interact with counter-anions to form hydrophobic ion pairs.

In addition to having desired molecular charges at physiological pH, these hydrophilic drugs have aqueous solubility of greater than 10 mg/mL and both drugs have been commercially available for the last several decades and are effective against a range of cancer cells. Despite their effectiveness, delivery of these drugs using nanoparticles have further improved efficacy through passive drug targeting while reducing side effects, but drug loading in polymeric nanoparticles have been limited by their hydrophilicity.

In addition to potential charge-charge interactions between positively charged drug molecules and negative charges of the anions to provide an active drug uptake into nanoparticles, the fused rings of doxHCl and VS may also have hydrophobic interactions

(pi-pi stacking) with aromatic rings of the lipophilic borates used, such as sodium tetraphenylborate.

1.5 Alternative applications of ion complexing/pairing polymeric nanoparticles

Drug delivery is only one of the applications for lipophilic anion-incorporated polymeric nanoparticles, but based on the potential for active drug and opposite charge uptake; other applications may also be possible for these versatile devices. Two of the potential applications include treatment for drug detoxification and water purification.

1.5.1 Drug detoxification

Drug overdose has been one of the major healthcare problems around the world and can result from causes such as therapeutic mishaps by physicians or nurses, illegal drug uses, or suicide attempts. Despite mounting morbidity and financial burdens, the majority of drug-induced toxicities still lack appropriate treatment (Litovitz 1998).

1.5.1.1 Current detoxification strategies

There are five primary detoxification methods widely used today. The most often cited is hemodialysis and hemofiltration, where semi-permeable membranes separate counter-current dialysate and extracorporeal blood to remove drugs. However, important shortcomings of this include suitability only for a small number of hydrophilic drugs with low molecular weight, low volume of distribution, and slow onset of action due to long procedure duration. A second method, similar to hemodialysis, is plasmapheresis, where extracorporeal exchange of plasma with treated donor plasma or saline takes place. Similar to hemodialysis, this strategy involves additional complexities related to exchange of plasma itself. The third method is use of drug-specific antibodies through either direct injection or extracorporeal immunoadsorption. However, due to limited binding sites, large quantities of antibodies need to be administered in order to be effective. To date, only Digibind®, used for treating digoxin toxicity, has been commercially available. The fourth method is the traditional use of drug-specific antidotes, although only two, atropine and naloxone, have been manufactured and

available to treat muscarinic-cholinergic and narcotic receptor antagonists. Although rarely used, the last method involves direct infusion of enzymes to degrade drugs into inactive metabolites, such as the use of butyrylcholinesterase to degrade cocaine (Dennis, Martin et al. 2001; Kaminski and Rosengart 2005).

Although these are the primary methods, other cheaper but effective methods include induced vomiting and stomach washes.

1.5.1.2 Nanoparticle detoxification strategies

Due to limitations of the existing detoxification methods, a few nanoparticle systems have been explored as potential detoxifying agents. Early research in this area include the use of custom-designed microemulsions to extract lipophilic drugs into lipophilic inner cores (Morey, Varshney et al. 2004; Varshney, Morey et al. 2004), magnetic nanoparticles that can capture toxins through surface-conjugated receptors (Kaminski and Rosengart 2005; Mertz, Kaminski et al. 2005), and larger derivatized oligochitosan molecules that achieve rapid amitriptyline adsorption through pi-pi complexation (Lee and Baney 2004; Lee, Flint et al. 2005). Despite successful drug uptake, shortcomings of these systems include relative instability of microemulsions in a physiological system and complex synthesis and characterization for derivatized magnetic particles and chitosan as well as uncertainty regarding how well these systems work physiologically.

A new biodegradable polymeric nanoparticle system could overcome these shortcomings. By taking advantage of and selecting best-available commercially available polymers, such as poly(lactic acid) (PLA), poly(ε-caprolactone) (PCL), and FDA-approved poly(lactide-*co*-glycolide) (PLGA) (Astete and Sabliov 2006) as well as incorporation of a lipophilic anion that improves drug partitioning into the nanoparticle, we can synthesize an effective, stable and simple system for detoxification.

1.5.2 Hard water treatment

Another potential application of ion-complexing nanoparticles may be water treatment. Water hardness, due to the presence of heavy metals magnesium and calcium,

pose significant problems for cleaning (domestic applications such as laundry and bathing and industrial scale applications), causing buildup in pipes which restrict water flow over time, and causing buildups in thermal generators (water heating element) which increases the cost of heating water over time (Robison 2008). For humans, water hardness may increase the risk of acute myocardial infarction (Yang, Chang et al. 2006; Kousa, Havulinna et al. 2008) and irritant contact dermatitis (Warren, Ertel et al. 1996). Because of these challenges, research to reduce heavy metal content have been extensive and numerous scientist have explored ion-exchange mechanisms for metal removal. Examples include cross-linked poly(styrenesulfonamide) with iminoacetic acid (Bicak, Senkal et al. 1998) and use of mixture of calcium hydroxide, iron sulfate, lime and chlorine to precipitate and sediment heavy metals such as calcium (Sale, Darr et al. 1988).

Lipophilic anion-incorporated polymeric nanoparticles in this project may be applicable for this process. Presence of lipophilic anions inside nanoparticles and anionic charges of PLGA polymers provide a natural ion-exchange mechanism for cationic molecules such as heavy metals. Potential aggregation of regular (unPEGylated) nanoparticles after surface charge neutralization (due to drug adsorption/binding) also provides a built-in mechanism of metal ion removal. In addition, PLGA is biodegradable and biocompatible, while selection of lipophilic anion selection should be more carefully considered to limit the inherent toxicity associated with this strategy.

1.6 Specific aims

With all of the above information in mind, there are several objectives that I would like to accomplish for this project:

1) Test the ion pairing ability of a group of alkyl sulfates with a model drug, doxorubicin hydrochloride, and determine the solubility of resulting complexes in various organic solvents and lastly, examine how well they incorporate into polymeric nanoparticles.

2) Test the ion-pairing ability of a group of borate-based compounds by determining their solubility in various organic solvents and ability to extract (ion-pair with) doxHCl into an organic phase.

3) Examine incorporation and loading of borate-based lipophilic anions and model drugs, doxorubicin hydrochloride and vinblastine sulfate, into polymeric nanoparticles, with drug loading achieved using an optimized incubation adbsorption method; and test drug uptake under simulated physiological environment.

4) Compare drug loading (by weight) and release properties, for ion-pairing nanoparticles, with drug loaded using either absorption drug loading strategy or traditional encapsulation/entrapment strategy for a model drug, doxorubicin hydrochloride.

Figure 1. 1. Marketed forms of A) Cialis®, B) Ambien®, and C) Nicoderm®.

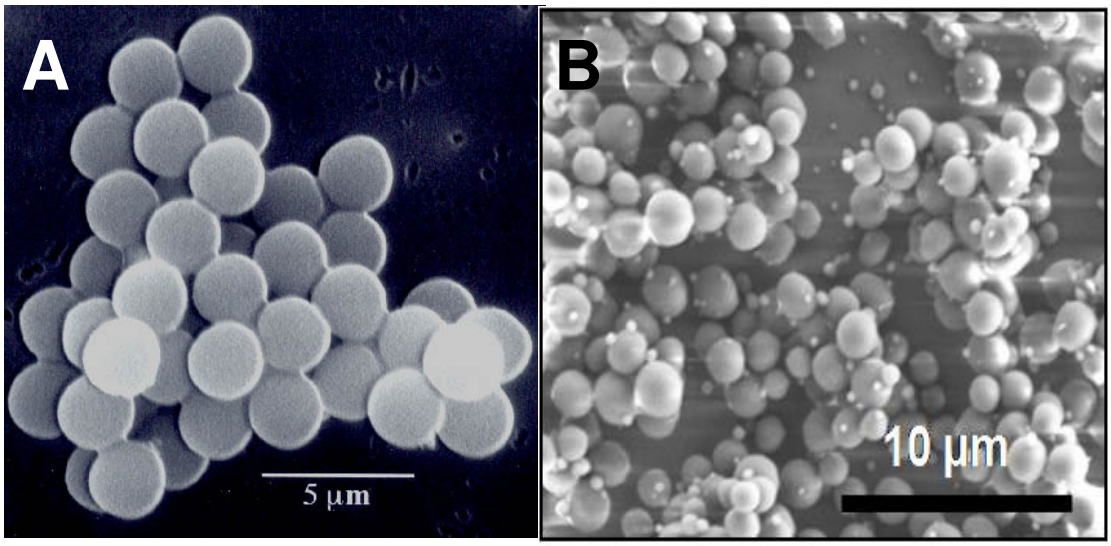

Figure 1. 2. Representative albumin (A) and polyvinylpyrrolidone (B) microspheres as seen by SEM.

Figure 1. 3. Norplant® millicylinder implants (Sold by Wyeth®).

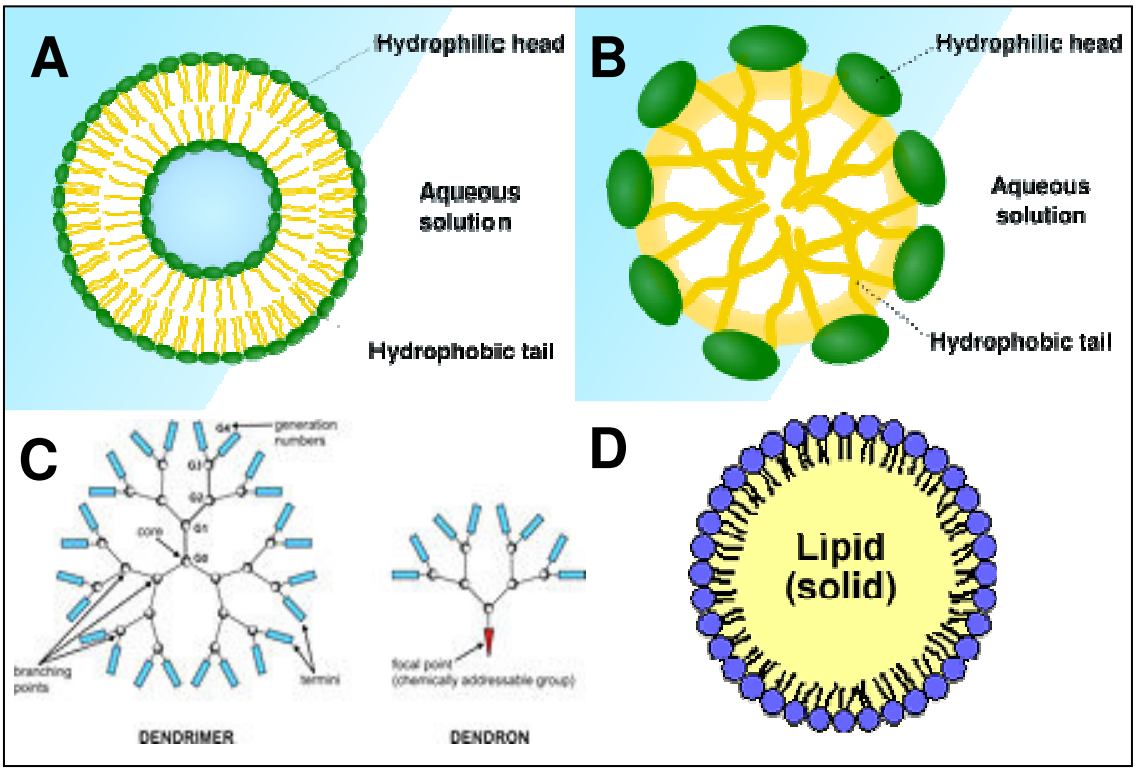

Figure 1. 4. Representative liposomes (A), micelle (B), dendrimer (C), and solid lipid nanoparticles (D).

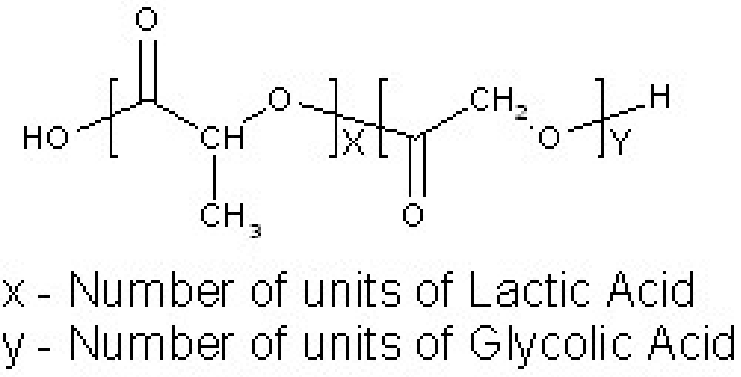

Figure 1. 5. Chemical formula of PLGA.

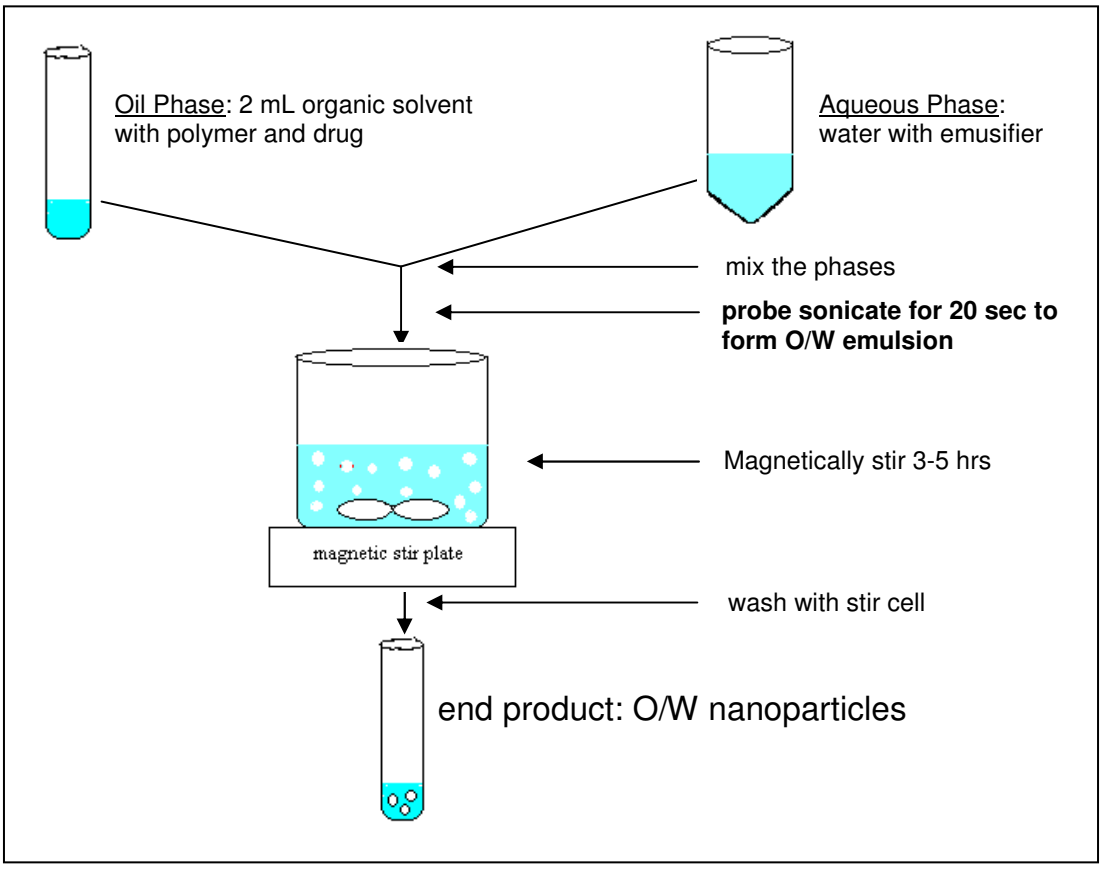

Figure 1. 6. General formulation procedure for O/W nanoparticles.

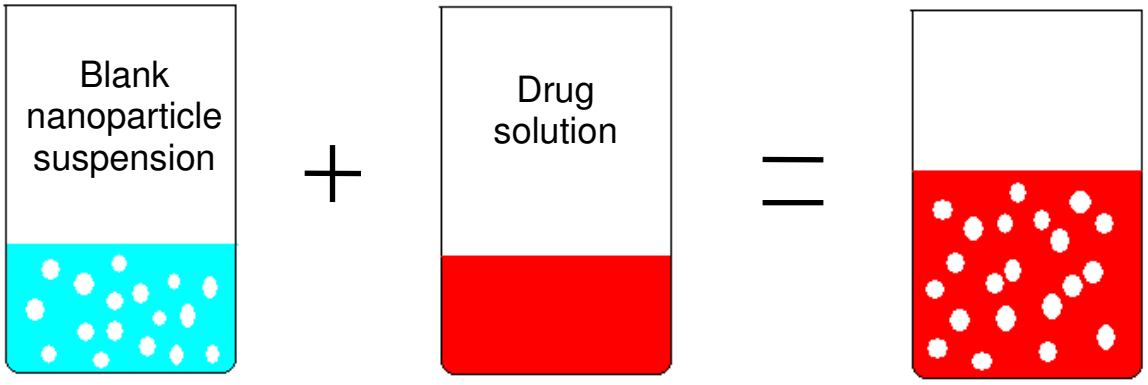

Figure 1. 7. Incubation/absorption drug loading process involving simple mixing of two components.

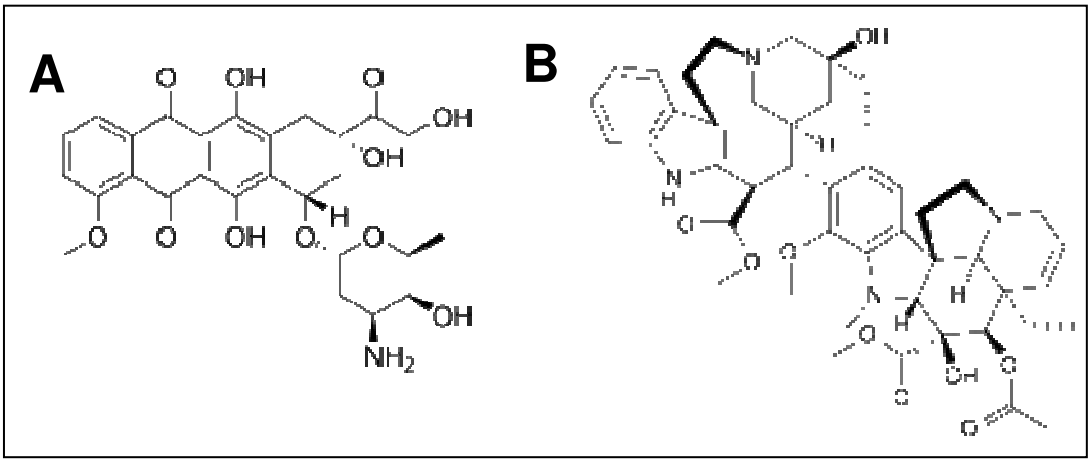

Figure 1. 8. Structure of doxorubicin hydrochloride (A) and vinblastine sulfate (B).

List of References:

Abdekhodaie, M. J. and X. Y. Wu (2006). "Drug loading onto ion-exchange microspheres: Modeling study and experimental verification." Biomaterials **27**(19): 3652-3662.

Astete, C. E. and C. M. Sabliov (2006). "Synthesis and characterization of PLGA nanoparticles." Journal of Biomaterials Science-Polymer Edition **17**(3): 247-289.

Bae, Y., T. A. Diezi, et al. (2007). "Mixed polymeric micelles for combination cancer chemotherapy through the concurrent delivery of multiple chemotherapeutic agents." Journal of Controlled Release **122**: 324-330.

Bagalkot, V., L. Zhang, et al. (2007). "Quantum dot - Aptamer conjugates for synchronous cancer imaging, therapy, and sensing of drug delivery based on Bi-fluorescence resonance energy transfer." Nano Letters **7**: 3065-3070.

Banerjee, R. (2001). "Liposomes: Applications in medicine." Journal of Biomaterials Applications **16**(1): 3-21.

Bangham, A. D. (1993). "Liposomes - the Babraham Connection." Chemistry and Physics of Lipids **64**(1-3): 275-285.

Bertin, P. A., D. D. Smith, et al. (2005). "High-density doxorubicin-conjugated polymeric nanoparticles via ring-opening metathesis polymerization." Chemical Communications(30): 3793-3795.

Bibby, D. C., J. E. Talmadge, et al. (2005). "Pharmacokinetics and biodistribution of RGD-targeted doxorubicin-loaded nanoparticles in tumor-bearing mice." International Journal of Pharmaceutics **293**(1-2): 281-290.

Bicak, N., B. F. Senkal, et al. (1998). "Crosslinked poly(styrenesulfonamide) with iminoacetic acid chelating groups for hard-water treatment." Macromolecular Chemistry and Physics **199**(12): 2731-2735.

Bindschaedler, C., R. Gurny, et al. (1988). Process for preparing a powder of water-insoluble polymer which can be redispersed in a liquid phase, the resulting powder and utilization thereof. Switzerland. **WO 88/08011**.

Brannon-Peppas, L. and J. O. Blanchette (2004). "Nanoparticle and targeted systems for cancer therapy." Advanced Drug Delivery Reviews **56**(11): 1649-1659.

Brigger, I., C. Dubernet, et al. (2002). "Nanoparticles in cancer therapy and diagnosis." Advanced Drug Delivery Reviews **54**(5): 631-651.

Budhian, A., S. J. Siegel, et al. (2008). "Controlling the in vitro release profiles for a system of haloperidol-loaded PLGA nanoparticles." International Journal of Pharmaceutics **346**(1-2): 151-159.

Cafaggi, S., E. Russo, et al. (2007). "Preparation and evaluation of nanoparticles made of chitosan or N-trimethyl chitosan and a cisplatin-alginate complex." Journal of Controlled Release **121**(1-2): 110-123.

Cai, C., U. Bakowsky, et al. (2008). "Charged nanoparticles as protein delivery systems: A feasibility study using lysozyme as model protein." Eur J Pharm Biopharm **69**(1): 31-42.

Cao, Y. H. (2004). "Antiangiogenic cancer therapy." Seminars in Cancer Biology **14**(2): 139-145.

Cavalli, R., M. R. Gasco, et al. (2002). "Solid lipid nanoparticles (SLN) as ocular delivery system for tobramycin." International Journal of Pharmaceutics **238**(1-2): 241-245.

Chavanpatil, M. D., A. Khdair, et al. (2007). "Surfactant-polymer nanoparticles overcome P-glycoprotein-mediated drug efflux." Molecular Pharmaceutics **4**: 730-738.

Chavanpatil, M. D., A. Khdair, et al. (2007). "Surfactant-polymer nanoparticles: A novel platform for sustained and enhanced cellular delivery of water-soluble molecules." Pharmaceutical Research **24**(4): 803-810.

Chavanpatil, M. D., A. Khdair, et al. (2007). "Polymer-surfactant nanoparticles for sustained release of water-soluble drugs." Journal of Pharmaceutical Sciences **96**: 3379-3389.

Chen, J. H., L. Wang, et al. (2004). "Body distribution of nanoparticle-containing adriamycin injected into the hepatic artery of hepatoma-bearing rats." Digestive Diseases and Sciences **49**(7-8): 1170-1173.

Croy, S. R. and G. S. Kwon (2006). "Polymeric micelles for drug delivery." Current Pharmaceutical Design **12**(36): 4669-4684.

Dennis, D. M., C. R. Martin, et al. (2001). Detoxification and decontamination using nanotechnology therapy. USPTO. United States, Univ, Florida. **6977171**.

Dreis, S., F. Rothweller, et al. (2007). "Preparation, characterisation and maintenance of drug efficacy of doxorubicin-loaded human serum albumin (HSA) nanoparticles." International Journal of Pharmaceutics **341**(1-2): 207-214.

Duncan, G., T. J. Jess, et al. (2005). "The influence of protein solubilisation, conformation and size on the burst release from poly(lactide-co-glycolide) microspheres." Journal of Controlled Release **110**(1): 34-48.

Dutta, R. C. (2007). "Drug carriers in pharmaceutical design: Promises and progress." Current Pharmaceutical Design **13**(7): 761-769.

Eroglu, H., H. S. Kas, et al. (2001). "The in-vitro and in-vivo characterization of PLGA : L-PLA microspheres containing dexamethasone sodium phosphate." Journal of Microencapsulation **18**(5): 603-612.

Farhood, H., N. Serbina, et al. (1995). "The Role of Dioleoyl Phosphatidylethanolamine in Cationic Liposome-Mediated Gene-Transfer." Biochimica Et Biophysica Acta-Biomembranes **1235**(2): 289-295.

Freiberg, S. and X. Zhu (2004). "Polymer microspheres for controlled drug release." International Journal of Pharmaceutics **282**(1-2): 1-18.

Galindo-Rodriguez, S., E. Allemann, et al. (2004). "Physicochemical parameters associated with nanoparticle formation in the salting-out, emulsification-diffusion, and nanoprecipitation methods." Pharmaceutical Research **21**(8): 1428-1439.

Gou, M. L., M. J. Huang, et al. (2007). "Preparation of anionic poly(epsilon-caprolactone)-poly(ethylene glycol)poly(epsilon-caprolactone) copolymeric nanoparticles as basic protein antigen carrier." Growth Factors **25**: 202-208.

Govender, T., S. Stolnik, et al. (1999). "PLGA nanoparticles prepared by nanoprecipitation: drug loading and release studies of a water soluble drug." Journal of Controlled Release **57**(2): 171-185.

Gref, R., Y. Minamitake, et al. (1994). "Biodegradable Long-Circulating Polymeric Nanospheres." Science **263**(5153): 1600-1603.

Gulyaev, A. E., S. E. Gelperina, et al. (1999). "Significant transport of doxorubicin into the brain with polysorbate 80-coated nanoparticles." Pharmaceutical Research **16**(10): 1564-1569.

Harada, A. and K. Kataoka (1998). "Novel polyion complex micelles entrapping enzyme molecules in the core: Preparation of narrowly-distributed micelles from lysozyme and poly(ethylene glycol)-poly(aspartic acid) block copolymer in aqueous medium." Macromolecules **31**(2): 288-294.

Huang, H., E. Pierstorff, et al. (2007). "Active nanodiamond hydrogels for chemotherapeutic delivery." Nano Letters **7**: 3305-3314.

Husseini, G. A., M. A. D. de la Rosa, et al. (2007). "Release of doxorubicin from unstabilized and stabilized micelles under the action of ultrasound." Journal of Nanoscience and Nanotechnology **7**(3): 1028-1033.

Hyung, W., H. Ko, et al. (2008). "Novel hyaluronic acid (HA) coated drug carriers (HCDCs) for human breast cancer treatment." Biotechnology and Bioengineering **99**: 442-454.

Iwasaki, Y., H. Maie, et al. (2007). "Cell-specific delivery of polymeric nanoparticles to carbohydrate-tagging cells." Biomacromolecules **8**: 3162-3168.

Jain, T. K., M. A. Morales, et al. (2005). "Iron oxide nanoparticles for sustained delivery of anticancer agents." Molecular Pharmaceutics **2**(3): 194-205.

Jalil, R. and J. R. Nixon (1990). "Biodegradable Poly(Lactic Acid) and Poly(Lactide-Co-Glycolide) Microcapsules - Problems Associated with Preparative Techniques and Release Properties." Journal of Microencapsulation **7**(3): 297-325.

Janes, K. A., M. P. Fresneau, et al. (2001). "Chitosan nanoparticles as delivery systems for doxorubicin." Journal of Controlled Release **73**(2-3): 255-267.

Jang, J. H. and L. D. Shea (2006). "Intramuscular delivery of DNA releasing microspheres: Microsphere properties and transgene expression." Journal of Controlled Release **112**(1): 120-128.

Jeong, Y. I., K. C. Choi, et al. (2006). "Doxorubicin release from core-shell type nanoparticies of poly(DL-lactide-co-glycolide)-grafted dextran." Archives of Pharmacal Research **29**(8): 712-719.

Jeong, Y. I., H. S. Na, et al. (2006). "Adriamycin release from self-assembling nanospheres of poly(DL-lactide-co-glycolide)-grafted pullulan." International Journal of Pharmaceutics **322**(1-2): 154-160.

Jung, S. W., Y. I. Jeong, et al. (2005). "Drug release from core-shell type nanoparticles of poly(DL-lactide-co-glycolide)-grafted dextran." Journal of Microencapsulation **22**(8): 901-911.

Jung, T., A. Breitenbach, et al. (2000). "Sulfobutylated poly(vinyl alcohol)-graft-poly(lactide-co-glycolide)s facilitate the preparation of small negatively charged biodegradable nanospheres." Journal of Controlled Release **67**(2-3): 157-169.

Kaminski, M. D. and A. J. Rosengart (2005). "Detoxification of blood using injectable magnetic nanospheres: A conceptual technology description." Journal of Magnetism and Magnetic Materials **293**(1): 398-403.

Kataoka, K., A. Harada, et al. (2001). "Block copolymer micelles for drug delivery: design, characterization and biological significance." Advanced Drug Delivery Reviews **47**(1): 113-131.

Katayose, S. and K. Kataoka (1998). "Remarkable increase in nuclease resistance of plasmid DNA through supramolecular assembly with poly(ethylene glycol) poly(L-lysine) block copolymer." Journal of Pharmaceutical Sciences **87**(2): 160-163.

Kohane, D. (2006). "Microparticles and nanoparticles for drug delivery." Biotechnology and Bioengineering **96**(2): 203-209.

Kousa, A., A. S. Havulinna, et al. (2008). "Magnesium in well water and the spatial variation of acute myocardial infarction incidence in rural Finland." Applied Geochemistry **23**(4): 632-640.

Kramer, P. A. (1974). "Albumin microspheres as vehicles for achieving specificity in drug delivery." J. Pharmaceut. Sci. **63**: 1646-1647.

Kreuter, J. (1996). "Nanoparticles and microparticles for drug and vaccine delivery." Journal of Anatomy **189**: 503-505.

Kumar, P. S., S. Ramakrishna, et al. (2006). "Influence of microencapsulation method and peptide loading on formulation of poly(lactide-co-glycolide) insulin nanoparticles." Pharmazie **61**(7): 613-617.

Lamprecht, A., H. Yamamoto, et al. (2003). "Microsphere design for the colonic delivery of 5-fluorouracil." Journal of Controlled Release **90**(3): 313-322.

Langer, K., S. Balthasar, et al. (2003). "Optimization of the preparation process for human serum albumin (HSA) nanoparticles." International Journal of Pharmaceutics **257**(1-2): 169-180.

Langer, R. (1996). "Controlled release of a therapeutic protein." Nature Medicine **2**(7): 742-743.

Langer, R. and J. Folkman (1976). "Polymers for Sustained-Release of Proteins and Other Macromolecules." Nature **263**(5580): 797-800.

Lee, C. C., E. R. Gillies, et al. (2006). "A single dose of doxorubicin-functionalized bow-tie dendrimer cures mice bearing C-26 colon carcinomas." Proceedings of the National Academy of Sciences of the United States of America **103**(45): 16649-16654.

Lee, C. C., J. A. MacKay, et al. (2005). "Designing dendrimers for biological applications." Nature Biotechnology **23**(12): 1517-1526.

Lee, D. W. and R. H. Baney (2004). "Oligochitosan derivatives bearing electron-deficient aromatic rings for adsorption of amitriptyline: Implications for drug detoxification." Biomacromolecules **5**(4): 1310-1315.

Lee, D. W., J. Flint, et al. (2005). "Aromatic-aromatic interaction of amitriptyline: Implication of overdosed drug detoxification." Journal of Pharmaceutical Sciences **94**(2): 373-381.

Lee, G. Y., K. Park, et al. (2006). "Anti-tumor and anti-metastatic effects of gelatin-doxorubicin and PEGylated gelatin-doxorubicin nanoparticles in SCC7 bearing mice." Journal of Drug Targeting **14**(10): 707-716.

Leo, E., R. Cameroni, et al. (1999). "Dynamic dialysis for the drug release evaluation from doxorubicin-gelatin nanoparticle conjugates." International Journal of Pharmaceutics **180**(1): 23-30.

Li, L. and S. P. Schwendeman (2005). "Mapping neutral microclimate pH in PLGA microspheres." Journal of Controlled Release **101**(1-3): 163-173.

Lian, T. and R. J. Y. Ho (2001). "Trends and developments in liposome drug delivery systems." Journal of Pharmaceutical Sciences **90**(6): 667-680.

Litovitz, T. (1998). "The TESS database - Use in product safety assessment." Drug Safety **18**(1): 9-19.

Liu, B., S. Q. Jiang, et al. (2006). "Novel biodegradable HSAM nanoparticle for drug delivery." Oncology Reports **15**(4): 957-961.

Madhankumar, A. B., B. Slagle-Webb, et al. (2006). "Interleukin-13 receptor-targeted nanovesicles are a potential therapy for glioblastoma multiforme." Molecular Cancer Therapeutics **5**(12): 3162-3169.

Mehnert, W. and K. Mader (2001). "Solid lipid nanoparticles - Production, characterization and applications." Advanced Drug Delivery Reviews **47**(2-3): 165-196.

Mertz, C. J., M. D. Kaminski, et al. (2005). "In vitro studies of functionalized magnetic nanospheres for selective removal of a simulant biotoxin." Journal of Magnetism and Magnetic Materials **293**(1): 572-577.

Missirlis, D., R. Kawamura, et al. (2006). "Doxorubicin encapsulation and diffusional release from stable, polymeric, hydrogel nanoparticles." European Journal of Pharmaceutical Sciences **29**(2): 120-129.

Morey, T. E., M. Varshney, et al. (2004). "Treatment of local anesthetic-induced cardiotoxicity using drug scavenging nanoparticles." Nano Letters **4**(4): 757-759.

Na, K., E. S. Lee, et al. (2003). "Adriamycin loaded pullulan acetate/sulfonamide conjugate nanoparticles responding to tumor pH: pH-dependent cell interaction, internalization and cytotoxicity in vitro." Journal of Controlled Release **87**(1-3): 3-13.

Nasongkla, N., E. Bey, et al. (2006). "Multifunctional polymeric micelles as cancer-targeted, MRI-ultrasensitive drug delivery systems." Nano Letters **6**(11): 2427-2430.

Newkome, G. R., Z. Q. Yao, et al. (1985). "Micelles .1. Cascade Molecules - a New Approach to Micelles - a [27]-Arborol." Journal of Organic Chemistry **50**(11): 2003-2004.

Nie, S. M., Y. Xing, et al. (2007). "Nanotechnology applications in cancer." Annual Review of Biomedical Engineering **9**: 257-288.

Papagiannaros, A., K. Dimas, et al. (2005). "Doxorubicin-PAMAM dendrimer complex attached to liposomes: Cytotoxic studies against human cancer cell lines." International Journal of Pharmaceutics **302**(1-2): 29-38.

Poznansky, M. J. and R. L. Juliano (1984). "Biological Approaches to the Controlled Delivery of Drugs: A Critical Review." Pharmacol Rev. **36**(4): 277-336.

Raffin, R. P., D. S. Jornada, et al. (2006). "Sodium pantoprazole-loaded enteric microparticles prepared by spray drying: Effect of the scale of production and process validation." International Journal of Pharmaceutics **324**(1): 10-18.

Rapoport, N., Z. G. Gao, et al. (2007). "Multifunctional nanoparticles for combining ultrasonic tumor imaging and targeted chemotherapy." Journal of the National Cancer Institute **99**(14): 1095-1106.

Ren, Y., S. M. Wong, et al. (2007). "Folic acid-conjugated protein cages of a plant virus: A novel delivery platform for doxorubicin." Bioconjugate Chemistry **18**(3): 836-843.

Reszka, R., P. Beck, et al. (1997). "Body distribution of free, liposomal and nanoparticle-associated mitoxantrone in B16-melanoma-bearing mice." Journal of Pharmacology and Experimental Therapeutics **280**(1): 232-237.

Robison, M. L. (2008, April 30, 2008). "Hard vs. Soft Water." from http://www.naturalhealthtechniques.com/BasicsofHealth/Water_files/waterhardvssoft.htm.

Sale, G., H. Darr, et al. (1988). Water purification process. http://www.freepatentsonline.com/4724079.html. United States.

Shchors, K. and G. Evan (2007). "Tumor angiogenesis: Cause or consequence of cancer?" Cancer Research **67**(15): 7059-7061.

Society, A. C. (2006). What are the different types of chemotherapy drugs?

Soma, C. E., C. Dubernet, et al. (2000). "Investigation of the role of macrophages on the cytotoxicity of doxorubicin and doxorubicin-loaded nanoparticles on M5076 cells in vitro." Journal of Controlled Release **68**(2): 283-289.

Soma, C. E., C. Dubernet, et al. (2000). "Reversion of multidrug resistance by co-encapsulation of doxorubicin and cyclosporin A in polyalkylcyanoacrylate nanoparticles." Biomaterials **21**(1): 1-7.

Soppimath, K. S., T. M. Aminabhavi, et al. (2001). "Biodegradable polymeric nanoparticles as drug delivery devices." Journal of Controlled Release **70**(1-2): 1-20.

Stolnik, S., L. Illum, et al. (1995). "Long circulating microparticulate drug carriers." Advanced Drug Delivery Reviews **16**(2-3): 195-214.

Svenson, S. and D. A. Tomalia (2005). "Commentary - Dendrimers in biomedical applications - reflections on the field." Advanced Drug Delivery Reviews **57**(15): 2106-2129.

Tang, N., G. J. Du, et al. (2007). "Improving penetration in tumors with nanoassemblies of phospholipids and doxorubicin." Journal of the National Cancer Institute **99**(13): 1004-1015.

Tewa-Tagne, P., S. Briancon, et al. (2006). "Spra-dried microparticles containing polymeric nanocapsules: Formulation aspects, liquid phase interactions and particles characteristics." International Journal of Pharmaceutics **325**(1-2): 63-74.

Tewes, F., E. Munnier, et al. (2007). "Comparative study of doxorubicin-loaded poly(lactide-co-glycolide) nanoparticles prepared by single and double emulsion methods." European Journal of Pharmaceutics and Biopharmaceutics **66**(3): 488-492.

Tian, Y., L. Bromberg, et al. (2007). "Complexation and release of doxorubicin from its complexes with pluronic P85-b-poly(acrylic acid) block copolymers." Journal of Controlled Release **121**: 137-145.

Tomalia, D. A., H. Baker, et al. (1985). "A new class of polymers - starburst-dendritic Macromolecules." Polymer Journal **17**(1): 117-132.

Ubrich, N., P. Bouillot, et al. (2004). "Preparation and characterization of propranolol hydrochloride nanoparticles: a comparative study." Journal of Controlled Release **97**(2): 291-300.

Varshney, M., T. E. Morey, et al. (2004). "Pluronic microemulsions as nanoreservoirs for extraction of bupivacaine from normal saline." Journal of the American Chemical Society **126**(16): 5108-5112.

Verdun, C., F. Brasseur, et al. (1990). "Tissue Distribution of Doxorubicin Associated with Polyisohexylcyanoacrylate Nanoparticles." Cancer Chemotherapy and Pharmacology **26**(1): 13-18.

Wang, J., Y. Tabata, et al. (2006). "Aminated gelatin microspheres as a nasal delivery system for peptide drugs: Evaluation of in vitro release and in vivo insulin absorption in rats." Journal of Controlled Release **113**(1): 31-37.

Warren, R., K. D. Ertel, et al. (1996). "The influence of hard water (calcium) and surfactants on irritant contact dermatitis." Contact Dermatitis **35**(6): 337-343.

Wissing, S. A., O. Kayser, et al. (2004). "Solid lipid nanoparticles for parenteral drug delivery." Advanced Drug Delivery Reviews **56**(9): 1257-1272.

Wong, H. L., R. Bendayan, et al. (2007). "Chemotherapy with anticancer drugs encapsulated in solid lipid nanoparticles." Advanced Drug Delivery Reviews **59**(6): 491-504.

Wong, H. L., R. Bendayan, et al. (2004). "Development of solid lipid nanoparticles containing lonically complexed chemotherapeutic drugs and chemosensitizers." Journal of Pharmaceutical Sciences **93**(8): 1993-2008.

Wong, H. L., A. M. Rauth, et al. (2006). "A new polymer-lipid hybrid nanoparticle system increases cytotoxicity of doxorubicin against multidrug-resistant human breast cancer cells." Pharmaceutical Research **23**(7): 1574-1585.

Yadav, A. K., P. Mishra, et al. (2007). "Development and characterization of hyaluronic acid-anchored PLGA nanoparticulate carriers of doxorubicin." Nanomedicine-Nanotechnology Biology and Medicine **3**: 246-257.

Yang, C. Y., C. C. Chang, et al. (2006). "Calcium and magnesium in drinking water and risk of death from acute myocardial infarction in Taiwan." Environmental Research **101**(3): 407-411.

Yang, H. and W. Y. J. Kao (2006). "Dendrimers for pharmaceutical and biomedical applications." Journal of Biomaterials Science-Polymer Edition **17**(1-2): 3-19.

Yang, J., E. J. Cho, et al. (2008). "Enhancement of cellular binding efficiency and cytotoxicity using polyethylene glycol base triblock copolymeric nanoparticles for targeted drug delivery." Journal of Biomedical Materials Research Part A **84A**: 273-280.

Yang, Y. Y., Y. Wang, et al. (2006). "Polymeric core-shell nanoparticles for therapeutics." Clinical and Experimental Pharmacology and Physiology **33**(5-6): 557-562.

Yi, Y. W., J. H. Kim, et al. (2005). "A polymeric nanoparticle consisting of mPEG-PLA-Toco and PLMA-COONa as a drug carrier: Improvements in cellular uptake and biodistribution." Pharmaceutical Research **22**(2): 200-208.

Yokoyama, M. (2005). "Drug targeting with nano-sized carrier systems." J. Artif. Organs **8**(2): 77-84.

Yoo, H. S., J. E. Oh, et al. (1999). "Biodegradable nanoparticles containing doxorubicin-PLGA conjugate for sustained release." Pharmaceutical Research **16**(7): 1114-1118.

Yu, J. J., H. A. Lee, et al. (2007). "Bio-distribution and anti-tumor efficacy of PEG/PLA nano particles loaded doxorubicin." Journal of Drug Targeting **15**(4): 279-284.

Yun, Y. H., D. J. Goetz, et al. (2004). "Hyaluronan microspheres for sustained gene delivery and site-specific targeting." Biomaterials **25**(1): 147-157.

Zhang, J., X. G. Chen, et al. (2007). "Self-assembled nanoparticles based on hydrophobically modified chitosan as carriers for doxorubicin." Nanomedicine-Nanotechnology Biology and Medicine **3**: 258-265.

Zhang, J. and R. D. K. Misra (2007). "Magnetic drug-targeting carrier encapsulated with thermosensitive smart polymer: Core-shell nanoparticle carrier and drug release response." Acta Biomaterialia **3**: 838-850.

Chapter 2

Ion Complexation of DoxHCl With Anionic Sulfates and Potential Encapsulation of These Hydrophobic Complexes Into Nanoparticles

2.1 Abstract

The purpose of this study was to synthesize hydrophobic complexes of doxorubicin hydrochloride (doxHCl) with a series of alkyl sulfates via ionic interactions to enhance drug encapsulation into hydrophobic polymeric core of nanoparticles. Doxorubicin/alkyl sulfate complexes were prepared through different mixing methods and characteristics such as aqueous solubility, partitioning between methylene chloride and phosphate-buffered saline (PBS) phases, and cell cytotoxicity relative to doxHCl were analyzed. Attempts were made to encapsulate these novel drug complexes into polymeric nanoparticles using either solid-in-oil-in-water (S/O/W) or modified water-in-oil-in-water (W/O/W) methods. Results showed that hydrophobic drug complexes had reduced aqueous solubility and increased methylene chloride/PBS partition coefficient relative to doxHCl and cell cytotoxicity against K562 leukemia cells were similar for drug complexes relative to doxHCl based on EC_{50} measurements. However, subsequent attempts to encapsulate drug complexes into polymeric nanoparticles using S/O/W or modified W/O/W emulsions failed as the complexes did not dissolve in organic solvents commonly used for nanoparticle preparation and the amphiphilic nature of alkyl sulfates actually may have promoted drug loss from nanoparticles. Based on these results, more hydrophobic alkyl sulfates or new classes of lipophilic anions need to be utilized for ion compexation or ion pairing with doxHCl to promote nanoparticle encapsulation.

2.2 Introduction

Doxorubicin hydrochloride (doxHCl) is a widely used anticancer chemotherapeutic belonging to a family of anticancer drugs known as anthracyclines.

This drug is made up of fused rings linked to a sugar moiety with an attached amine group with a pKa of 8.2 (Fig. 2.1). Since FDA approval in the 1970s, this drug has been successfully used to treat a range of cancers including various leukemias, breast cancer, ovarian cancer, various lymphomas, etc. (Information; Langer and Folkman 1976; Beijnen 1991). Despite its potent activity, doxHCl has a number of disadvantages including short plasma circulation half-life, long elimination half-life, and nonspecific cell-cytotoxicity. These shortcomings can lead to dose-limiting side effects including cardiomyopathy and myelosuppression (Abraham, Waterhouse et al. 2005; Kang, Cheon et al. 2006).

One way to overcome these problems is to encapsulate doxHCl in drug carriers; ones that have been experimentally tested include polymer micelles (Kataoka, Matsumoto et al. 2000; Lee, Na et al. 2005), polymeric nanoparticles (Yoo, Oh et al. 1999; Soma, Dubernet et al. 2000; Yoo, Lee et al. 2000), liposomes (Medina 2004; Abraham, Waterhouse et al. 2005), microspheres (Defail 2006; Missirlis, Kawamura et al. 2006), and hydrogels (Kang, Cheon et al. 2006). Use of depot formulations such as microspheres and hydrogels can reduce toxic side effects while providing extended drug release that may last up to months. Use of nanoparticulate carriers such as polymeric micelles, polymeric nanoparticles and liposomes to deliver doxHCl can confer additional advantages such as prolonged circulation half-life and increased accumulation in tumors due to EPR (enhanced permeation and retention) effect, where the leaky vasculature and poor lymphatic drainage around tumors improve drug retention.

Polymeric nanoparticles have gained considerable attention due to their ease of production, stability, optimal size distribution, increased hydrophobic drug loading and controlled/extended drug delivery potential through the use of different polymer(s) (Jeong, Cheon et al. 1998; Kataoka, Matsumoto et al. 2000; Yokoyama 2005). DoxHCl delivery to tumors could also benefit from the aforementioned attributes, however, due to its hydrophilicity, previous studies of doxHCl loading into nanoparticles have shown problems such as low encapsulation efficiency and loading into nanoparticles and burst release within a few hours after administration leading to significant drug loss and potential toxicity. To improve doxHCl loading into and release from polymeric nanoparticles, scientists have utilized strategies such as chemical conjugation of

doxorubicin to hydrophobic polymers (Yoo, Oh et al. 1999; Yoo, Lee et al. 2000) and chemical conversion of doxHCl into its free base (hydrophobic) form through a chemical reaction with triethylamine (TEA) (Kataoka, Matsumoto et al. 2000; Gao, Lee et al. 2005; Missirlis, Kawamura et al. 2006).

In this study, a simple process known as hydrophobic ion pairing (HIP), where a drug of interest is electrostatically paired with oppositely charged ionic molecule, will be used to modify doxorubicin hydrochloride into a new hydrophobic complex in order to improve drug loading into and release from polymeric nanoparticles. Here, alkyl sulfates such as sodium dodecyl sulfate are complexed with doxHCl; these sulfates have a negative sulfate group for pairing with cationic protonated amine group of doxHCl while a hydrophobic carbon chain may confer hydrophobicity to the complexes synthesized. Properties of the new complexes, such as solubility, partition coefficient, NMR-deduced structure and cell cytotoxicity will be compared to doxorubicin hydrochloride. Lastly, these complexes will be formulated into nanoparticles and loading and release determination. This strategy will be simpler than the aforementioned strategies for improving drug loading and release and hydrophobic drug complexes may prove to be more potent than the original doxHCl against cancer cells.

2.3 Materials and Methods

2.3.1 Materials

Sodium octyl sulfate (95% purity), sodium dodecyl sulfate (>98% purity), sodium tetradecyl sulfate (95% purity), and sodium octadecyl sulfate (93% purity), were purchased from Sigma-Aldrich. Doxorubicin hydrochloride (doxHCl) (>99% purity, lyophilized powder) was purchased from Hisun Pharmaceuticals (China). Poly(D,L-lactide-*co*-glycolide), 50/50, with inherent viscosity of 0.34 dL/g and MW_w of 38 kDa (resomer 503H) was purchased from Boehringer Ingelheim, and inherent viscosity of >1 dL/g (high IV, end-capped) was purchased from Alkermes. Poly(vinyl alcohol) (PVA) of MW_w of 25 kDa (88% hydrolyzed) was purchased from Polysciences Inc. Deuterated methanol (>99% purity) was purchased from Cambridge Isotope Laboratories. All other

chemicals and solvents were of analytical grade or higher and purchased from commercial suppliers.

K562 cells were a generous gift from Dr. Gustavo Rosania (University of Michigan). RPMI 1640 with and without L-glutamine and pencillin/streptomycin were purchased from Gibco Inc. Fetal serum albumin, heat-inactivated, and Vybrant® MTT cell proliferation assay kit were purchased from Invitrogen®. Costar 96 well round bottom cell culture plates, sterile, was purchased from Fisher Scientific. All other materials used for cell assays were sterile grade.

2.3.2 Doxorubicin complex synthesis

2.3.2.1 Sodium octyl sulfate/doxHCl (doxSOS): 1.1:1 molar ratio of SOS and doxHCl were dissolved in 2 mL of 5 mM sodium citrate buffer, pH 4. 2 mL of methylene chloride was added into the buffered solution followed by vortex mixing. The mixture was shaken for 1 hour on a shaker plate (Ika KS130) at 200 shakes/min followed by centrifugation at 5,000 RPM for 10 minutes. Aqueous phase was collected and spun down at 13,200 RPM for 6 minutes to collect the drug complex precipitate. The precipitate was washed twice with deionized water (DIW) and lyophilized.

2.3.2.2 Sodium dodecyl sulfate/doxHCl (doxSDS): 0.95:1 molar ratio of SDS and doxHCl were each dissolved in 2 mL of DIW. The SDS solution was slowly titrated into the doxHCl solution and red precipitate formed immediately. The precipitate was collected by centrifugation at 13,200 RPM for 6 minutes and washed twice with DIW followed by lyophilization.

2.3.2.3 Sodium tetradecyl sulfate/doxHCl (doxSTS): 0.95:1 molar ratio of STS and doxHCl was used. STS was dissolved in 0.1 mL of methanol and doxHCl was dissolved in 5 mL of DIW. STS solution was slowly titrated into the doxHCl solution and red precipitate formed immediately. The precipitate was collected by centrifugation at 13,200 RPM for 6 minutes and washed twice with DIW followed by lyophilization.

2.3.2.4 Sodium octadecyl sulfate/doxHCl (doxSODS): 0.95:1 molar ratio of SODS and doxHCl was used. SODS was suspended in 0.1 mL of methanol (suspension with white powder) and homogenized by sonication in a sonicating waterbath. DoxHCl was dissolved in 6 mL of DIW. SODS suspension was added into the doxHCl solution and red precipitate formed immediately. The precipitate was collected by centrifugation at 13,200 RPM for 6 minutes and washed twice with DIW followed by lyophilization.

2.3.3 NMR analysis of complexes

DoxHCl and the four drug complexes synthesized were weighed out and dissolved in 0.75 mL of methanol-D^4. The five samples were analyzed using Bruker Avance DRX 500.

2.3.4 HPLC analysis of doxHCl concentration

A Waters HPLC system (Waters, Milford, MA) was used for chromatographic separation of doxHCl. It consisted of a 1525 Binary HPLC pump, 717 plus autosampler, and 474 scanning fluorescence detector. Waters Breeze® chromatography software was used to acquire and process data. A Waters Nova-Pak® C_{18} column (3.9 x 150 mm I.D.) (Waters, Milford, MA) was used with a filtered and degassed ACN : 20 mM, pH 3 potassium phosphate : TFA (30:70:0.1, v/v/v) mobile phase. Chromatography was performed at a flow rate of 1 ml/min and fluorescence detection was set at $\lambda_{excitation}$ of 480 nm and $\lambda_{emission}$ of 590 nm at room temperature.

DoxHCl in the samples were identified by comparing retention time with corresponding standards injected separately.

2.3.5 Drug complex solubility determination

Excess amounts of doxHCl or doxorubicin/sulfate complexes were incubated in either phosphated-buffered saline (PBS) or deionized water (DIW) at 37^{o}C with shaking (200 shakes/min) for 12 hours. Samples were centrifuged at 13,200 RPM for 5 min after incubation and supernatant was collected and analyzed for doxHCl concentration by HPLC.

2.3.6 Partition coefficient measurements

The partition coefficients of doxorubicin/sulfate complexes were determined in methylene chloride/phosphate-buffered saline (PBS) mixture at 37°C. Doxorubicin/sulfate complexes were weighed and dissolved in methylene chloride at a concentration of 5 µg/ml. Equal volume of PBS was added to each drug complex solution followed by vortex mixing and shaking (200 shakes/min) for 24 hour at 37°C to reach equilibrium. DoxHCl concentration in PBS, after partitioning, was determined by HPLC assay. Partition coefficients were calculated as follows:

$$Partition\ Coefficient_{\ pbs\ /\ mc} = \frac{Conc_{\ pbs}}{Conc_{\ mc} - Conc_{\ pbs}}$$

2.3.7 In vitro experiments

2.3.7.1 Cell culture

K562 cells were maintained in tissue culture medium (RPMI 1640 supplemented with 10% FBS and 1% penicillin/streptomycin at 37°C with 5% CO_2). Experiments were done with cells in logarithmic growth phase (0.2-1 x 10^6 cells/mL)

2.3.7.2 Cell viability experiment

Cytotoxicity of doxHCl and various doxorubicin/sulfate complexes were determined using the MTT cell proliferation assay. Briefly, drug solutions at various concentrations (0, 0.01, 0.1, 0.25, 0.5, 1, 10, and 100 µg/ml), each containing 200,000 cells/mL, were made by spiking concentrated drug solutions in methanol into RPMI solutions containing 200,000 cells/ml to reach the desired drug concentration. Samples were plated at 100 µL/well (20 K cells/well; n = 5) and incubated 48 hours at 37°C and 5% CO_2, before starting MTT cytotoxicity assay to determine cell viability. Standard curve of various cell concentrations (25,000, 50,000, 100,000, 200,000, and 400,000 cell/mL) were made for the 48 hour incubation samples and methanol was added to cell

solutions at each concentration to ensure same volume ratio of methanol/RPMI relative to drug solutions. Results were expressed in terms of EC_{50} (μg/mL or μM of doxHCl or doxorubicin complex) as determined from dose-response curves and defined as the concentration of drug complex that produced a 50% reduction in cell viability compared to doxHCl. Sigmoidal dose-response curves were fit to the data using SigmaPlot (Systat Software Inc.) and used to compute EC_{50} for each experiment.

2.3.8 Nanoparticle formulation procedure

2.3.8.1 Solid-in-oil-in-water (S/O/W) emulsion formulation

Drug complex precipitates were encapsulated into nanoparticles via S/O/W emulsion/solvent evaporation procedure. Different amounts of solid drug were weighed and suspended in 2 mL methylene chloride (containing 80 mg dissolved polymer) and sonicated (60 seconds) on ice using a probe sonicator (Sonics VibraCell) at 100% power. The S/O suspension was further emulsified in 4 mL 3% PVA solution by sonication (60 seconds) on ice using a probe sonicator (Sonics VibraCell) at 100% power. The S/O/W emulsion was diluted into 80 mL of 1% PVA solution under rapid magnetic stirring for 4-5 hours. Nanoparticle suspensions were collected and dialyzed (Spectra/Por 7, MWCO: 50,000) to remove unencapsulated drug.

2.3.8.2 Modified water-in-oil-in-water (W/O/W) formulation

Drug-loaded nanoparticles were formulated using a water-in-oil-in-water (W/O/W) emulsion/solvent evaporation procedure. DoxHCl was dissolved in 0.3 ml deionized water (DIW) at predetermined concentration and emulsified, in a mixture of 1.9 ml methylene chloride with 80 mg dissolved polymer and 0.1 ml methanol with 1 mg SOS, by sonication (60 seconds) on ice using a probe sonicator (Sonics VibraCell) at 100% power. The primary emulsion (W/O) was further emulsified in 4 mL 3% PVA solution by sonication (30 seconds) on ice using a probe sonicator (Sonics VibraCell) at 100% power. The W/O/W emulsion was diluted into 80 mL 1% PVA solution under rapid magnetic

stirring for 4-5 hours. Nanoparticle suspensions were collected and dialyzed (Spectra/Por 7, MWCO: 50,000) to remove PVA and unencapsulated drug.

2.3.9 Drug loading determination

Briefly, drug-loaded nanoparticles were lyophilized and weighed into 2 mL polypropylene tubes. 0.1 mL methylene chloride was added to nanoparticles, followed by shaking for 10 minutes, then addition of 1.5 mL methanol and shaking for over 12 hours. These suspensions were spun down at 13,200 RPM for 8 min. Supernatant containing dissolved drug was diluted as appropriate using methanol. Drug concentration was analyzed using UV doxHCl concentration determination.

For UV analysis, a Beckman DU650 spectrophotometer was used. Samples or standards containing doxHCl were analyzed using a quartz spectrophotometer cell (Starna Cells Inc.) at a scanning rate of 1200/min and scanning range of 400-750 nm. Absorbance wavelength was set at 480 nm and all samples had baseline reading set at 750 nm.

2.3.10 Nanoparticle physical characterization

2.3.10.1 Particle size/zeta potential determination

Nanoparticle suspensions were diluted to 0.5 mg/mL and transferred into fold capillary cells for both zeta potential and particle size determination. Samples were analyzed using a Malvern ZetaSizer Nano ZS (Malvern Instruments).

2.3.10.2 SEM morphological analysis

Nanoparticle suspensions were diluted to 50 µg/mL and dried overnight on viewing stubs. Morphology was observed by scanning electron microscopy (Philips XL30 Field Emission Gun Scanning Electron Microscopy).

2.4 Results and Discussion

2.4.1 Doxorubicin complex synthesis

Many attempts have been made to increase doxorubicin hydrochloride (doxHCl) loading into nanoparticles. However, because of its hydrophilicity (>10 mg/ml solubility in deionized water), doxHCl loss during formulation and low drug loading/encapsulation efficiency were common. To improve doxHCl loading, a potentially effective strategy was formation of hydrophobic drug complexes through pairing with lipophilic anions and encapsulation of these complexes in nanoparticles. Here, we have tested a series of anionic sulfates (Table 2.1) for this strategy. The sulfates had increasing hydrophobicity based on theoretical logP values and structure; they were amphiphilic with a hydrophobic carbon chain and hydrophilic charged sulfate group. Formation of ion complexes between sulfates and doxHCl (Fig. 2.1) could neutralize charged portions of both molecules to form a hydrophobic ion pair.

Based on complex preparation conditions, ion pairing was the dominant interaction between sulfate and doxHCl molecules. This was shown when molar ratios of 1.1:1, 0.95:1, and 0.95:1 between SDS:doxHCl, STS:doxHCl, and SODS:doxHCl, respectively, when mixed in water, formed red complex precipitates and left no visible trace of dissolved drug in solution (dissolved doxHCl in water gave a red solution while very little or no drug gave a colorless solution). Of the 4 complexes tested, doxSOS complex was the least stable (highest aqueous solubility) and hardest to form in large quantities while formation of other complexes occurred readily (within seconds of mixing) and completely (almost all the dissolved drug had form precipitates with sulfates). This was reasonable considering sodium octyl sulfate was the most water-soluble of the four sulfates and the short alkyl chain (8 carbons) was not enough to impart the desired levels of hydrophobicity.

2.4.2 Drug complex characterization

2.4.2.1 NMR analysis

DoxHCl and its hydrophobic sulfate complexes were dissolved in deuterated methanol and analyzed. Despite subtle differences, the NMR spectrum of doxHCl (Fig.

2.2) obtained here was similar to previously reported spectrum (Xu, Yang et al. 2005). Overlay of the different spectra (Fig. 2.2) showed characteristic peaks associated with doxHCl (bottom-most spectrum) and sulfate detergents. Even though characteristic peaks of anionic sulfates and doxHCl were observed, there was no peak shift for any doxHCl peaks upon complexation with sulfates, which was surprising.

Normally, changes in the polarity of hydrogen atoms, caused by events such as ion complexation or chemical conjugation, would lead to a shift of the corresponding NMR hydrogen peak. Here, even though ion complexation occurred between protonatable amine group of doxorubicin and anionic sulfates, there was no peak shift for the amine hydrogens of doxorubicin. A potential explanation has to do with methanol solvent used for NMR analysis. Since methanol molecules were polar with numerous hydroxyl groups, they could cause dissociation of the drug complexes dissolved in it and form cages where its hydroxyl groups surround and stabilize the lone charges.

Even though empirical evidence demonstrated the formation of hydrophobic drug/sulfate complexes, NMR spectra did not directly prove this observation.

2.4.2.2 Solubility of doxorubicin sulfate complexes

Solubility of doxorubicin sulfate complexes was compared to that for doxHCl (Table 2.2) to ensure the complexes were more hydrophobic. Drug complexes and doxHCl were dissolved in either deionized water (DIW) or phosphate-buffered saline (PBS), with salt composition and concentrations that mimicked physiological fluids.

In PBS, doxSOS solubility was about 30% of doxHCl solubility while doxSDS and doxSODS had about 3% of doxHCl solubility. Surprisingly, doxSTS, not doxSODS, had the lowest PBS solubility at about 1.5% of doxHCl solubility, or 66.7 times lower aqueous solubility. In DIW, differences in solubility were even more pronounced. Using a reported doxHCl solubility value of greater than 17.24 mM in deionized water, doxSOS solubility was 7.5% that of doxHCl solubility, doxSDS solubility was 1.7% that of doxHCl solubility, while doxSTS and doxSODS had the lowest solubility at only 0.6% of doxHCl solubility. Overall, solubility trends in both PBS and DIW were not surprising as doxSOS complexes were the hardest to synthesize under aqueous conditions while other complexes formed readily. DoxSTS and doxSODS were expected to have the lowest

aqueous solubility due to longer alkyl chain lengths (14 and 18 carbons, respectively), although it was uncertain why doxSTS, not doxSODS, had the lowest solubility in PBS; however, because PBS solubilities of doxSTS and doxSODS were very low to begin with, a solubility difference of 1.5% was not significant and could simply be due to experimental error.

Solubility of the complexes could take two forms, they could either dissolve as a whole complex in either DIW or PBS, which was minimal due to its hydrophobicity, or the complexes may dissociate in the presence of counterions in PBS and each component would on its own. With this in mind, in the presence of PBS, doxHCl and doxSOS solubilities were 5-10 times lower than corresponding solubilities in DIW (no salt present) while doxSDS, doxSTS, and doxSODS showed slightly higher solubilities in PBS than in DIW. Higher DIW solubility for doxHCl, relative to that in PBS, matched previously known information which suggested they may crash out of solutions at high salt concentrations (PBS). Because doxSOS was the most hydrophilic drug complex with properties most similar to doxHCl, its dissolution in DIW was also expected to be greater than in PBS, where the complexes had a lower solubility and dissociation of the complex was limited by solubility of doxorubicin itself. For the other complexes, DoxSDS, doxSTS, and doxSODS, which had much lower DIW solubilities relative to that in PBS, the situation was actually reversed as the complexes had very low solubilities in both DIW and PBS due to their hydrophobicity and the ability of the complexes to dissociate in PBS actually led to higher solubilities.

In all, these results suggested doxSDS, doxSTS, and doxSODS had significantly improved hydrophobicity over doxHCl, unlike doxSOS.

2.4.2.3 Partition coefficient measurements

Another important property of drug complexes was their partitioning between aqueous and organic phases. For this study, PBS was chosen as the aqueous phase to mimic drug release into physiological compartments, while methylene chloride, a solvent commonly used to formulate nanoparticles and encapsulate drugs, was chosen as the organic phase. The four doxorubicin sulfate complexes were dissolved in methylene chloride and equilibrated with equal volume of PBS to determine drug concentration and

partition coefficient. DoxHCl, with negligible solubility in methylene chloride and drastically higher PBS solubility, was not studied.

Results (Table 2.3) showed that doxSOS, with the highest aqueous solubility, had the lowest methylene chloride/PBS partition coefficient while doxSODS had the highest partition coefficient (more drug partitioning into methylene chloride phase). A surprising result was that doxSTS had lower partition coefficient relative to doxSDS, which should be less hydrophobic, and that doxSTS had partition coefficient of less than 1, indicating a higher drug concentration in the aqueous phase. This result was unexpected and may be due to experimental errors although it was also likely that actual properties of doxSTS may deviate from ones predicted based on their structure. Overall, though, the trend was as expected with doxSOS having much lower partitioning coefficients than the other three complexes.

Despite partition coefficients of >1, which indicated higher partitioning into methylene chloride phase and the potential for improved drug encapsulation and loading, a major problem encountered here was the low solubilities of the different hydrophobic complexes in methylene chloride (low µg/ml range, data not shown). This was a major limitation for traditional drug encapsulation strategies which required drug dissolution in organic solvents at high concentrations for significant drug loading.

2.4.3 *In vitro* cytotoxicity

To compare the cytotoxicity of doxorubicin complexes on cell viability relative to doxHCl, different amounts of doxHCl/doxorubicin complexes were administered to K562 lymphoma cells and then incubated in a drug-free medium for 48 hours. Cell viability after 48 hours was determined using MTT assay and compared to untreated controls. After 48 hours, sigmoidal dose-response curves were obtained (Fig. 2.3) for the different drugs and EC_{50} values for K562 cells were obtained (Table 2.4) based on these sigmoidal dose-response curves.

EC_{50} could be considered as the drug concentration where half of the initially incubated cells were killed after 48 hrs of incubation. On a molar basis, the values for the complexes were similar (Table 2.4) although they were slightly higher than that for doxHCl, which indicated the complexes had slightly lower efficacy relative to doxHCl

although it was not statistically significant. This result was reasonable considering doxHCl and doxorubicin complexes were administered to K562 cells at equivalent weight amounts, which meant there were less doxorubicin molecules administered in the form of hydrophobic complexes as the theoretical molecular weight of the complexes increased. Since doxorubicin molecules were the primary cytotoxic agents and the complexes required dissociation before doxorubicin can be released, it makes sense that the complexes have slightly lower cytotoxicity.

2.4.4 Solid-in-oil-in-water nanoparticle formulation

In this study, the ultimate goal was to load doxorubicin sulfate complexes into hydrophobic core of polymeric nanoparticles at high concentrations. However, initial studies found traditional emulsion/solvent evaporation strategies (O/W or W/O/W) were not useful because the drug complexes had low solubilities in methylene chloride, chloroform, and ethyl acetate (data not shown), organic solvents commonly used for nanoparticle formulation. An alternative formulation strategy utilized was solid-in-oil-in-water (S/O/W) technique (Bilati, Allemann et al. 2005). Using this strategy, large amounts of drug complex precipitates may be suspended in methylene chloride, and after intense sonication, their size may be reduced enough for encapsulation into polymeric nanoparticles (Fig. 2.4).

Initial observations of S/O/W nanoparticle emulsions containing doxSDS, doxSTS, or doxSODS showed relatively clear red suspensions (not shown) without large particles or aggregates. However, after sitting overnight, a thin layer of precipitates sedimented in the nanoparticle suspension, which does not occur normally with pure nanoparticle suspensions and indicated presence of micrometer (or larger) sized particles. Even though initial particle sizing data (not shown) showed a unimodal size distribution between 150-200 nm in diameter, SEM images of nanoparticle suspensions (Fig. 2.5) showed nanoparticles intermixed with large amounts of micrometer sized strands. This was the first time strands like these had been observed. Various attempts were made to separate the strands from nanoparticles using differential centrifugation (spinning down at different speed). However, the attempts failed and this formulation strategy was unsuccessful.

An initial hypothesis for the identity of these strands focused on drug complex precipitates. Because the complexes were sonicated in methylene chloride before encapsulation, their size may not have been reduced enough and ended up in the micrometer instead of nanometer size range. To test this hypothesis, blank nanoparticles (without drug complex addition) were formulated using the same S/O/W formulation procedure and SEM image (Fig. 2.6A) showed good nanoparticles without any strands. Another study, where only doxSODS precipitate was sonicated in blank methylene chloride, and then immediately viewed under SEM, showed drug complex strands in the micrometer size range (Fig. 2.6B). These results confirmed the hypothesis that drug complex precipitates hindered successful nanoparticle formulation and without a sonication device that produces significantly higher sonication power, an alternative formulation strategy was required.

2.4.5 Modified W/O/W nanoparticle formulation

Knowing that doxorubicin sulfate complexes could not reach nanometer size range via sonication with the device on hand and they had low solubility in a range of organic solvents, a possible alternative was to first dissolve doxHCl and sulfate molecules in different phases and form drug complex precipitates during nanoparticle formation. To facilitate this, a modified W/O/W nanoparticle formulation strategy could be employed (Fig. 2.4) with doxHCl dissolved in the inner aqueous phase and sulfates dissolved in the organic phase. Unfortunately, none of the four sulfates studied dissolve well in methylene chloride, chloroform, or ethyl acetate, solvents commonly used for nanoparticle formulation. To resolve this problem, a possible alternative solution was to dissolve the sulfates, at high concentrations, in another organic solvent miscible with methylene chloride and mix that with methylene chloride for nanoparticle formulation. The organic solvents tested for this were methanol, acetone, and acetonitrile.

Initial studies with STS and SODS had demonstrated poor solubilities in a number of organic solvents (not shown), so attention was focused on SOS and SDS. Results showed that between SDS and SOS and the three organic solvents tested, only SOS was soluble in methanol at a high concentration of >10 mg/ml (Table 2.5), so this combination was chosen to formulate W/O/W nanoparticles with doxHCl in the inner

aqueous phase and a combination of 1.9 ml methylene chloride with dissolved polymer and 0.1 ml methanol with dissolved SOS as the organic phase.

Nanoparticle emulsion was successfully formulated as clear red nanoparticle suspensions and no sedimentation was observed overnight. SEM images (Fig. 2.7) confirmed the observations as ~200 nm spherical nanoparticles were observed without the presence of micrometer sized strands. However, doxHCl loading determination for these nanoparticles, using ones without any SOS incorporation as control, showed similar values (Table 2.6) with SOS-loaded nanoparticles actually having slightly lower drug loading (1.36% vs. 1.41%) and encapsulation efficiency (23.0% vs. 23.2%). This result was very surprising considering SOS should stay in the polymer phase and provide additional anionic charges for ion pairing with doxorubicin to reduce their loss from nanoparticles. A possible explanation for this could be due to the nature of the anionic sulfates. These sulfates were amphiphilic in nature, and as a result, they may preferentially localize to the surface of nanoparticles where the hydrophobic carbon chain portion intercalate into the polymer core while the hydrophilic sulfate portion orient toward the outer aqueous phase. During nanoparticle hardening, organic solvent movement/escape into bulk aqueous phase may facilitate movement of dissolved sulfate molecules toward nanoparticle surface and because of ion pairing between sulfates and doxorubicin, this could lead to drug loss (Fig. 2.8).

2.5 Conclusions

To the best of our knowledge, this is the first time that doxorubicin hydrochloride has been modified into hydrophobic ion pair with small molecule alkyl sulfates for encapsulation into polymeric nanoparticles. Direct observations demonstrated drug complex formation while solubility and partition coefficient studies showed increasing hydrophobicity of these complexes. Doxorubicin sulfate complexes did not significantly change cell cytotoxicity (molar EC_{50} measurement) relative to free doxHCl, suggesting that it was the doxorubicin molecules, and not the complexes, that predominantly cause toxicity.

Despite improvements in hydrophobicity, low dissolution of the drug complexes in organic solvents commonly used for nanoparticle formulation precluded traditional

formulation strategies. Alternative nanoparticle formulation methods also encountered significant obstacles for drug complex loading or showed no improvements relative to existing processes.

The above information demonstrated several important things. First, anionic sulfates were not appropriate ion pairing agents because even though hydrophobic drug complexes could form easily, their limited solubility in organic solvents precluded successful encapsulation. Second, their hydrophobicity, even though improved, was still relatively low and perhaps more hydrophobic versions of the sulfate molecules (even longer carbon chain) or a whole new class of lipophilic anions may be used to further improve drug hydrophobicity and loading into nanoparticles. Third, even though micrometer sized strands were obtained and could not be used for nanoparticle formulation, these products may be effective for alternative purposes such as microsphere drug delivery and that could be an area for future studies.

Table 2. 1. Alkyl sulfates tested as hydrophobic ion pairing agents with doxorubicin hydrochloride

Anionic pairing agent	**Chemical formula**	**Molecular weight (g/mol)**	**CMC [1,2] (mM)**	**LogP [3]**
Sodium octyl sulfate (SOS)	$C_8H_{17}O_4SNa$	232.28	100	1.44
Sodium dodecyl sulfate (SDS)	$C_{12}H_{25}O_4SNa$	288.38	8	3.6
Sodium tetradecyl sulfate (STS)	$C_{14}H_{29}O_4SNa$	316.44	1.6	4.55
Sodium octadecyl sulfate (SODS)	$C_{18}H_{37}O_4SNa$	372.55	0.45	6.03

1. Colloids & Polymer Sci. 1984, 262: 657-661
2. Colloids & Polymer Sci. 1987, 265: 604-612
3. www.logp.com

Table 2. 2. Drug complex solubility data for various drug complexes and doxHCl after 12 hours of incubation

Drug or Drug Complex	Concentration (mM)	
	in PBS	in DIW
doxHCl	1.41 ± 0.01	ND [#]
doxSOS	0.41 ± 0.02	1.30 ± 0.30
doxSDS	0.039 ± 0.001	0.029 ± 0.002
doxSTS	0.014 ± 0.000	0.010 ± 0.001
doxSODS	0.044 ± 0.000	0.011 ± 0.001

[#] Solubility of doxorubicin HCl in water reportedly >10 mg/mL (17.24 mM)

Table 2. 3. Partition coefficients of doxorubicin hydrochloride from organic (methylene chloride) to an aqueous (PBS) phase at equilibrium

Drug Complex	**Partition Coefficient ($P_{MC/PBS}$ ± S.D.)**
doxSOS	0.33 ± 0.09
doxSDS	1.34 ± 0.41
doxSTS	0.82 ± 0.16
doxSODS	2.49 ± 0.26

Table 2. 4. EC_{50} values for doxHCl or drug complexes from 48 h dose-response curve (n = 5). Measurements were done using SigmaPlot software to find the best-fit curve

DoxHCl / Dox complex	**MW (g/mol)**	**EC_{50}-48 h (µg/ml ± Std. Err.)**	**EC_{50}-48 h (µM ± Std. Err.)**
doxHCl	580	0.12 ± 0.02	0.21 ± 0.03
doxSOS	812	0.27 ± 0.02	0.33 ± 0.03
doxSDS	868	0.28 ± 0.04	0.24 ± 0.03
doxSTS	896	0.21 ± 0.03	0.23 ± 0.04
doxSODS	953	0.27 ± 0.06	0.29 ± 0.07

Table 2. 5. Solubility of different sulfates in methanol, acetone, or acetonitrile (STS and SODS are known to have low solubility in these organic solvent)

Sulfate detergent	**Solvent**	**Solubility**
1 mg SDS	0.1 or 0.2 ml methanol	Insoluble
1 mg SDS	0.1 or 0.2 ml acetone	Insoluble
1 mg SDS	0.1 or 0.2 ml acetonitrile	Insoluble
1 mg SOS	0.1 or 0.2 ml acetone	Insoluble
1 mg SOS	*0.1 ml methanol*	*Soluble*

Table 2. 6. DoxHCl loading and encapsulation efficiency for nanoparticles with and without sodium octyl sulfate (SOS) in the oil phase ($n = 2$)

Nanoparticle sample	**Theoretical doxHCl loading (%)**	**Calculated doxHCl loading (%)**	**Encapsulation Efficiency (%)**
W/O/W-doxHCl	6.07	1.41	23.2
W/O/W-doxHCl and SOS	5.92	1.36	23.0

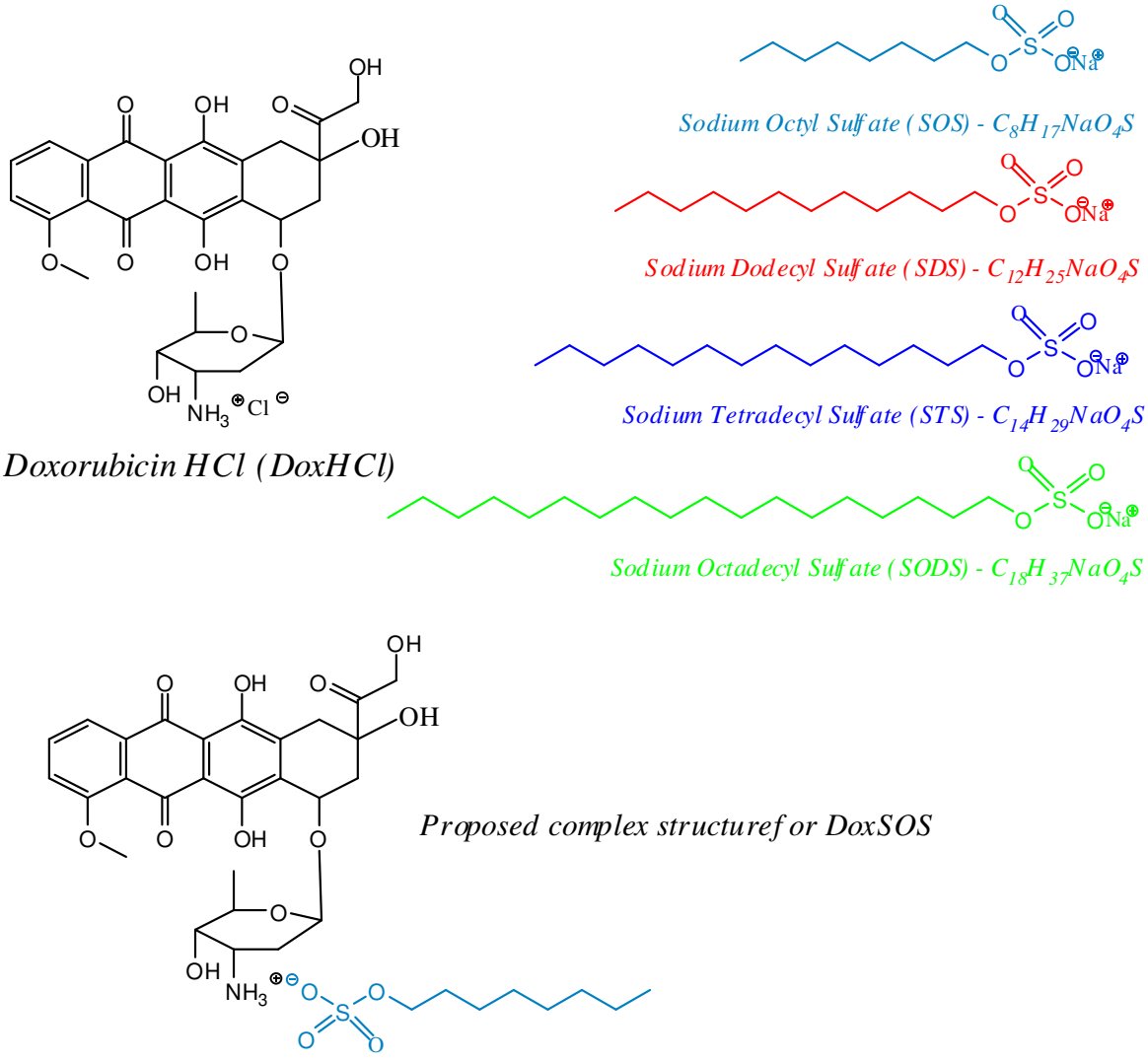

Figure 2. 1. Structures of doxorubicin hydrochloride and the 4 sulfate-based anions and a proposed structure of the complex formed.

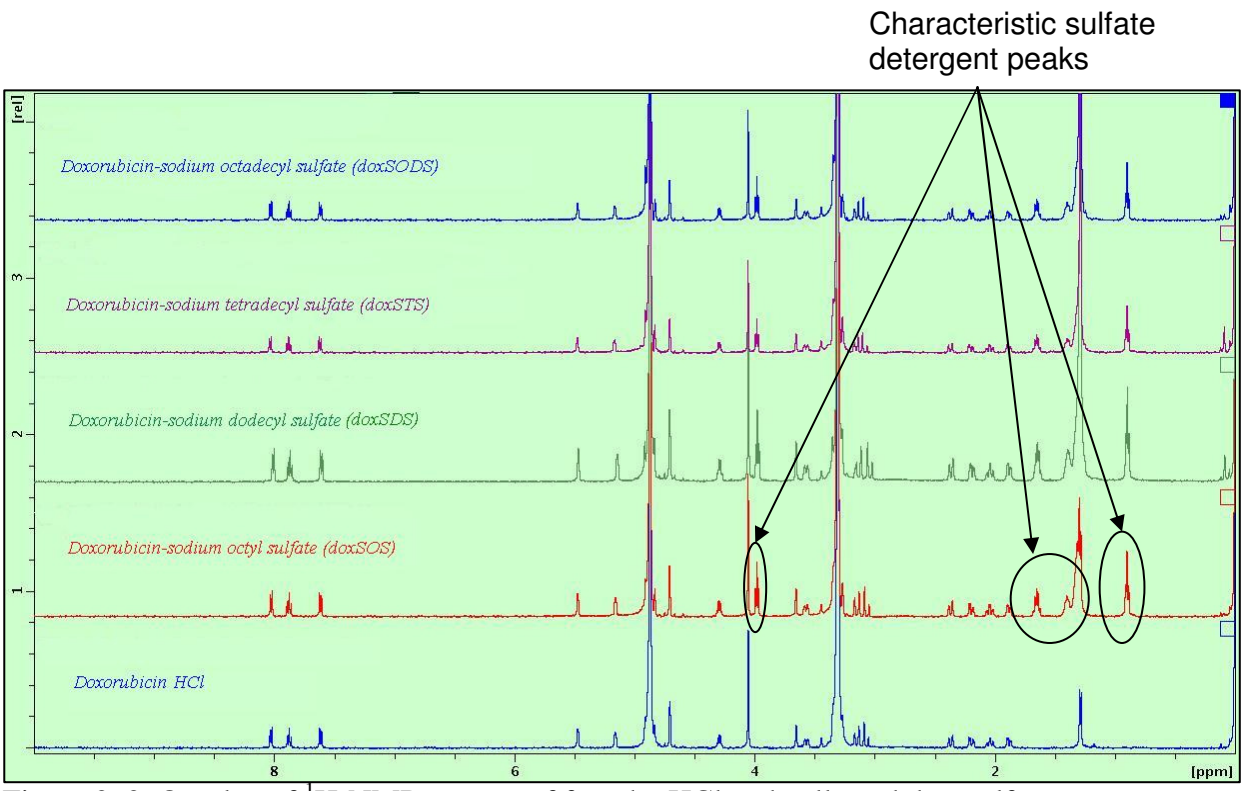

Figure 2. 2. Overlay of ^{1}H-NMR spectra of free doxHCl and collected dox-sulfate complexes in deuterated methanol (Bruker Avance DRX 500).

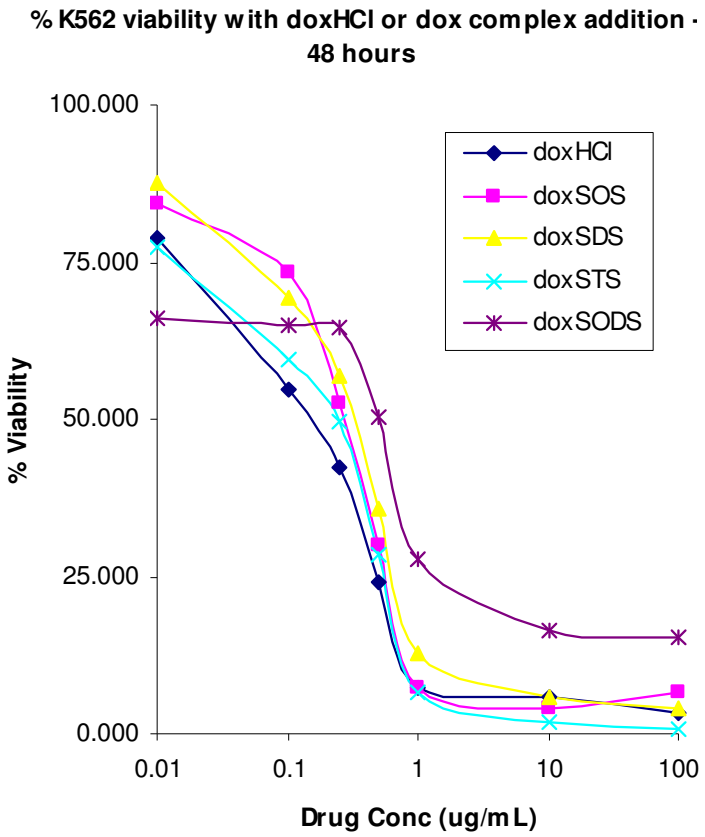

Figure 2. 3. Dose-response curve showing inhibition of growth of K562 cells by different doses of doxHCl and doxorubicin complexes.

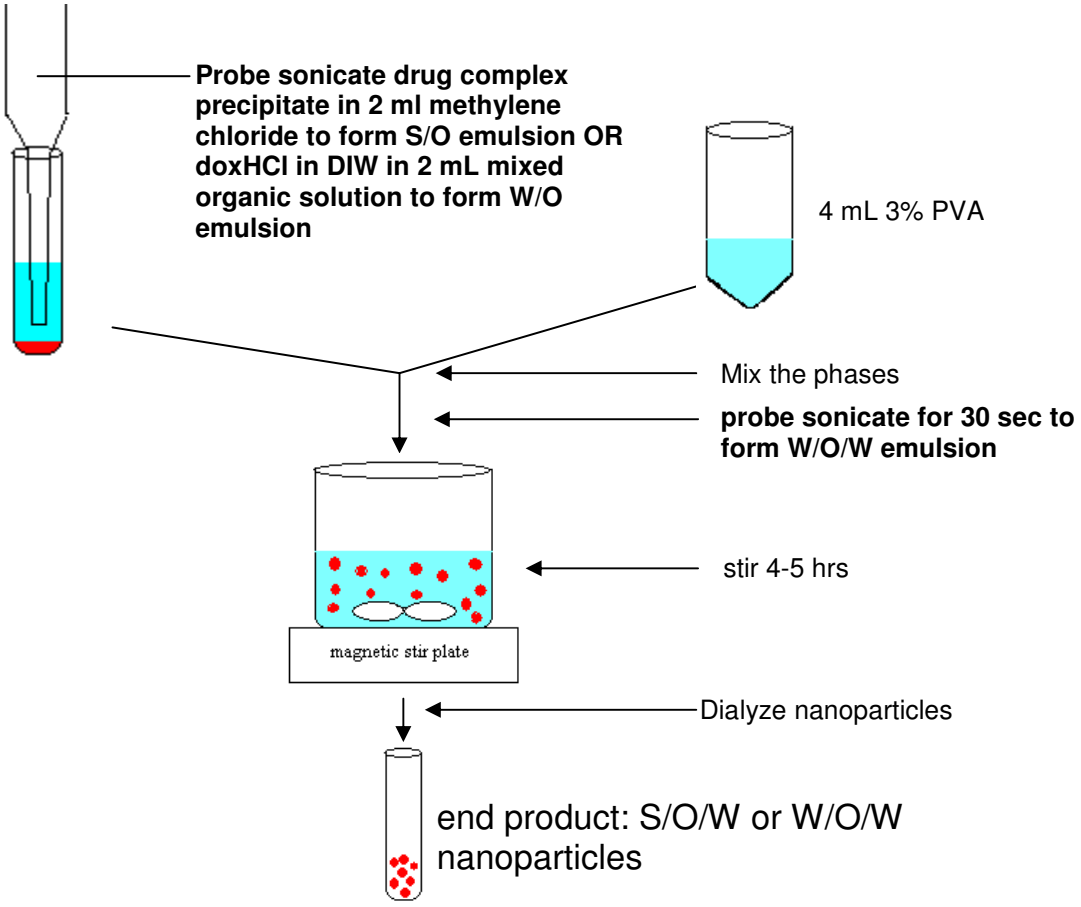

Figure 2. 4. Formulation procedure for S/O/W or W/O/W nanoparticles.

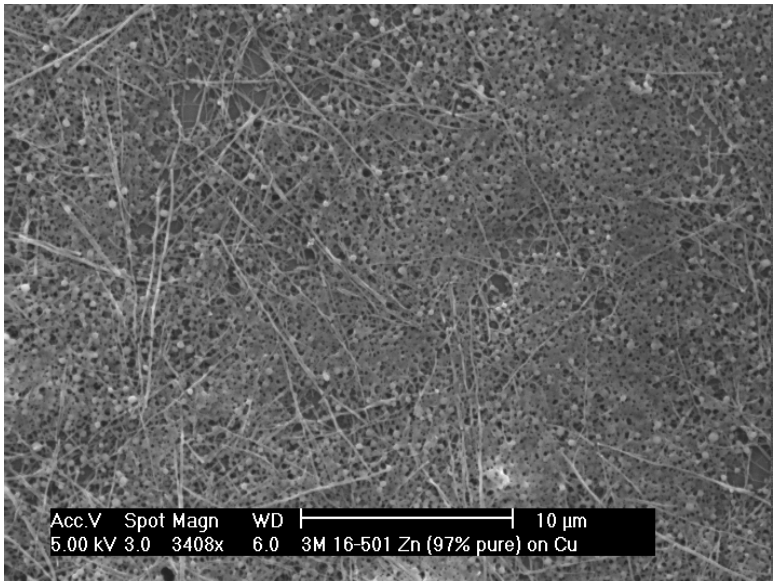

Figure 2. 5. Representative SEM image of S/O/W nanoparticles.

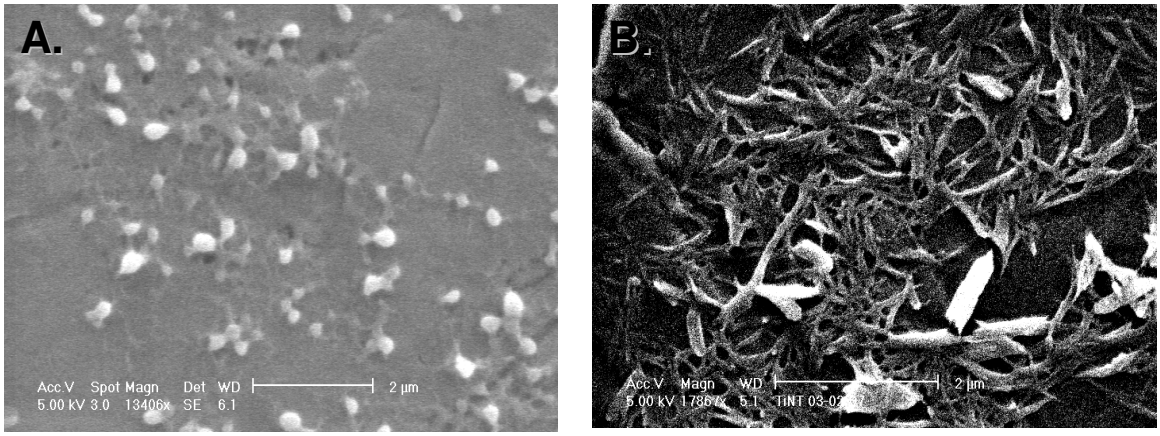

Figure 2. 6. SEM images of blank polymer nanoparticles without drug or sulfate encapsulation (A) and SODS sonicated in methylene chloride (B).

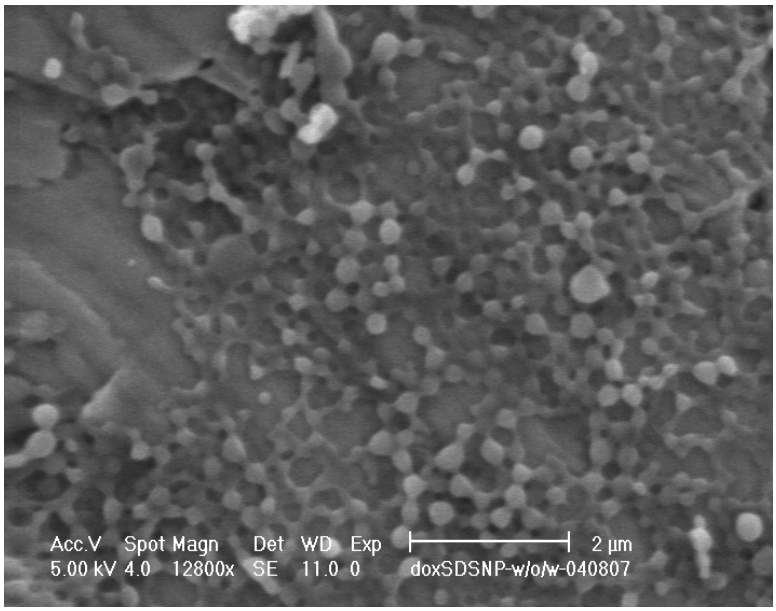

Figure 2. 7. SEM image of doxHCl and SOS-loaded W/O/W nanoparticles.

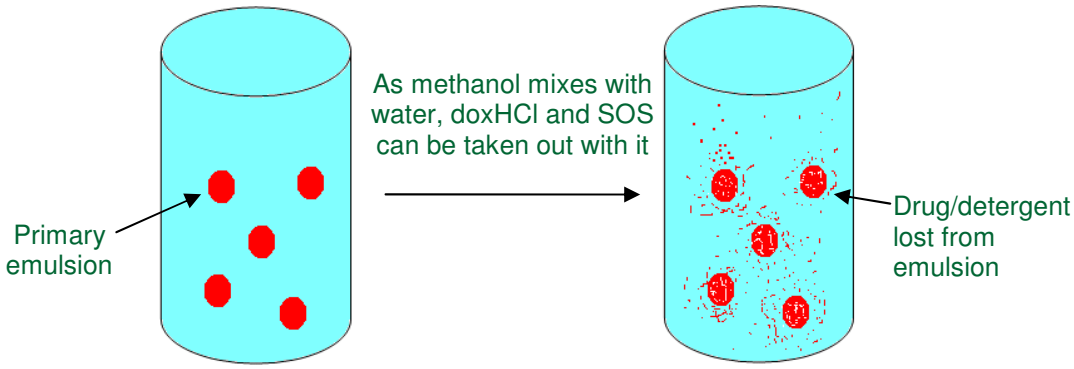

Figure 2. 8. Schematic drawing of potential doxHCl loss from nanoparticles during organic solvent evaporation.

List of references:

Abraham, S. A., D. N. Waterhouse, et al. (2005). The liposomal formulation of doxorubicin. Liposomes, Pt E. **391:** 71-97.

Beijnen, J. H., P.L. Meenhorst, R. Van Gijn, M. Fromme, H. Rosing, and W.J.M. Underberg (1991). "HPLC determination of doxorubicin, doxorubicinol and four aglycone metabolites in plasma of AIDS patients." Journal of Pharmaceutical & Biomedical Analysis **9**(10-12): 995-1002.

Bilati, U., E. Allemann, et al. (2005). "Nanoprecipitation versus emulsion-based techniques for the encapsulation of proteins into biodegradable nanoparticles and process-related stability issues." AAPS PharmSciTech **6**(4): E594-604.

Defail, A. J., H.D. Edington, S. Matthews, W.C. Lee, and K.G. Marra (2006). "Controlled release of bioactive doxorubicin from microspheres embedded within gelatin scaffolds." J. Biomed. Mater. Res. A.

Gao, Z. G., D. H. Lee, et al. (2005). "Doxorubicin loaded pH-sensitive micelle targeting acidic extracellular pH of human ovarian A2780 tumor in mice." Journal of Drug Targeting **13**(7): 391-397.

Information, A.-F. P. "Adriamycin-Full Prescribing Information." from www.meds.com/leukemia/idamycin/adriamycin.html.

Jeong, Y. I., J. B. Cheon, et al. (1998). "Clonazepam release from core-shell type nanoparticles in vitro." Journal of Controlled Release **51**(2-3): 169-178.

Kang, G. D., S. H. Cheon, et al. (2006). "Controlled release of doxorubicin from thermosensitive poly(organophosphazene) hydrogels." International Journal of Pharmaceutics **319**(1-2): 29-36.

Kataoka, K., T. Matsumoto, et al. (2000). "Doxorubicin-loaded poly(ethylene glycol)-poly(beta-benzyl-l-aspartate) copolymer micelles: their pharmaceutical characteristics and biological significance." Journal of Controlled Release **64**(1-3): 143-153.

Langer, R. and J. Folkman (1976). "Polymers for Sustained-Release of Proteins and Other Macromolecules." Nature **263**(5580): 797-800.

Lee, E. S., K. Na, et al. (2005). "Doxorubicin loaded pH-sensitive polymeric micelles for reversal of resistant MCF-7 tumor." Journal of Controlled Release **103**(2): 405-418.

Medina, O. P., Y. Zhu, and K. Kairemo (2004). "Targeted liposomal drug delivery in cancer." Current Pharmaceutical Design **10**: 2981-2989.

Missirlis, D., R. Kawamura, et al. (2006). "Doxorubicin encapsulation and diffusional release from stable, polymeric, hydrogel nanoparticles." European Journal of Pharmaceutical Sciences **29**(2): 120-129.

Soma, C. E., C. Dubernet, et al. (2000). "Investigation of the role of macrophages on the cytotoxicity of doxorubicin and doxorubicin-loaded nanoparticles on M5076 cells in vitro." Journal of Controlled Release **68**(2): 283-289.

Xu, X., L. Yang, et al. (2005). "Ultrafine medicated fibers electrospun from W/O emulsions." Journal of Controlled Release **108**(1): 33-42.

Yokoyama, M. (2005). "Drug targeting with nano-sized carrier systems." J. Artif. Organs **8**(2): 77-84.

Yoo, H. S., K. H. Lee, et al. (2000). "In vitro and in vivo anti-tumor activities of nanoparticles based on doxorubicin-PLGA conjugates." Journal of Controlled Release **68**(3): 419-431.

Yoo, H. S., J. E. Oh, et al. (1999). "Biodegradable nanoparticles containing doxorubicin-PLGA conjugate for sustained release." Pharmaceutical Research **16**(7): 1114-1118.

Chapter 3

Systematic Study of Important Variables in Absorption Drug Loading into Specially Formulated Ion-Pairing PLGA Nanoparticles Using Doxorubicin Hydrochloride as Model Drug

3.1 Abstract

An effective drug loading procedure should be simple and time-efficient to maximize drug loading or uptake; adsorption drug loading, when optimized, could provide an important tool to fulfill these requirements. With this in mind, the purpose of this study was fourfold. First, evaluate the ion pairing potential between borate-based lipophilic anions and a model cationic drug, doxorubicin hydrochloride (doxHCl), in organic solvents, to introduce attractive force for absorption loading. Second, formulate blank polymeric nanoparticles incorporating borate-based lipophilic anions using oil-in-water (O/W) emulsion for adsorption drug loading. Third, systematically study and optimize absorption loading of doxHCl into the aforementioned nanoparticles by analyzing different variables. Lastly, having optimized the drug uptake conditions, evaluate doxHCl uptake by nanoparticles in plasma.

Results showed an almost 1:1 molar attraction between lipophilic anions and doxHCl as well as successful formulation of PLGA or PLGA/PEG-PLA polymeric nanoparticles incorporating one of the borates, potassium tetrakis(4-chlorophenyl)borate (KTpClPB). These nanoparticles were spherical and XPS confirmed the presence of PEG polymer on their surface. Adsorption drug loading was optimized using polymers with high acid number (502H), maximizing KTpClPB incorporation, increasing incubation/uptake temperature, increasing drug:nanoparticle incubation ratio, and using PEGylated nanoparticles (those containing PEG-PLA). Under optimized conditions, doxHCl loading reached as high as 6%. Studies with another model drug, vinblastine sulfate (VS), confirmed the utility of this loading procedure and specially formulated

nanoparticles. Plasma drug uptake study showed marginal reduction of plasma drug concentration at concentrations near the normal therapeutic dose of doxHCl while the nanoparticle system effectively reduced drug concentration by almost 16%, when plasma drug concentration was 4 times the normal therapeutic dose (200 µg/mL). Favorable results supported the use of borate-encapsulated polymeric nanoparticles for improved model drug loading via absorption/extraction loading procedure under different conditions.

3.2 Introduction

Nanoparticulate polymeric drug delivery systems have been the subject of intense research due to advantages including extended blood circulation time, improved passive or active drug targeting, reduced side effects and wasted drug, prolonged drug release for extended dosing intervals, and biocompatibility of different biodegradable polymers available for nanoparticle formulation (Soppimath, Aminabhavi et al. 2001; Yang, Wang et al. 2006; Park 2007).

An important feature of these systems is drug loading, which may help to directly reduce total drug amount per dose and total dosing time while indirectly improving total release period as well as drug accumulation at target sites. For polymeric nanoparticles, many drug loading procedures have been established to improve loading of different drugs, each with their unique properties. Two commonly cited strategies are drug entrapment, where drug molecules are trapped in the hydrophobic polymer matrix of nanoparticles during formulation, and drug conjugation, where drug molecules are covalently linked to polymer strands before or after nanoparticle formulation. Three commonly cited entrapment methods are emulsification/solvent-evaporation, nanoprecipitation, and polymerization. Emulsification/solvent-evaporation method takes advantage of phase separation between oil and water to promote homogenization/ sonication-driven nanoparticle formation and examples include oil-in-water (O/W) or water-in-oil-in-water (W/O/W) emulsions. Nanoprecipitation method involves partitioning of water-soluble oil phase into an aqueous phase to promote emulsification without power input. The polymerization method, as the name suggests, is where nanoparticles are prepared through chemical polymerization of monomers (Soppimath,

Aminabhavi et al. 2001; Galindo-Rodriguez, Allemann et al. 2004). These different strategies differ in that each may be tailored to maximize loading of different types of drugs as well as facilitate the use of special polymers (Zobel, Zimmer et al. 1999; Krauel, Davies et al. 2005; Arias, Ruiz et al. 2008). Despite the effectiveness of entrapment methods, drug release from these nanoparticles have shown a large initial burst within the first 1-3 h of release and minimal release afterwards (Soma, Dubernet et al. 2000; Wong, Bendayan et al. 2004; Missirlis, Kawamura et al. 2006). To overcome this, drug conjugation can be utilized where drug molecules are chemically linked to polymer strands followed by use of these conjugates for particle formulation or linked to pre-formed nanoparticles (Yoo, Oh et al. 1999). Even though zero-order drug release can be achieved through hydrolysis-limiting drug release, drug loading is low due to limited availability of conjugation sites.

Another strategy now more commonly used to complement entrapment and conjugation loading methods is the absorption method, which, as the name suggests, achieves drug loading through incubation of blank nanoparticles with a concentrated drug solution (Asuri, Karajanagi et al. 2007; Arias, Linares-Molinero et al. 2008). This method originates from the need to encapsulate protein/peptide drugs into nanoparticles, where drugs could lose efficacy during stressful entrapment and conjugation loading procedures while the more passive adsorption loading process preserved drug integrity and efficacy. In studies cited thus far, the passive drug concentration gradient and potential hydrophobic interactions between the polymer and protein/peptide have played important roles in improving drug loading.

Recently, the concept of ion pairing has been incorporated into nanoparticles undergoing adsorption loading. Here, electrostatic interactions are integrated into nanoparticles, by using charged polymers to formulate charged nanoparticles, to provide additional attractive forces with oppositely charged drug molecules. Examples of the above strategy include using sulfobutylated poly(vinyl alcohol)-graft-poly(lactide-*co*-glycolide) to incorporated tetanus toxoid (Jung, Breitenbach et al. 2000), poly(ε-caprolactone)-poly(ethylene glycol)-poly(ε-caprolactone) to enhance human basic fibroblast growth factor incorporation (Gou, Huang et al. 2007)and using poly(styrene-co-4-styrene-sulfonate) to enhance lysozyme loading (Cai, Bakowsky et al. 2008).

Existing absorption drug loading procedures incorporating ion complexation or ion pairing, despite their effectiveness, still has several shortcomings. One is that charged polymers may be difficult to synthesize, purify, and characterize. Second, the potential utility of absorption loading for small molecule drugs, especially cationic anti-cancer drugs such as doxorubicin hydrochloride and vinblastine sulfate, have not been systemically evaluated, especially compared to existing ones. Third, no existing studies have evaluated the effectiveness of PEGylated nanoparticles, those with a layer of hydrophilic poly(ethylene glycol) (PEG) polymer on the surface, for absorption drug loading. Lastly, alternative uses of charged polymeric nanoparticles have not been explored.

With the above issues in mind, there are several goals for this study. First, evaluate the ability of borate-based lipophilic anions to extract a model cation drug, doxorubicin hydrochloride, from aqueous to the organic phase. Second, a new anionic polymeric nanoparticle will be formulated using an FDA-approved polymer, PLGA, and borate-based lipophilic anions and properties such as borate incorporation, particle size and morphology will be evaluated. Third, absorption loading of doxHCl by the specially formulated nanoparticles will be studied systemically to optimize loading. Fourth, PEGylated nanoparticles will be formulated to evaluate its absorption drug uptake potential. Lastly, drug uptake in plasma will be explored to evaluate alternative uses for this nanoparticle system.

3.3 Materials and Methods

3.3.1 Materials

Potassium tetrakis(2-thienyl)borate (KTTB), potassium tetrakis(4-chlorophenyl)borate (KTpClPB), and potassium tetrakis[3,5-bis(trifluoromethyl)phenyl]borate (KTBTFMPB) were purchased from Sigma-Aldrich. Sodium tetraphenylborate (NaTPB) was a kind gift from Dr. Mark Meyerhoff. Doxorubicin hydrochloride (doxHCl) (>99% purity, lyophilized powder) was purchased from Hisun Pharmaceuticals (China). Poly(D,L-lactide-*co*-glycolide), 50/50, with inherent viscosity of 0.2 dl/g and MW_w of 15 kDa (resomer 502H), 0.34 dL/g and MW_w

of 38 kDa (resomer 503H), and 0.42 dL/g and MW_w of 45 kDa (resomer 503), were purchased from Boehringer Ingelheim. Poly(vinyl alcohol) (PVA) with MW_w of 25,000 (88% hydrolyzed) was purchased from Polysciences Inc. L-lactide (>99% purity) was purchased from Sigma-Aldrich. Methoxy-poly(ethylene glycol) (mPEG-NH_2, MW_w = 5,000) was purchased from Nektar Therapeutics. Spectra/por 7 dialysis bags (MWCO: 10-12K or 50K, Spectrum) were purchased from Fisher Scientific All other chemicals and solvents were of analytical grade and purchased from commercial suppliers.

3.3.2 Borate solubility

Borates were weighed into glass tubes followed by addition of different organic solvents in 0.5 mL incremental volumes at room temperature. After shaking for 30 s, solubility was determined as the concentration when the solution was completely clear.

3.3.3 DoxHCl extraction into borate-dissolved ethyl acetate phase

DoxHCl was dissolved in deionized water (DIW) at 1.72 mM. KTTB, KTpClPB, and KTBTFMPB were dissolved in ethyl acetate at 0.5:1, 1:1, or 2:1 molar ratios with doxHCl. For extraction, 1 mL of either blank or borate-dissolved ethyl acetate solution was added to 1 mL doxHCl solution followed by vortexing for 30 s and shaking for 10 min. The mixture was centrifuged at 5,000 RPM for 5 min, and the doxHCl concentration in the aqueous phase before and after extraction was determined by HPLC (see below).

Percent doxHCl extraction was calculated as:

$$\%\ Drug\ Extraction = \frac{DoxHCl\ Conc_{\ before\ extraction} - DoxHCl\ Conc_{\ after\ extraction}}{DoxHCl\ Conc_{\ before\ extraction}} \times 100\%$$

3.3.4 DoxHCl concentration determination methods

3.3.4.1 HPLC method

A Waters HPLC system (Waters, Milford, MA) was used for chromatographic separation of doxHCl. It consisted of a 1525 Binary HPLC pump, 717 plus autosampler, and 474 scanning fluorescence detector. Waters Breeze® chromatography software was used to acquire and process data. A Waters Nova-Pak® C_{18} column (3.9 x 150 mm I.D.) (Waters, Milford, MA) was used with a filtered and degassed ACN : 20 mM, pH 3 potassium phosphate : TFA (30:70:0.1, v/v/v) mobile phase. Chromatography was performed at a flow rate of 1 mL/min and fluorescence detection was set at $\lambda_{excitation}$ of 480 nm and $\lambda_{emission}$ of 590 nm at room temperature.

DoxHCl in the samples were analyzed using corresponding standards injected separately.

3.3.4.2 UV method

A Beckman DU650 spectrophotometer was used for UV analysis. Samples or standards containing doxHCl in methanol were analyzed using a quartz spectrophotometer cell (Starna Cells Inc.) at a scanning rate of 1200/min and scanning range of 400-750 nm. Absorbance wavelength was set at 480 nm and all sample had baseline reading set at 750 nm.

3.3.5 PEG-PLA copolymer synthesis and characterization

Methoxy-poly(ethylene glycol)-poly(lactic acid) (PEG-PLA) was synthesized by a standard ring opening polymerization. Briefly, L-lactide (Sigma, 98% purity) was pre-purified by recrystallization from ethyl acetate and the catalyst, stannous octoate (Tin(II) 2-ethylhexanoate, Sigma, 95% purity), was pre-purified by distillation. The desired molar ratio of L-lactide to mPEG-NH_2 was weighed out and added to the reaction flask followed by addition of stannous octoate at equivalent molar ratio to mPEG-NH_2. Dry toluene (10 mL / 1.5 g of reactants) was added to dissolve and mix the reagents. The reaction proceeded with stirring at 110^{o}C for 2 hours under moisture-free argon atmosphere. At the end of the polymerization step, copolymer was purified and recovered as follows. The copolymer crystallized upon cooling and was dissolved with cooled dichloromethane followed by ether addition to reprecipitate the copolymer. The previous

procedure was repeated and the copolymer was collected by filtration on a Buchner funnel. They were then dried at 37^{o}C in a vacuum oven overnight.

PEG-PLA was analyzed by ^{1}H-NMR spectroscopy using a Bruker DRX 500 spectrometer (Bruker Biospin Inc., Billerica, MA) operating at 500 MHz. Peak areas for different hydrogens were used for PEG-PLA molecular weight determination.

3.3.6 General nanoparticle formulation

Nanoparticles were formulated using an oil-in-water (O/W) emulsion/solvent evaporation procedure (Fig. 3.6). Different amounts of polymer were dissolved in 2 mL ethyl acetate (oil phase) and emulsified by sonication (20 s) on ice using a probe sonicator (Sonics VibraCell) at 50% power in 2 mL 3% PVA solution (aqueous or water phase). The O/W emulsion was diluted into 40 mL of 0.075% PVA solution under rapid magnetic stirring for 4-5 hours. Nanoparticle suspensions were collected and washed using an Amicon Stirred Cell with a 50 nm Millipore nitrocellulose filter.

KTpClPB-loaded nanoparticles were formulated using the same O/W procedure above except that predetermined amounts of KTpClPB were dissolved in the ethyl acetate phase along with polymer.

PEGylated nanoparticles were formulation using the same O/W procedure above with modifications. 502H PLGA and KTpClPB were dissolved in 2 mL ethyl acetate and mixed with PEG-PLA dissolved in 0.2 mL methylene chloride. This oil phase was emulsified in 2.2 mL of 3% PVA solution. All other steps were unchanged.

3.3.7 Nanoparticle characterization

3.3.7.1 Particle size/zeta potential determination

Nanoparticle suspensions were diluted to 0.5 mg/mL and transferred into fold capillary cells for both zeta potential and particle size determination. Samples were analyzed using a Malvern ZetaSizer Nano ZS (Malvern Instruments).

3.3.7.2 SEM morphological analysis

Nanoparticle suspensions were diluted to 50 µg/mL and dried overnight on viewing stubs. Morphology was observed by scanning electron microscopy (Philips XL30 Field Emission Gun Scanning Electron Microscopy).

3.3.7.3 Surface chemistry analysis

Surface chemistry of nanoparticle with or without PEG-PLA (no drug loaded) as well as PEGylated nanoparticles with doxHCl loaded was characterized by X-ray photoelectron spectroscopy (XPS, Kratos Axis Ultra, Kratos Analytical) equipped with a monochromatized aluminum X-ray source (powered at 10 mA and 14 kV). The angle between the normal to the sample surface and the lens axis was 0^{o}. A survey scan spectrum (0-1000 eV, average of 4 scans) and regional scan for C_{1s} (265-295 eV, average of 10 scans) were recorded for each sample. The analyzer was set at pass energies of 160 eV or 20 eV for the survey or regional scans, respectively. Analysis of data was done with CasaXPS program (Casa Software Ltd., UK) with a Gaussian/Lorentzian product function. Chemical shifts for the C_{1s} regional scans were referenced to hydrocarbon at 285 eV.

3.3.8 KTpClPB loading determination

KTpClPB was extracted from nanoparticles by adding 0.1 mL methylene chloride followed by 1.5 mL methanol to pre-weighed nanoparticle powder. The suspension was shaken overnight for complete extraction and spun down at 13,200 RPM for 8 minutes. Supernatant containing KTpClPB was diluted 4-fold by addition of methanol and sample concentration was determined using HPLC with corresponding standards injected separately.

Waters HPLC system (Waters, Milford, MA) was used. It consisted of a 1525 Binary HPLC pump, 717 plus autosampler, and 2487 Dual λ absorbance detector. Waters Breeze® chromatography software was used to acquire and process data. No column was used. Chromatography was performed using 100% acetonitrile as the mobile phase, at a flow rate of 1 mL/min and UV detection was set at 232 nm.

3.3.9 General drug absorption loading into nanoparticles

Drug was dissolved to desired concentrations in deionized water (DIW). Both the drug solution and a nanoparticle suspension (known concentrations) were added consecutively into an aqueous phase so that 1) drug and nanoparticle reached desired concentrations and relative weight ratios and 2) final suspension volume reached 4 mL. Mixtures were shaken (Ika KS130) for different lengths of time at different temperatures.

After drug loading, mixtures were dialyzed in Spectra/por 7 dialysis bag (MWCO: 50,000, Spectrum) against 1 liter of DIW (replaced every hour during the first 3 h) over 24 h. Dialyzed suspensions were used for size, zeta potential, and drug loading determination.

3.3.10 Drug loading determination

This procedure is similar to KTpClPB loading determination. Briefly, drug loaded nanoparticle samples were lyophilized and weighed into 2 mL polypropylene tubes. 0.1 mL methylene chloride was added to nanoparticles, followed by shaking for 10 min, then addition of 1.5 mL methanol and shaking for over 12 h. These suspensions were spun down at 13,200 RPM for 8 min. Supernatant containing dissolved drug was diluted as appropriate using methanol. Drug concentration was analyzed using UV doxHCl concentration determination procedure above.

3.3.11 Vinblastine sulfate uptake study

Two types of nanoparticles were used for this study. 502H:PEG-PLA(7:1, wt/wt) mixed polymeric nanoparticles with or without incorporation of maximal amount of KTpClPB in the organic phase formulated at total polymer concentration of 20 mg/mL in ethyl acetate. Different nanoparticle formulations were loaded with vinblastine sulfate (VS) using the incubation method with variations.

Formulation	Drug uptake temperature (^{o}C)	KTpClPB presence
1	Room temp	No
2	37	No
3	37	Yes

The above table describes the three groups of nanoparticles incubated with vinblastine sulfate. Nanoparticles were mixed polymeric nanoparticles with 20 mg/mL polymeric concentration in ethyl acetate.

For the incubation drug uptake procedure, 7.5 mg of blank nanoparticles were mixed with 1.5 mg of VS in a total of 4 mL DIW and incubated at different temperature, with shaking, for 30 min. Drug loaded nanoparticles were dialyzed (spectra/por 7, MWCO: 50K) against 1 L of DIW (replaced every hour for the first 3 h) over 24 h. Nanoparticles were lyophilized and then weighed out. VS was extracted from nanoparticles by adding 0.1 mL methylene chloride and 1.5 mL methanol to pre-weighed nanoparticles followed by shaking for 12 h. The suspension was spun down and supernatant containing VS was injected into HPLC for concentration determination.

A Waters HPLC system used for doxHCl detection was also used for VS detection. No HPLC column was used and the mobile phase was methanol:10 mM sodium phosphate (60:40). Flow rate was 1 mL/min and injection volume was 100 µL. UV detection was set at 270 nm and VS in the samples were analyzed using corresponding standards injected separately.

3.3.12 Plasma drug extraction procedure

Goat plasma was aliquoted into 36 – 3 mL portions and divided into 12 groups of 3 portions each. Into six of the groups (control groups), 10 mg/mL doxHCl solution was added to plasma to reach either 15 µg/mL, 30 µg/mL, 50 µg/mL, 100 µg/mL, 150 µg/mL, or 200 µg/mL followed by addition of 25 µL of deionized water (DIW). Into the remaining six groups, 10 mg/mL doxHCl was added to reach the above concentrations followed by addition of 25 µL (0.95 mg) of blank PEGylated nanoparticle suspension.

The 12 groups were shaken at 37^{o}C for 30 minutes. Six groups containing nanoparticles were first centrifuged at 21,000 RPM for 25 minutes to spin down the

nanoparticles; supernatant samples were transferred to labeled tubes. 0.4 mL of plasma from each sample in each group was transferred into 15 mL polypropylene tubes followed by addition of 4 mL methanol:chloroform (3:1, v/v), 1 minute vortexing, and shaking for 10 minutes. Samples were then centrifuged at 12,000 RPM for 10 minutes and 2 mL of the organic phase was transferred into 50 mL polypropylene tubes and dried.

Dried phase was reconstituted using 0.3 mL methanol (for 15 – 100 µg/mL doxHCl samples) or 0.6 mL methanol (for 150 and 200 µg/mL doxHCl samples) and drug concentration was analyzed using HPLC (with no column) with corresponding standards injected separately.

3.4 Results and Discussion

3.4.1 Borate selection and properties

Borate-based lipophilic anions have traditionally been utilized as exchangers in ion-selective electrodes (Ganjali, Norouzi et al. 2006; Gupta, Singh et al. 2008). For this reason, different properties for these anions, relevant for nanoparticle encapsulation, either have not been studied or have not been published. For this project, two critical properties of borates were logP, or partition coefficient of the anions between hydrophobic and hydrophilic phases, and solubilities in different organic solvents. The former could give a rough estimate of compatibility of these anions with hydrophobic cores of nanoparticles while the latter may suggest solvents appropriate for nanoparticle formulation. For borate-based compounds in this study (Fig. 3.2), logP values were obtained as estimates using ChemDraw program (Table 3.1) and their solubilities in different organic solvents were determined by incremental addition of organic solvents to each borate compound (Fig. 3.2).

Borate anions demonstrated increasing logP values (increasing hydrophobicity), which indicated good hydrophobicity and compatible with nanoparticle cores (Fig. 3.2, Table 3.1). With addition of halogen and carbon atoms to the aromatic rings of the borates, hydrophobicity increased dramatically and could suggest design patterns which may be helpful when synthesizing new biocompatible lipophilic anions more appropriate for human usage. There did not appear to be a correlation between increasing logP values

and solubility in organic solvents (Table 3.1, Fig. 3.3). KTTB was not soluble in any organic solvents tested and was not studied. For polymeric nanoparticle formulations, the most commonly used organic solvents for preparation are methylene chloride, chloroform, and ethyl acetate. Because methylene chloride and chloroform dissolved the borates very poorly, ethyl acetate, which dissolved the borates up to 2.5 mg/mL, was chosen as the organic solvent for nanoparticle preparation.

3.4.2 DoxHCl extraction by borate molecules

Knowing that borates could dissolve in ethyl acetate, it was important to show that they could also extract a model hydrophilic drug, doxorubicin hydrochloride (doxHCl), from aqueous to the ethyl acetate phase. By itself, doxHCl had negligible solubility in ethyl acetate (Fig. 3.4A) and could not be extracted, but with increasing amounts of borates in the ethyl acetate phase, doxHCl extraction improved significantly (Fig. 3.4B). Quantitatively, doxHCl extraction was 93.4% for NaTPB, 97.0% for KTpClPB, and 94.9% for KTBTFMPB at 1:1 molar ratio of borate to drug (Fig. 3.5). This suggested the extraction process was primarily due to electrostatic interactions between anionic borates and cationic drug molecules and demonstrated the potential for doxorubicin to enter hydrophobic cores of borate-loaded nanoparticles.

Previous studies using NaTPB as ion exchangers showed leaching of the electrostatically bound material, suggesting it was not the best borate for future studies; while KTBTFMPB was 20 times more expensive than the other borate anions. For the above reasons, KTpClPB was chosen as the model lipophilic anion for nanoparticle studies.

3.4.3 Nanoparticle formulation with encapsulated KTpClPB

KTpClPB has not been associated with nanoparticle formulations in previous publications. For this study, an oil-in-water (O/W) emulsion method was used to formulate KTpClPB-loaded polymeric nanoparticles (Fig. 3.7). Because both the polymer chosen, PLGA, and the borate-based anion, KTpClPB, could dissolve in ethyl acetate, the procedure was simple as ethyl acetate with dissolved KTpClPB and PLGA was

emulsified into an outer aqueous phase to formulate the particles. To validate successful nanoparticle formation, particle sizing was done to determine the number and size of nanoparticle population(s) and scanning electron microscopy (SEM) was done to observe the morphology of the nanoparticles. The results were positive as particle size (not shown here) showed a unimodal (one population or peak) distribution with an average size below 200 nm depending on the initial amounts of KTpClPB added and SEM images (Fig. 3.8) showed spherical nanoparticles with similar sizes range of between 100-250 nm.

3.4.3.1 KTpClPB presence and quantification in nanoparticles

Despite a monomodal size distribution, direct evidence of KTpClPB incorporation into the nanoparticles was still needed and two other experiments were done to confirm its incorporation. First, the O/W emulsion procedure was repeated except that only KTpClPB, and no polymer, was dissolved in the ethyl acetate phase. The resulting emulsion was clear, filtered through the stir cell membrane filter system (used for washing nanoparticles) rapidly unlike nanoparticle suspensions with KTpClPB encapsulated, which did not filter through at all. This demonstrated that any KTpClPB not encapsulated into nanoparticles would be removed from the nanoparticle solution during the washing procedure and any changes in particle size or drug loading for KTpClPB-loaded versus KTpClPB-free nanoparticles was due to KTpClPB actually associated with nanoparticles. Second, and more importantly, KTpClPB was extracted from lyophilized nanoparticles with 0 or 10.7% theoretical KTpClPB loading (Table 3.2). HPLC analysis of extracted supernatant from KTpClPB-loaded nanoparticles showed a large peak which was not present for extracted supernatant of KTpClPB-free nanoparticles. Another important result from this HPLC experiment was that incubation of KTpClPB-loaded nanoparticles in different solutions (PBS or DIW) for 1 h or less did not appear to cause KTpClPB loss as calculated percent loading results for non-incubated and incubated nanoparticles were similar. In addition, it was observed that only 40% of the initial KTpClPB added was actually encapsulated (Table 3.2), which suggested an upper limit on how much KTpClPB could actually be incorporated. The above results clearly demonstrated encapsulation of KTpClPB into the nanoparticles although more

than half of the KTpClPB was lost during formulation. This experiment, however, did not show the location of these molecules in nanoparticles (core or surface or both).

3.4.4 Optimization of incubation drug loading

Under optimal conditions, absorption drug loading, where drug is incubated with and extracted into pre-formulated nanoparticles, may prove to be a versatile strategy to improve drug loading and other properties using PLGA-based nanoparticles. To optimize these conditions, various factors were analyzed including 1) PLGA acid number, 2) increasing KTpClPB loading, 3) impact of temperature, 4) different weight ratios of nanoparticles to drug in the incubation media, and 5) impact of PEGylation of nanoparticles.

3.4.4.1 Polymer (PLGA) selection

Many different polymers have been specially synthesized for the purpose of absorption drug loading, however, PLGA, the most readily available polymer approved by the FDA for clinical use, has not been systemically studied for absorption loading/uptake purposes much less in combination with KTpClPB. For this study, three different PLGA 50/50 polymers were selected (Table 3.3) to formulate blank nanoparticles (no KTpClPB added) to isolate the property most important for choosing the best PLGA. Of the three, 502H had the smallest molecular weight and viscosity, indicating that nanoparticles formulated using this polymer should be smaller than particles formulated using the more viscous polymers. More importantly, the acid numbers of the polymers were quite different. Resomer 503 was end-capped with acid number of <1, meaning the majority of carboxylic acid groups at the end of each polymer strand were "capped" by an alkyl group to form alkyl esters. Because carboxylic acid groups could contribute negative charges for electrostatic attraction to cationic drugs, the polymer with the highest acid number, resomer 502H, was expected to produce nanoparticles with the highest drug loading. Results confirmed this hypothesis as 502H nanoparticles (ethyl acetate organic phase) showed substantially higher extraction efficiency and drug loading (Fig. 3.10A) relative to nanoparticles made with other

polymers, reaching 1.44% drug loading and 44.6% extraction efficiency. In comparison, nanoparticles formulated using resomer 503, the end-capped PLGA, showed negligible drug loading of 0.09% loading and 2.8% extraction efficiency (Fig. 3.10B), which was expected considering they are end-capped. Another interesting result from this figure was that resomer 503H nanoparticles made with ethyl acetate organic phase, which were smaller than ones made with methylene chloride, had twice the drug loading and significantly improved encapsulation efficiency.

The results confirmed that acid number was important for enhancing drug loading and encapsulation efficiency and polymers with highest acid number should be selected while smaller particles, with greater surface area-to-volume ratio and potentially higher polymer density, was also important for improving adsorption drug loading.

3.4.4.2 KTpClPB incorporation

Even though anionic polymers or copolymers have been synthesized in the past to increase electrostatic interactions with cationic drugs, small molecule lipophilic anions such as KTpClPB have not been studied for this purpose and optimal amount of KTpClPB for nanoparticle incorporation was uncertain.

As the data showed, increasing KTpClPB incorporation increased extraction efficiency (measure of how much drug initially present in the incubation media was taken up by the particles) from 48% to 75% at the highest KTpClPB loading, and drug loading from 3.0% without KTpClPB addition to 4.8% at maximal KTpClPB loading (Fig 3.11A). These results clearly demonstrated the benefits of lipophilic anions and also suggested that additional KTpClPB incorporation would continue to increase drug loading; however, since KTpClPB incorporation in this study was limited by its solubility in ethyl acetate, further improvements in drug uptake was unlikely.

Previous results had shown approximately 40% encapsulation efficiency of KTpClPB into nanoparticles (Table 3.2). Based on this result, when maximal KTpClPB amount was loaded into nanoparticles (4.8 mg KTpClPB for 80 mg polymer nanoparticles), only 2.16 mg of KTpClPB was actually encapsulated in 80 mg of polymer nanoparticles. Since doxHCl loading was improved by 1.8% (3% to 4.8% as stated above) due to maximal KTpClPB addition, this meant an additional 1.44 mg of doxHCl was

loaded for every 80 mg of polymer in nanoparticles due to KTpClPB presence. Together, 2.16 mg KTpClPB and 1.44 mg doxHCl meant a KTpClPB:doxHCl molar ratio of 1.75:1, which suggested not all the encapsulated KTpClPB was paired with a drug molecule and anionic charges were still available. However, KTpClPB may be buried deep within the nanoparticles, precluding drug access. Furthermore, the results did not clearly indicate if hydrophobic interactions (pi-pi stacking) played a factor in the increased drug loading.

Another interesting observation was that in the presence of increasing KTpClPB, nanoparticle size decreased dramatically from 182.5 nm to 117.1 nm (Fig. 3.11B). One hypothesis for this was that increasing KTpClPB may lead to more drug loading and more hydrophobic drug-KTpClPB ion pair formation, especially on particle surface. These hydrophobic ion pairs could drive water away from, or even out of, nanoparticles and lead to a smaller hydrodynamic radius recognized by the particle sizing instrument.

3.4.4.3 Temperature effect on adsorption uptake

With increasing KTpClPB loading into 502H nanoparticles, doxHCl loading and extraction efficiency could be improved significantly, as results showed. Even though the previous KTpClPB uptake studies were done at 37^{o}C, the physiological temperature, it was important to discern the effects of temperature on drug loading and extraction efficiency. Comparison of drug adsorption loading for KTpClPB-loaded nanoparticles at room and physiological temperatures showed a very interesting trend where all other conditions being equal, higher temperature generated approximately 30% higher drug loading at all KTpClPB loadings (Fig. 3.12A) as well as similar increases in extraction efficiency (data not shown). For example, drug loading for nanoparticles with no KTpClPB incorporated improved from 1.4% to 3.0% while nanoparticles with maximized KTpClPB loading improved from 3.7% to 4.8%. These data demonstrated temperature-dependent drug loading improvement was actually due to the polymer used (502H) themselves rather than because of KTpClPB. A hypothesis for this increase focused on polymer rearrangement in nanoparticles. Polymeric nanoparticles could be envisioned as a ball of polymer strands with each strand having random motion. Hydration of nanoparticles and residence in an environment where temperature was above the glass transition temperature (T_g) for the polymer were known to significantly

increase the polymer strand motion and lead to rearrangement within a nanoparticle. For PLGA, an experimentally determined T_g value was approximately 31^oC (Blasi, D'Souza et al. 2005), which was in between the room temperature and physiological temperatures studied and led to the conclusion that in this case, increasing polymer rearrangement due to temperature increase led to increased drug molecule partitioning into the polymer phase and ion-pair formation with polymer carboxylic acids and KTpClPB. This phenomenon was also cited in a previous article from Kang and colleagues (Kang and Schwendeman 2003), where partitioning of small hydrophobic probes into polymer films increased with increasing temperature.

3.4.4.4 Effect of drug:nanoparticle ratio on drug uptake

For absorption loading, relative amounts of nanoparticle and drug in solution could be important due to a passive drug concentration gradient. However, it was uncertain how much KTpClPB presence could impact this and at what drug:nanoparticle weight ratio further increases in drug amount would make no difference.

For this study, fixed amount of KTpClPB-loaded nanoparticles were incubated with increasing amounts of doxHCl in solution up to 1.5 mg. However, at the highest ratio of 1.5 mg:15 mg (drug:nanoparticle), nanoparticle aggregation and sedimentation occurred during incubation. Between additions of 0.25 mg to 1 mg doxHCl, though, results (Fig. 3.13A) showed almost complete doxHCl extraction efficiency (95% or above) with 0.25 mg or 0.5 mg doxHCl in solution and 75% when 1 mg doxHCl was present. Drug loading also increased from 1.6% (with 0.25 mg doxHCl added) to 4.8% (with 1 mg doxHCl added); this was logical given the higher drug concentration gradient explained before and higher driving force for partitioning into nanoparticles. Nanoparticle zeta potential was more positive with drug adsorption loading (changing from -35 mV to ~ -26 mV), which was reasonable considering surface negative charges were being neutralized; however, there was no significant change in zeta potential nor particle size with increasing amounts of drug (0.25 mg – 1 mg) in the incubation media (Fig. 3.13B). This suggested that additional loaded drug were below the top layer of nanoparticles, supporting the polymer strand rearrangement theory in the previous temperature study.

Drug loading versus amount of doxHCl added curve increased in an almost linear fashion without reaching a plateau, suggesting that not all potential drug binding sites were occupied on nanoparticles and higher loading could be achieved if nanoparticle aggregation problem could be resolved.

3.4.4.5 PEGylated nanoparticles

Traditionally, it was known that hydrophilic moiety (polymer) could be grafted onto nanoparticle surface to form a hydrophilic surface layer that repels protein adsorption onto nanoparticle surface as well as reduce potential aggregation between particles. A commonly used hydrophilic polymer for this purpose is poly(ethylene glycol) (PEG) (Heald, Stolnik et al. 2002), a biodegradable polymer used in commercial products. For formulation purposes, PEG was usually incorporated through direct conjugation to a hydrophobic polymer, such as poly(lactic acid) (PLA), to form a diblock copolymer, which may be used by itself or in combination with other polymers to form nanoparticles. As copolymer nanoparticles form, PLGA or PLA segment intertwine to form a hydrophobic nanoparticle core while the hydrophilic PEG segments extend out to form a hydrophilic shell (Fig. 3.14).

3.4.4.5.1 NMR characterization

Here, PEGylated nanoparticles were made from a mixture of resomer 502H and synthesized PEG-PLA although the total polymer concentration for these PEGylated nanoparticles was the same as regular nanoparticles made with only resomer 502H. NMR spectrum of the copolymer (Fig. 3.6A) matched those in previously published papers (Olivier, Huertas et al. 2002) and based on comparison of the various peaks obtained, calculated molecular weights of between 19,408 – 22,689 Da were obtained which was similar to the theoretical value of 25,000 Da found based on the weight ratio of L-lactide and mPEG-NH_2 used to synthesize the copolymer (Fig. 3.6B).

3.4.4.5.2 XPS characterization

X-ray photoelectron spectroscopy (XPS) has been used extensively for surface analysis of various polymeric materials. Using this technique, binding energies of electrons associated with different atoms in the top 2-10 nm of a surface can be measured to collect elemental and chemical information (Scholes, Coombes et al. 1999; Dong and Feng 2004). Here, XPS was utilized to analyze six nanoparticle samples including 1) blank PLGA (502H), 2) blank PEG-PLA, 3) blank PLGA:PEG-PLA (7:1, wt/wt) nanoparticles, all without KTpClPB addition; as well as 4) blank PLGA (502H), 5) blank PLGA:PEG-PLA (7:1, wt/wt), and 6) doxorubicin-loaded PLGA:PEG-PLA (7:1, wt/wt), all 3 of which had maximal KTpClPB incorporation. These samples were investigated for chemical composition as well as the presence of doxHCl and PEG polymers on nanoparticle surface.

Survey scans of the nanoparticle samples (Fig. 3.15) were done to detect carbon, oxygen and nitrogen atoms on nanoparticle surface and their percent composition. Of the materials present in nanoparticles, only the drug, doxorubicin hydrochloride (doxHCl), contained nitrogen atoms in its structure, thus presence of nitrogen peak at around 400 eV in the survey scans would indicate drug accumulation on nanoparticle surface. However, all six survey scans were similar in shape and showed visible C_{1s} and O_{1s} peaks, while no nitrogen peaks were present. Quantification results further confirmed this as all six samples, with the exception of blank KTpClPB-loaded PLGA (502H) nanoparticles, had zero nitrogen content (Table 3.4). Because the detection limit of this instrument is 0.1%, though, even the 0.1% nitrogen composition for blank KTpClPB-loaded PLGA nanoparticles was negligible. Upon analysis, this result was expected because based on the chemical formula of doxHCl, $C_{27}H_{29}NO_{11}Cl$, nitrogen has a theoretical percent atomic composition of 2.5% within doxorubicin; and when embedded into or onto nanoparticles, surrounded by numerous other carbon and oxygen atoms of polymers, this was easily reducible to less than 0.1%. From survey scan results, it was hard to draw conclusions regarding doxHCl localization within nanoparticles.

A surprising result from the survey spectra was that the percent atomic composition of carbon was similar to that of oxygen (Table 3.4), different from a previous study showing a 2:1 atomic ratio of carbon:oxygen (Pourcelle, Devouge et al. 2007), and different from predicted theoretical values of 2:1 for PEG, 2.5:2 for PLGA,

and 3:2 for PLA, all based on their respective chemical formulas. Considering that even the controls for this study, blank PLGA and blank PEG-PLA nanoparticles, both had low carbon:oxygen atomic ratios, this result could be due to a problem with instrument calibration where the intensity readings for the carbon peak was not fully optimized. From the atomic composition of carbon (Table 3.4), it was observed that carbon composition for blank PEG-PLA nanoparticles was 5% higher than blank PLGA nanoparticles (43.6% vs. 48.6%), which was expected given the higher theoretical carbon:oxygen ratio for PEG. Based on this, it was also not surprising to see blank PLGA:PEG-PLA nanoparticles with a percent carbon composition in between that of PLGA and PEG-PLA nanoparticles and this result was direct evidence of the presence of PEG strands on nanoparticle surfaces.

Results from Table 3.4 also showed that percent carbon composition for blank PLGA:PEG-PLA and blank PLGA/KTpClPB nanoparticles were similar (45.8% vs. 45.4%). Because there were no PEG-PLA in the KTpClPB loaded nanoparticles, a potential explanation for the increased carbon composition was due to KTpClPB, which has an amphiphilic structure (Fig. 3.2) that promoted localization on nanoparticle surfaces (similar to detergents) as well as a number of benzene rings in its structure which contribute to percent carbon composition. However, another potential cause could be polyvinyl alcohol (PVA), a surfactant added to all six formulations that could localize to the surface of nanoparticles to stabilize them. Like PEG, PVA also has 2:1 carbon:oxygen atomic ratio and the combinations of PVA + PEG-PLA and PVA + KTpClPB on nanoparticle surfaces could lead to similar carbon:oxygen ratios if enough PVA was present.

Lastly, results showed percent carbon composition for blank PLGA:PEG-PLA/KTpClPB and PLGA:PEG-PLA/KTpClPB/dox nanoparticles were significantly higher than the other four batches (Table 3.4). This result was surprising considering the magnitude of the increase relative to the control, blank PLGA nanoparticles (51.2 – 52.1% to 43.6%, 7-9% increase). Blank PLGA:PEG-PLA and blank PLGA/KTpClPB nanoparticles each had approximately 2% higher carbon composition relative to blank PLGA nanoparticles, which meant a combined increase of 4%, or around 47.6% theoretical carbon composition for nanoparticles with both PEG-PLA and KTpClPB

added. However, actual carbon compositions were 51.2% and 52.1%, or between 3-5% higher than expected, for PLGA nanoparticles containing PEG-PLA and KTpClPB. This phenomenon could be due to synergistic actions between PEG-PLA and KTpClPB, which multiplied rather than simply added the contributions of the components, when both components were present in nanoparticles. For example, by itself, PEG-PLA was miscible with PLGA and the combination of the two on nanoparticle surface led to a lower carbon:oxygen ratio than if only PEG-PLA was present on the surface. However, the presence of KTpClPB on nanoparticles appeared to reduce this miscibility and caused PEG-PLA to be pushed to the surface of nanoparticles, away from the PLGA core. Thus the combination of PEG-PLA with KTpClPB, with its many benzene rings and carbon atoms, formed a thick enough layer on nanoparticle surfaces to increase percent carbon composition readings.

Decomposition of C_{1s} envelope, based on previous studies (Shakesheff, Evora et al. 1997; Dong and Feng 2004; Pourcelle, Devouge et al. 2007), could further confirm the presence of PEG on nanoparticle surface (Fig 3.16). Ether carbons and hydrocarbons were primary constituents of PEG and ether carbons typically have a chemical shift of +1 to +1.3 eV relative to hydrocarbons referenced at 285 eV. In this study, 10.35% carbons were present at 286.3 eV (where ether carbons would be) for blank PLGA nanoparticles even though PEG was not present (Table 3.5). The presence of these carbons was again due to PVA, which was used to formulate all six nanoparticle formulations and was present on nanoparticle surfaces as a particle-stabilizing emulsifier. PVA has a carbon backbone with a hydroxyl group linked to every other carbon atom; hydroxyl carbons have similar chemical shifts as ether carbons and caused the 10.35% reading. Relative to blank PLGA standard, blank PEG-PLA nanoparticles had increased percentages of hydrocarbons as well as PEG carbons, which was expected since both PEG and PVA in these nanoparticles could contribute both types of carbons.

It was found that blank PLGA:PEG-PLA nanoparticles had slightly more hydrocarbons and PEG carbons relative to blank PLGA nanoparticles (less than 1 percent each, Table 3.5). Based on the fact that instrument detection limit was 0.1% and PEG-PLA only constituted 12.5% (wt/wt) of each nanoparticle, this again showed that some PEG was present on the surface layer. This result also matched previous percent carbon

composition results (Table 3.4), where blank PLGA:PEG-PLA nanoparticles had approximately 2% higher carbon composition relative to blank PLGA nanoparticles due to PEG presence.

Earlier, it was proposed that when both KTpClPB and PEG-PLA were incorporated into nanoparticles, PEG-PLA would have reduced miscibility with PLGA and PEG-PLA, along with KTpClPB, could form a surface layer that shielded the PLGA core. This was again confirmed through the carbon decomposition results (Table 3.5). For PLGA:PEG-PLA/KTpClPB nanoparticles with and without doxHCl, both hydrocarbons and PEG carbon percentages were much higher than polyester and carboxyl carbons, both of which were normally indicative of PLGA polymers. Furthermore, it was very interesting to see the PEG carbon percentages for these two nanoparticle formulations (32.79% and 34.20%) to be much higher than even blank PEG-PLA nanoparticles (18.04%) while polyester and carboxyl carbon percentages were much lower. This result indicated that the combination of KTpClPB with 12.5% weight percent PEG-PLA in PLGA nanoparticles may be a thicker layer than the PEG layer of pure PEG-PLA nanoparticles.

Lastly, an important observation from Table 3.5 was that PLGA:PEG-PLA/KTpClPB nanoparticles, with doxorubicin loaded, contained 42.99% hydrocarbons, while the batch with no doxorubicin had 40.47% hydrocarbons. Because the structure of doxorubicin (Fig. 3.1) contained many fused rings with numerous C-C, C-H (hydrocarbon) carbons, the 2.52% increase in hydrocarbon reading could be attributed to the presence of doxorubicin. Even though it was nearly impossible to calculate the number of doxorubicin molecules representing this 2.52% increase, qualitatively, it was safe to say that part of the doxorubicin loaded into these nanoparticles via incubation loading was in the surface layer.

3.4.4.5.3 SEM characterization

SEM images showed PEGylated nanoparticles, like regular ones, were spherical with size range of between 100-200 nm (Fig. 3.18). To study potential improvements of PEGylated nanoparticles, increasing amounts of doxHCl were again incubated with fixed amount of PEGylated nanoparticles up to 2 mg doxHCl. Because results at 2 mg doxHCl

addition were almost the same as those at 1.5 mg doxHCl addition, these results were not shown. With increasing doxHCl addition to PEGylated nanoparticles, no visible aggregation occurred; suggesting surface PEG strands were effective for repelling other particles. Despite no visible aggregation, particle sizing data of PEGylated nanoparticles (Fig 3.17C), after incubation with 1 mg and 1.5 mg doxHCl, showed increased particle size. This may be explained by transient particle-particle interactions where PEG strands momentarily intertwined and then came apart or where nanoparticle surfaces without PEG coverage interact to form transient complexes. Overall, particle size still remained below 350 nm, which was in line with or below many previously reported particle diameters.

3.4.4.5.4 Drug loading

DoxHCl extraction from solution, again, decreased with increasing drug in the incubation media while drug loading increased due to higher doxHCl concentration gradient (Fig. 3.17A). Extraction efficiency of PEGylated nanoparticles was slightly below that for regular nanoparticles, and with 1.5 mg doxHCl in the incubation media, extraction efficiency by PEGylated nanoparticles was still as high as 65%. The slightly lower extraction efficiency may be attributed to the outer shell of PEG strands that may repel a small percentage of doxHCl molecules in solution and slow their migration into the nanoparticle. Despite the substitution of PEG-PLA for a portion of resomer 502H, which reduced the number of carboxylic acids available for drug binding, drug loading values for regular and PEGylated nanoparticles were similar across the different drug:nanoparticle ratios. In fact, by preventing aggregation, PEGylated nanoparticles with maximal KTpClPB loading achieved up to 6% drug loading (Fig. 3.17B), which was much higher than most published drug loading values.

3.4.5. Vinblastine sulfate uptake

Vinblastine sulfate (VS), like doxorubicin hydrochloride, was commonly used for cancer treatment. As a small molecule drug, it has a molecular weight of 810.97 daltons with a number of fused rings in its structure (Fig. 3.19) that could be beneficial for

hydrophobic interactions, much like doxHCl. In terms of physicochemical properties, VS has moderate solubility in aqueous medium (greater than 10 mg/mL) and a reported *pKa* of 7.4 (Gaertner, Murray et al. 1998), which meant that under physiological conditions, around 50% of VS molecules should have a net positive charge. Because its intrinsic properties matched the type of drug whose loading we would like to improve using the specially formulated KTpClPB-loaded PEGylated nanoparticles, vinblastine sulfate was used as an additional model drug to demonstrate the potential utility of these nanoparticles toward this category of drug.

Several formulations were studied using either KTpClPB-free or KTpClPB-loaded PEGylated nanoparticles to further demonstrate improvements due to KTpClPB. PEGylated nanoparticles were loaded with vinblastine sulfate at either room temperature or 37^{o}C to see if the temperature-induced drug loading increase seen before also applied. KTpClPB-loaded PEGylated nanoparticles with no VS loaded was used as a control.

Results showed that as drug loading temperature increased from room temperature to 37^{o}C, actual drug loading improved from 3.77% to 5.98% while encapsulation efficiency improved from 22.6% to 35.9% (Table 3.6). This improvement again showed that the temperature effect on drug loading was dependent on the nanoparticles or polymer used and this system was effective for both doxHCl and VS. With KTpClPB incorporation into the nanoparticles, drug loading increased from 5.98% to 8.98% and encapsulation efficiency improved from 35.9% to 53.9% (Table 3.6). This was significant as almost half of the drug initially present in the incubation medium was taken up by the nanoparticles and further showed that KTpClPB presence significantly enhanced drug loading. It was also interesting to see that vinblastine sulfate loading into these nanoparticles was higher than for doxHCl and this could be due to the additional fused rings in its structure that provide improved stability in the hydrophobic core of nanoparticles. Alternatively, this loading difference relative to doxHCl may be due to the higher molecular weight of VS.

The above results with VS provided evidence that drug loading improvements using KTpClPB-loaded PEGylated nanoparticles were not exclusive to doxorubicin hydrochloride and it would be interesting to know if these particles and drug loading systems could be applied to other drugs.

3.4.6 Charge quantification calculations

Previous studies demonstrated significant increases in doxHCl and VS drug loading when the polymer, 502H, and KTpClPB were used to formulate the ion complexing nanoparticles. Assuming that all available charges of 502H polymer and KTpClPB could be used for ion pairing with drug molecules on a charge-for-charge basis, it would be interesting to calculate the theoretical drug loading in these nanoparticles.

First, the effect of 502H polymers on doxHCl loading was calculated. 502H polymers have an acid number of minimum 6 mg KOH/gram polymer according to the company (Boehringer Ingelheim) website. This meant that since KOH has a molecular weight of 56.1 g/mol, approximately 17.82 µmol of KOH may be neutralized by protons contributed by carboxylic acids in one grams of this polymer, which was also the same as saying that 17.82 µmol of doxorubicin could be neutralized by one gram of this polymer. Because 80 mg of 502H was used to make each batch of nanoparticles, this meant 1.426 µmol or 0.827 mg (doxHCl MW: 580 g/mol) of doxorubicin could be loaded into these nanoparticles by ion pairing. Finally, 0.827 mg of doxHCl in 80 mg of 502H nanoparticles would be equivalent to 1.02% drug loading. This theoretical drug loading was lower than the actual loadings observed in the temperature-dependent drug uptake study (Fig. 3.12A), where drug loadings in KTpClPB-free 502H nanoparticles were 1.4% and 3%, at room temperature and 37^{o}C, respectively. The increase in the actual drug loading could be due to hydrolysis of 502H during nanoparticle formulation which generated additional free acids in the polymer; although a more likely explanation was that the acid number reported by the manufacturer was only a minimum, and the actual acid number, was approximately 11.5 (determined by standard titration with potassium hydroxide by Dr. Ying Zhang), or twice the reported value. This meant the theoretical drug loading should have been 2.04%, which was closer to the actual values of 1.4% and 3%.

Because only 2 mL of ethyl acetate was used during nanoparticle formulation and KTpClPB had a solubility of 2.4 mg/mL in ethyl acetate, the maximal amount of KTpClPB that was theoretically added into each batch of nanoparticles was 4.8 mg. Since a previous KTpClPB extraction study found that encapsulation efficiency of KTpClPB in

nanoparticles was around 40% (Table 3.2), this meant that 1.92 mg of KTpClPB was actually encapsulated into each batch of nanoparticles. Assuming that each molecule of KTpClPB could ion pair with a molecule of doxHCl and that molecular weights of KTpClPB and doxHCl are 496 g/mol and 580 g/mol, respectively, this meant 1.92 mg of KTpClPB can bind to 2.25 mg of doxHCl. If 80 mg of 502H was used to formulate nanoparticles, this would have been equivalent to 2.67% increase in drug loading due to KTpClPB. Looking at actual result, there was an increase in drug loading from 3% to 4.8% between KTpClPB-free nanoparticles and nanoparticles with maximal KTpClPB incorporation (Fig 3.12A), which meant that presence of KTpClPB led to 1.8% increase in loading. Comparing the actual increase of 1.8% and theoretical increase of 2.67%, this meant that 2/3 of available KTpClPB were ion paired, which was substantial.

Lastly, it was observed that vinblastine sulfate loading into KTpClPB-free nanoparticles were 3.77% and 5.98% at room temperature and 37^{o}C, respectively (Table 3.6). Since 80 mg of 502H were used to make each batch of nanoparticles, based on reported acid number for 502H, this meant 1.426 µmol or 1.16 mg (vinblastine MW: 811 g/mol) of vinblastine could be loaded into these nanoparticles by ion pairing. 1.16 mg of vinblastine in 80 mg of 502H would have been equivalent to 1.43% theoretical drug loading (charge basis). However, since the measured acid number was almost twice the reported value, this meant the theoretical drug loading should have been almost 2.9%. This theoretical drug loading almost matched drug loading at room temperature, 3.77%, although it still fell short of the 5.98% achieved at 37^{o}C. One potential reason for the significantly higher drug loading relative to the theoretical value may be due to the structure of vinblastine, which contained more alkyl rings that may promote compatibility with the hydrophobic core of nanoparticles. In addition, if we again assume that 1.92 mg of KTpClPB was actually encapsulated into each batch of nanoparticles and that KTpClPB and vinblastine sulfate have molecular weights of 496 g/mol and 811 g/mol, respectively, this meant 1.92 mg of KTpClPB could bind 3.14 mg of vinblastine sulfate. Since 80 mg of 502H was used to formulate these nanoparticles, this meant the presence of KTpClPB led to an increase in theoretical loading of 3.7%. Because drug loading actually increased from 5.98% to 8.98% with incorporation of maximal amount of KTpClPB (Table 3.6), the 3% actual increase in drug loading was close to the theoretical

improvement of 3.7% and indicated that approximately 80% of available KTpClPB was bound to vinblastine molecules.

3.4.7 Plasma drug uptake study

Previous *in vitro* results demonstrated PEGylated nanoparticles in this study could effectively take up the model drugs, doxorubicin hydrochloride and vinblastine sulfate, after optimization. Ultimately, it was hoped that the successful *in vitro* results could translate into equivalent *in vivo* data; however, before conducting lengthy and difficult *in vivo* studies, a proof of concept should be done under simulated physiological conditions, or in plasma, which to the best of our knowledge, has not been done before. In this study, plasma suspensions containing different concentrations of dissolved doxHCl (from a normal therapeutic dose up to four times the therapeutic dose) were incubated with or without blank PEGylated nanoparticles and free drug concentration after incubation were determined.

To choose the proper conditions for this study, two things had to be calculated. One was an appropriate nanoparticle concentration in plasma, while the other was the normal therapeutic concentration of doxHCl in plasma (assuming 70% plasma protein drug binding). Doxil®, a nanoparticulate liposome containing doxHCl, was widely used clinically for cancer treatment, so its nanoparticle concentration per dose was used for this study. Normally, around 1 gram of liposomes was administered per dose and since an average person has around 3 liters of plasma, this calculated to a dose of 1 mg nanoparticle / 3 mL of plasma (**1 mg/3 mL**). For doxHCl dose calculation, the normal dose of Adriamycin®, i.e., 150 mg (60-75 mg/m^2 while an average 6 feet human was around 2 m^2) was used. Because the human body has around 3 liters of plasma, this translated to 50 µg/mL of total doxHCl concentration in plasma. Since doxHCl binding by plasma protein was 70%, free doxHCl concentration in plasma was 15 µg/mL. In addition to these two theoretical drug concentrations, a concentration in between these (30 µg/mL) as well as potentially toxic doses of 2X, 3X, and 4X the normal therapeutic concentration of 50 µg/mL were tested.

Plasma doxHCl concentrations, after drug extraction in the presence or absence of PEGylated nanoparticles, were measured while initial drug concentrations were used to

denote each formulation. Final free doxHCl concentrations, without addition of nanoparticles, were smaller than the theoretical drug concentrations due to plasma protein drug binding. Calculations showed that drug binding was consistently around 60% (not shown) while reported human plasma protein doxHCl binding was around 70% although values of between 50% and 70% have also been observed.

For the tested doxHCl concentrations near its normal therapeutic concentration (15 – 50 µg/mL) (Table 3.7), the effect of nanoparticles were relatively insignificant as the percent drug concentration reduction was between 7.7%-9.44%, which only translated to actual reduction of between 0.5-1.8 µg/mL. Nanoparticle drug loading here was only between 0.18-0.6%, which was insignificant considering these PEGylated could have a theoretical drug loading of up to 6 - 7%. Between 100 and 150 µg/mL (2X or 3X the normal dose of 50 µg/mL), the percent drug concentration reduction was 6.96% and 8.4%, respectively, which was comparable to those at normal drug dose, but drug loading improved slightly to 0.9% and 1.66%, showing that more drug molecules were starting to diffuse into the nanoparticles. At 200 µg/mL initial doxHCl concentration, absolute drug concentration reduction suddenly jumped to more than 13 µg/mL, or 15.71%. More importantly, drug loading of the nanoparticles increased to 4.35%, an almost 3-fold increase compared with the study done at 150 µg/mL.

The above results were surprising considering previous *in vitro* studies showed an active and quick uptake of doxHCl molecules by the PEGylated nanoparticles that was limited only by the maximal drug loading potential. However, these differences could be explained by the presence of dissolved plasma proteins, which were not present during the *in vitro* studies. These proteins have a tendency to reversibly adsorb to hydrophobic nanoparticle surface despite the presence of hydrophilic PEG polymers on the nanoparticles, which was only around 2.5% by total nanoparticle weight and was not effective for shielding the entire nanoparticle surface from the plasma proteins. Thus, any drug molecules that came into contact with nanoparticles was likely to first encounter an outer shell of plasma proteins and was preferentially bound by these proteins until gradually, available protein binding sites were saturated and excess drug could access and bind to nanoparticle itself.

Both percent plasma drug concentration reduction and drug loading results also suggested the PEGylated nanoparticles were not effective around the normal therapeutic concentration of 50 µg/mL, which was actually desirable considering a minimum therapeutic concentration was needed for treatment. At 4X the normal therapeutic concentration and above, the PEGylated nanoparticle could be very effective for treating potential drug overdose considering the high drug loading and quick uptake (30 minute incubation time). Although not tested here, drug loading results indicated that more drug uptake into the nanoparticles were possible considering these particles could reach up to 6% drug loading. Although only doxHCl was tested in this study, these nanoparticles could be effective for the broad category of small molecule drugs, including vinblastine sulfate, to reduce potential toxicity.

3.5 Conclusions

Anionic borates demonstrated great potential as model lipophilic anions with successful extraction of a model hydrophilic drug, doxorubicin hydrochloride (doxHCl), from aqueous to the organic phase via ion pairing. Of the borates studied, KTpClPB was most suitable for nanoparticle incorporation and was incorporated into regular or PEGylated nanoparticles at high concentrations to form spherical nanoparticles with PEG localized on the outer shell according to XPS.

In vitro incubation drug loading procedure, tested with these specially formulated nanoparticles, successfully extracted two model drugs, doxorubicin hydrochloride and vinblastine sulfate, into the particles at high concentrations. This drug loading process was optimized using polymers with high acid number (more negative charges for ion complexing), maximizing the KTpClPB loading into nanoparticles, increasing incubation temperature, maximizing drug:nanoparticle (wt/wt) ratio, and using PEGylated nanoparticles. These improvements enhanced loading by potentially increasing the density of available negative charges in nanoparticles for ion pairing, introducing potential hydrophobic interaction between drug and KTpClPB molecules to stabilize and enhance loading, and preventing or reducing potential particle aggregation through PEGylation.

Plasma doxHCl uptake, using optimized PEGylated nanoparticles, was negligible when the normal therapeutic dose of doxHCl was administered, which was desirable. However, such particles effectively reduced both plasma drug concentration and achieved high drug loading when 4X the normal therapeutic concentration was administered. This promising result suggested potential application of these nanoparticles as treatment for drug overdose of small molecule drugs with similar properties to doxHCl.

Overall, the combination of KTpClPB-loaded PEGylated nanoparticles and an optimized absorption/extraction loading process could significantly enhance active drug loading and provide a viable alternative to entrapment and conjugation-based drug loading methods.

Table 3. 1. Properties of the borate compounds studied

Compounds	**Molecular formula**	**MW (g/mol)**	**LogP** [#]
Potassium tetrakis(2-thienyl)borate (KTTB)	$C_{16}H_{12}BS_4K$	382.44	6.152
Sodium tetraphenyl borate (NaTPB)	$C_{24}H_{20}BNa$	342.23	7.568
Potassium tetrakis(4-chlorophenyl)borate (KTpClPB)	$C_{24}H_{16}BC_{14}K$	496.12	10.42
Potassium tetrakis[3,5-bis-(trifluoromethyl)phenyl]borate (KTBTFMPB)	$C_{32}H_{12}BF_{24}K$	902.32	14.632

[#]LogP values calculated by ChemDraw (octanol/water partition coefficient)

Table 3. 2. KTpClPB extraction from O/W nanoparticles with 40 mg total polymer/batch

Nanoparticle	**Theoretical KTpClPB (%)**	**Incubation**	**Actual loading (%)**	**Encapsulation Efficiency (%)**
7:1-502H/PEG-PLA	None	None	0	0
7:1-502H/PEG-PLA	10.7	None	4.19 ± 0.04	39.12
7:1-502H/PEG-PLA	10.7	1 hour in DIW	4.02 ± 0.1	37.54
7:1-502H/PEG-PLA	10.7	30 min in PBS	4.43 ± 0.10	41.36

Table 3. 3. Properties of different PLGA tested

PLGA polymer	Molecular Weight (g/mol)	Viscosity	Acid number
Resomer® RG 502H	~15,000	0.2 dl/g	min. 6 mg KOH/g
Resomer® RG 503H	~38,000	0.34 dl/g	min. 3 mg KOH/g
Resomer® RG 503	~45,000	0.42 dl/g	End-capped (max. 1 mg KOH/g)

Table 3. 4. Atomic % composition of C_{1s}, O_{1s}, and N_{1s}; of XPS C_{1s} core-level spectra of various nanoparticle samples

Nanoparticle samples	**Atomic composition (%)**		
	C_{1s}	**O_{1s}**	**N_{1s}**
PLGA	43.6	56.4	0.0
PEG-PLA	48.6	51.4	0.0
PLGA:PEG-PLA	45.8	54.2	0.0
PLGA + KTpClPB	45.4	54.6	0.1
PLGA:PEG-PLA + KTpClPB	51.2	48.8	0.0
PLGA:PEG-PLA + KTpClPB + doxorubicin	52.1	47.9	0.0

Table 3. 5. Decomposition of C_{1s} peak (% envelope ratios) of nanoparticle samples

Nanoparticle samples	Carbon peak components			
	C-C, C-H (hydrocarbon, 285 eV)	**C-O (PEG, 286.3 eV)**	**C-O (polyester, 287.2 eV)**	**O=C-O-C (carboxyl, 289.2 eV)**
PLGA	26.91	10.35	28.69	33.04
PEG-PLA	30.62	18.04	25.63	25.70
PLGA:PEG-PLA	27.79	11.15	29.58	31.49
PLGA + KTpClPB	29.50	11.02	27.38	32.09
PLGA:PEG-PLA + KTpClPB	40.47	32.79	11.70	15.04
PLGA:PEG-PLA + KTpClPB + doxorubicin	42.99	34.20	10.49	12.31

Table 3. 6. Drug loading and encapsulation efficiency for vinblastine sulfate

Nanoparticle formulation	**Drug loading (%)**	**E.E. (%)***
502H:PEG(7:1)-room temp	3.77 ± 0.54	22.6
502H:PEG(7:1)-37^{o}C	5.98 ± 0.90	35.9
502H:PEG(7:1)-KTpClPB	8.98 ± 0.76	53.9

*E.E.: encapsulation efficiency

Table 3. 7. Doxorubicin hydrochloride uptake by PEGylated nanoparticles in plasma

Formulations *	**Amt dox added/3.1 mL plasma (µg)**	**Final Conc-no nanoparticle (µg/mL)**	**Final Conc-with nanoparticle (µg/mL)**	**% Drug extraction** #	**Nanoparticle drug loading (%)**
15 µg/mL	45	7.01 ± 0.31	6.47 ± 0.16	7.70	0.18
30 µg/mL	90	12.21 ± 0.59	11.21 ± 0.40	8.19	0.33
50 µg/mL	150	19.38 ± 0.40	17.55 ± 0.71	9.44	0.60
100 µg/mL	310	39.82 ± 1.93	37.05 ± 0.56	6.96	0.90
150 µg/mL	470	60.71 ± 2.28	55.61 ± 1.33	8.40	1.66
200 µg/mL	620	84.85 ± 3.17	71.52 ± 2.06	15.71	4.35

* Formulations denoted by theoretical doxHCl concentrations originally present in plasma

Percent drug extraction:

$$\%\ Drug\ Extraction = \frac{Drug\ Conc_{\ no\ nanoparticles} - Drug\ Conc_{\ with\ nanoparticles}}{Drug\ Conc_{\ no\ nanoparticles}} \times 100\%$$

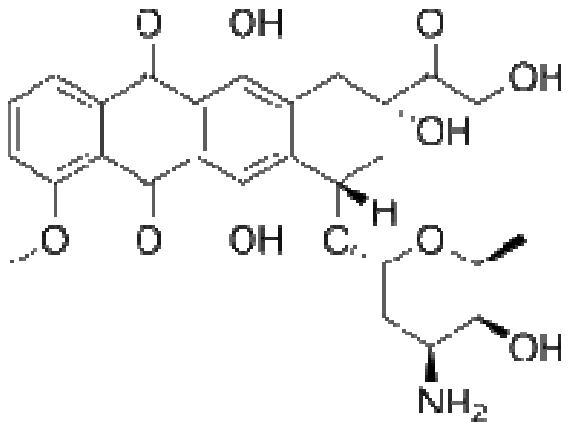

Figure 3. 1. Structure of doxorubicin hydrochloride (doxHCl).

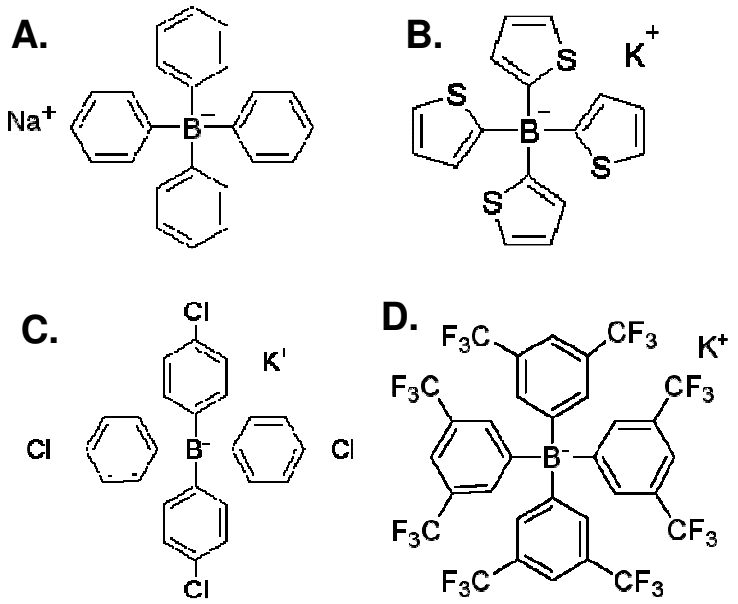

Figure 3. 2. Structures of the borate compounds studied, (A) sodium tetraphenylborate (NaTPB), (B) potassium tetrakis(2-thienyl)borate (KTTB), (C) potassium tetrakis(4-chlorophenyl)borate (KTpClPB), and (D) potassium tetrakis[3,5-bis(trifluoromethyl)phenyl]borate (KTBTFMPB).

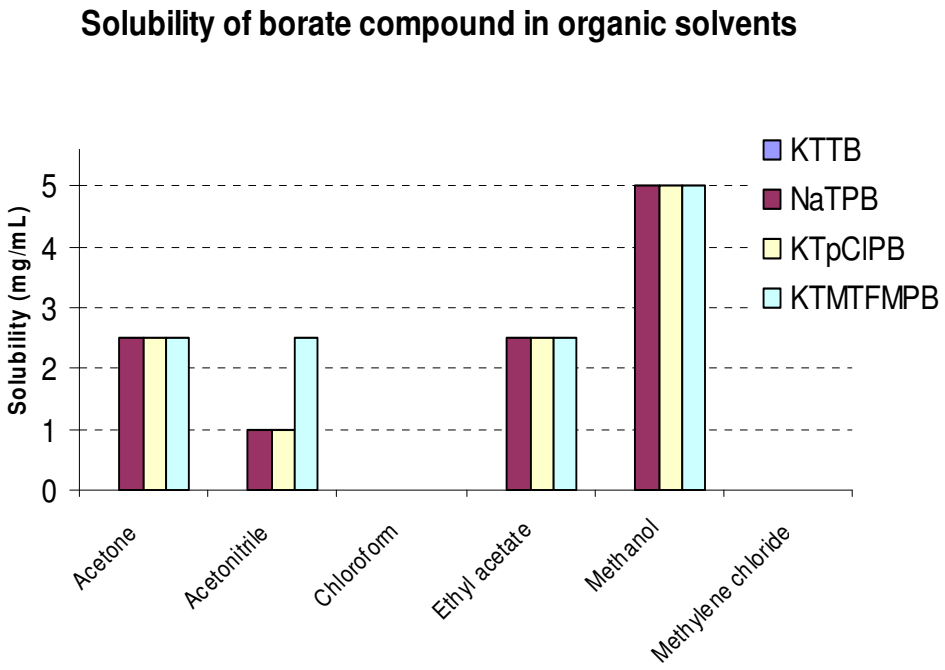

Figure 3. 3. Borate solubilities in various organic solvents.

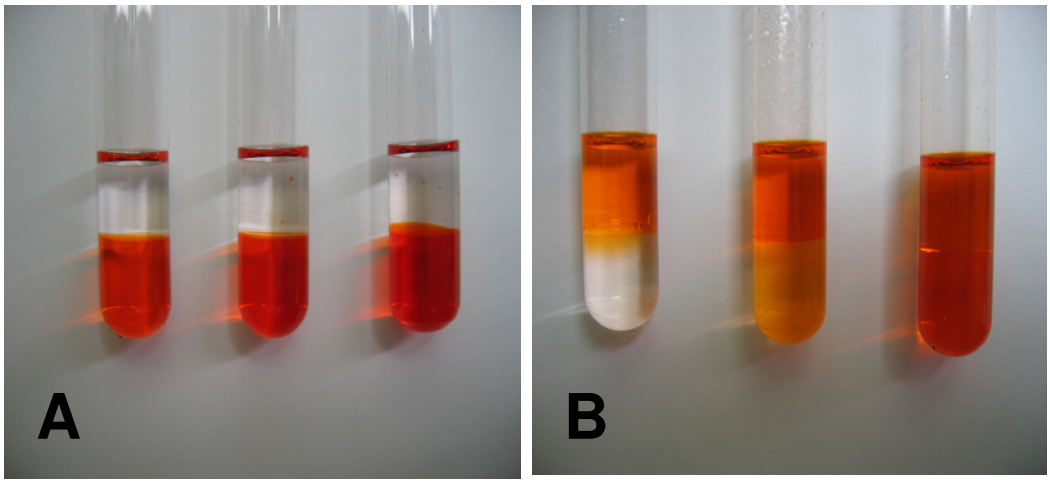

Figure 3. 4. Doxorubicin hydrochloride extraction into blank ethyl acetate at different aqueous doxHCl concentrations (A) or at 1:0.5, 1:1, and 1:1.5 molar ratios (left to right, photo B) of representative borate:doxHCl.

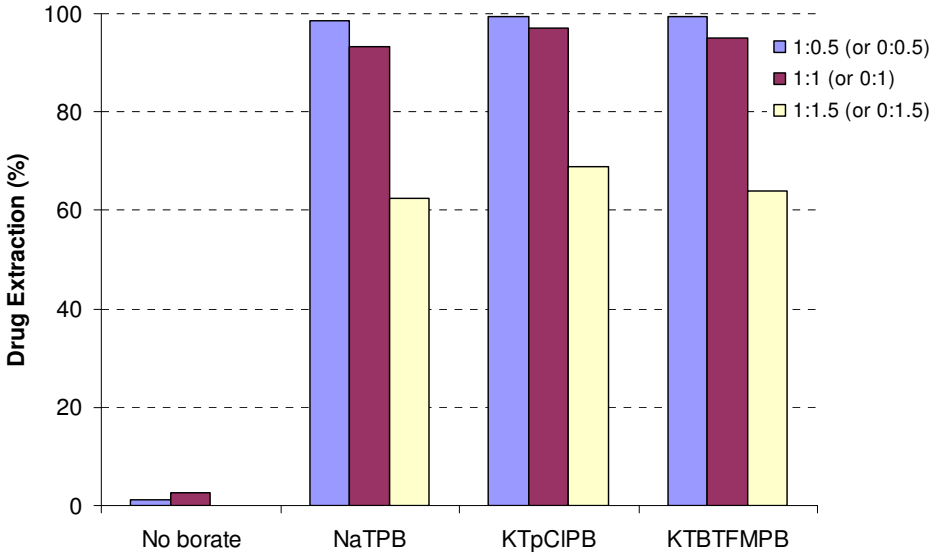

Figure 3. 5. Percent doxHCl extraction into ethyl acetate phase with and without dissolved borates. Three different molar ratios (1:0.5, 1:1, and 1:1.5) of borate:doxHCl were studied.

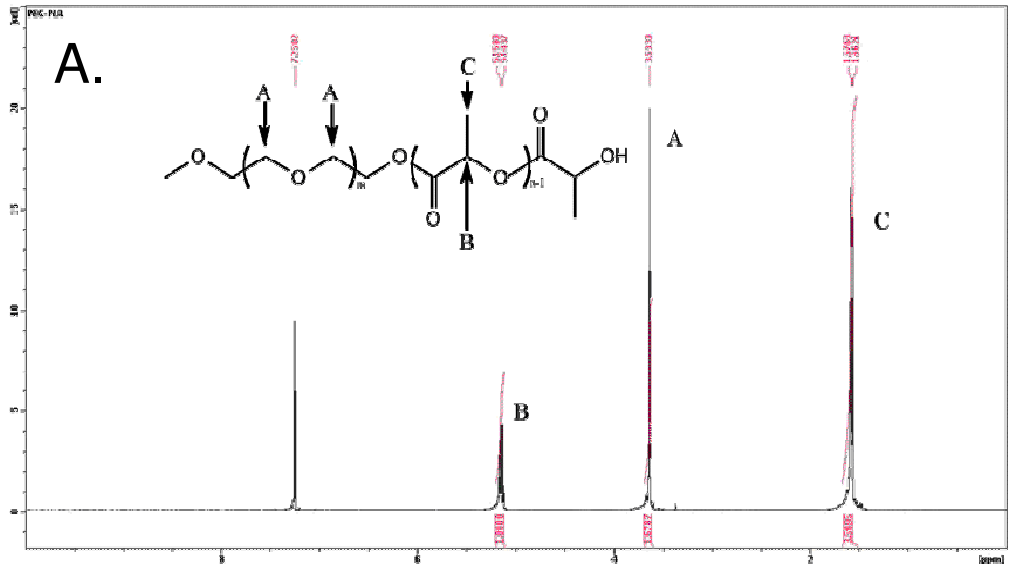

B.

PEG MW (g/mol)	PEG-PLA theoretical MW[1] (g/mol)	PEG-PLA calculated MW[2] (g/mol)	PEG-PLA calculated MW[3] (g/mol)
5,000	25,000	19,408.54	22,689.8

1. Calculated based on wt ratios of PEG and L-lactide added during PEG-PLA synthesis
2. Calculated based on area ratios of peaks A and B
3. Caclulated based on area ratios of peaks A and C

Figure 3. 6. (A) ^{1}H-NMR spectrum of methoxyPEG-PLA copolymer in deuterated chloroform and (B) associated table with theoretical and calculated molecular weights of the copolymer based on peak area ratios.

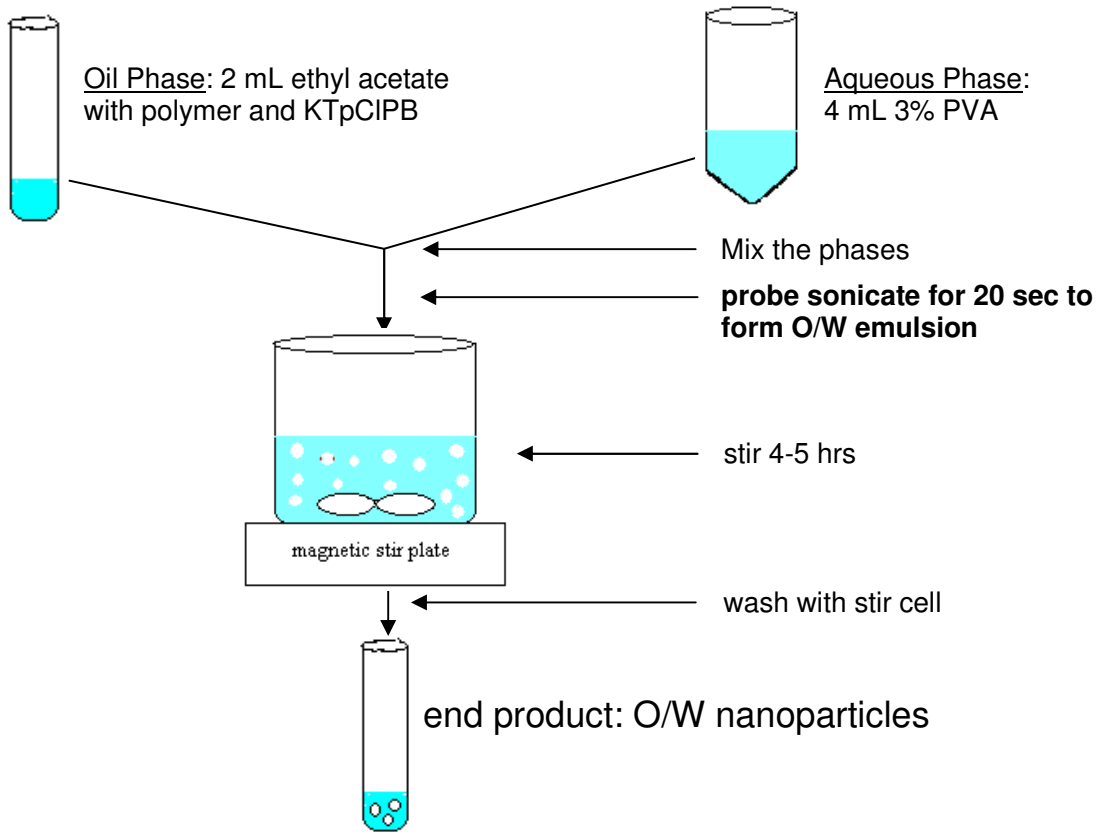

Figure 3. 7. General oil-in-water (O/W) blank nanoparticle formulation procedure.

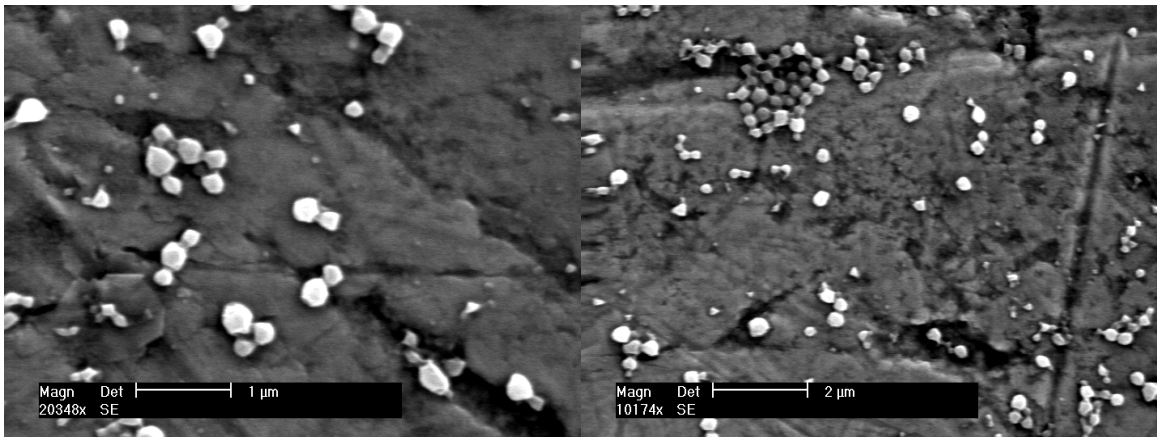

Figure 3. 8. SEM images of KTpClPB-loaded O/W nanoparticles at different magnifications (Philips XL30 FEG SEM).

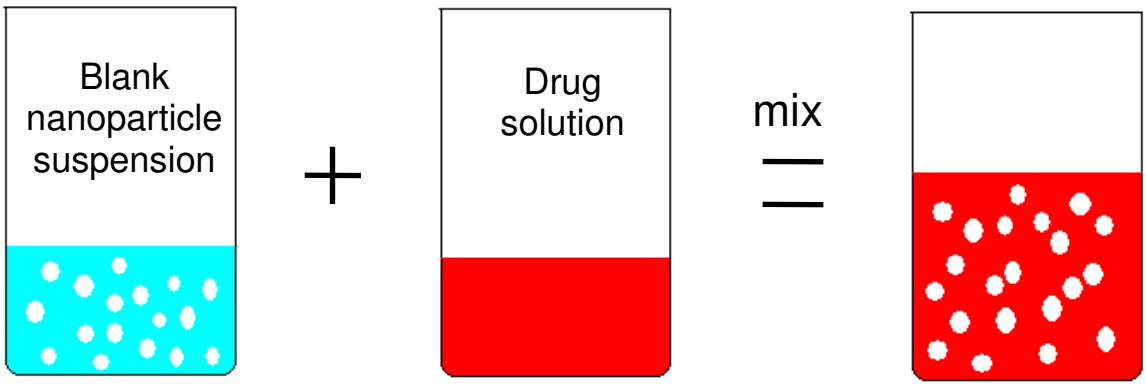

Figure 3. 9. General drug extraction/absorption loading into nanoparticle process.

A.

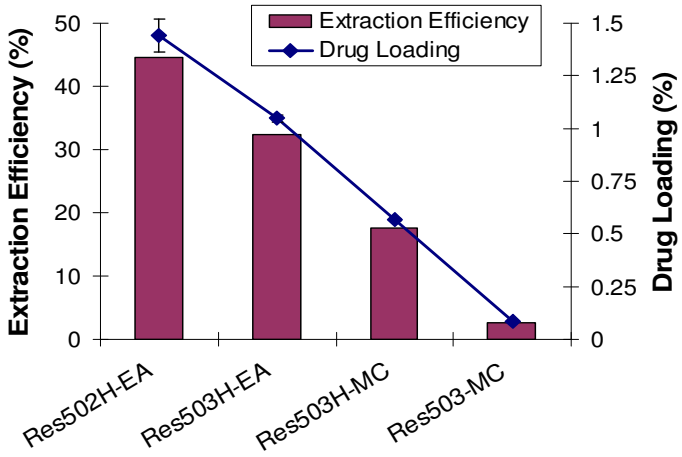

B.

Sample	Zeta potential-before extraction (mV)	Zeta potential-after extraction (mV)	Particle size (nm)	Polydispersity
Res502H-EA	-30.3	-14.7	179.5	0.155
Res503H-EA	-25.5	-14.5	189.8	0.133
Res503H-MC	-33.7	-23.1	229.4	0.108
Res503-MC	-36.2	-18.9	240.2	0.159

Figure 3. 10. DoxHCl extraction/absorption into nanoparticles made with different polymers with extraction efficiency and drug loading (A) and associated table of zeta potential and size of drug-loaded nanoparticles (B).

A.

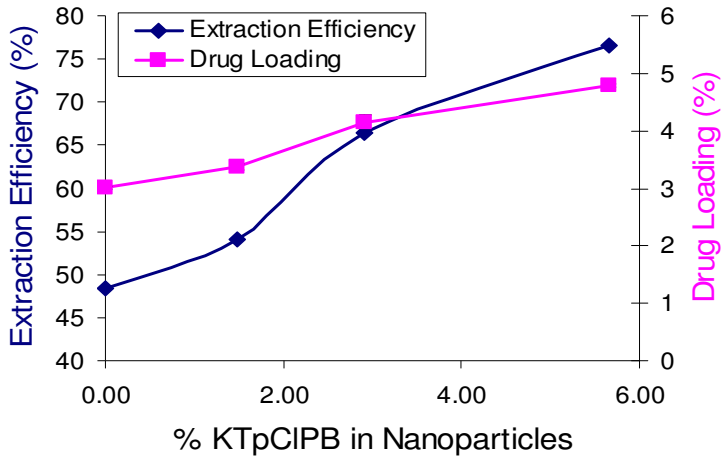

B.

Theoretical % KTpClPB present	Theoretical amt KTpClPB/batch NP (mg)	Zeta potential-before extraction (mV)	Zeta potential-after extraction (mV)	Particle size (nm)
0.00	0	-30.4	-21.3	182.5
1.48	1.2	-33.8	-18	161.7
2.91	2.4	-37.2	-15.7	142.6
5.66	4.8	-35.4	-17.3	117.1

Figure 3. 11. DoxHCl extraction/absorption into nanoparticles made with different polymers with extraction efficiency and drug loading (A) and associated table of zeta potential and size of drug-loaded nanoparticles (B).

A.

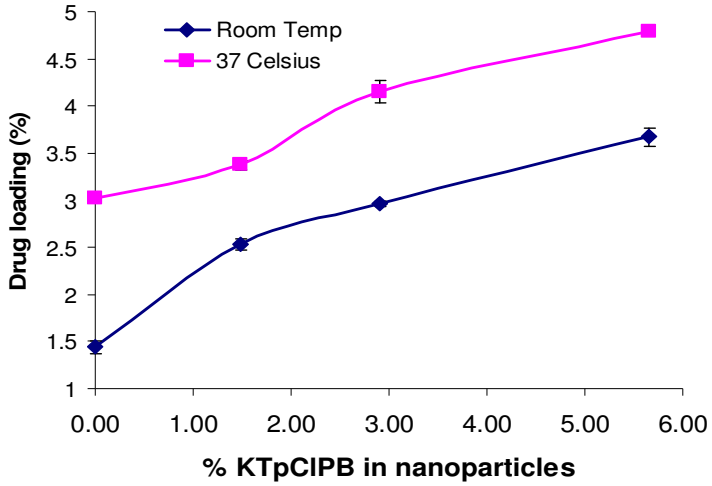

B.

Theoretical percent KTpClPB present	Zeta potential-before extraction (mV)	Zeta potential after extraction (mV)		Particle size (nm)	
		Room temp	37°C	Room temp	37°C
0.00	-30.4	-21.3	-22.3	178.4	182.5
1.48	-33.8	-18.0	-18.9	166.1	161.7
2.91	-37.2	-15.7	-20.9	145.1	142.6
5.66	-35.4	-17.3	-22.2	128.0	117.1

Figure 3. 12. DoxHCl extraction/absorption into KTpClPB-loaded 502H nanoparticles at different temperatures with extraction efficiency and drug loading (A) and associated table of zeta potential and size of drug-loaded nanoparticles at the two temperatures (B).

A.

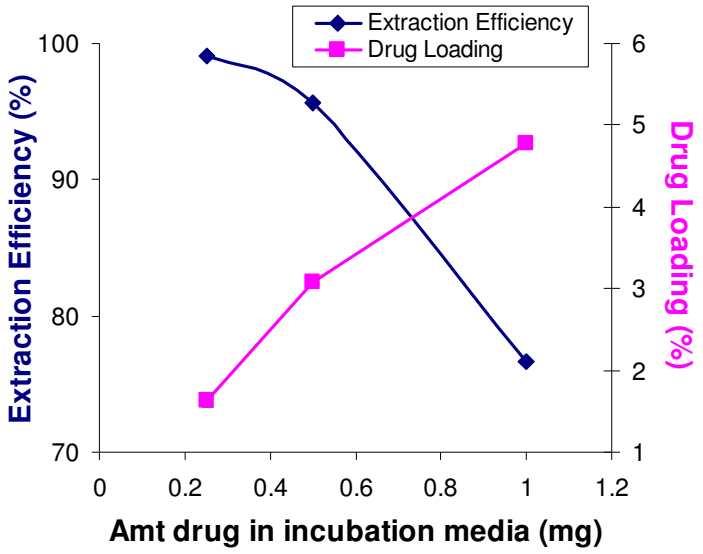

B.

DoxHCl in incubation media (mg)	Zeta potential- before extraction (mV)	Zeta potential- after extraction (mV)	Particle size (nm)
0.25	-35.4	-24.5	120.2
0.5	-35.4	-26.6	123.0
1	-35.4	-22.1	117.1

Figure 3. 13. DoxHCl extraction/absorption into KTpClPB-loaded 502H nanoparticles at different amounts of doxHCl to 15 mg nanoparticles with extraction efficiency and drug loading (A) and associated table of zeta potential and size of drug-loaded nanoparticles at the two temperatures (B).

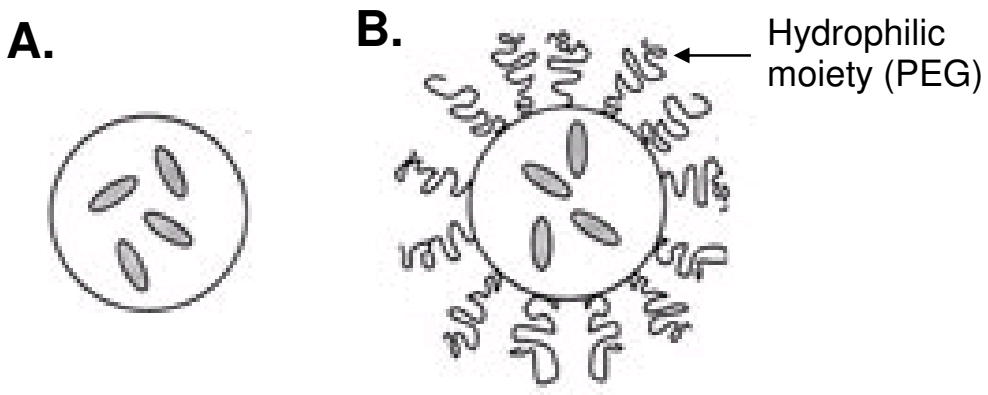

Figure 3. 14. Schematic of (A) regular vs. (B) PEGylated nanoparticles.

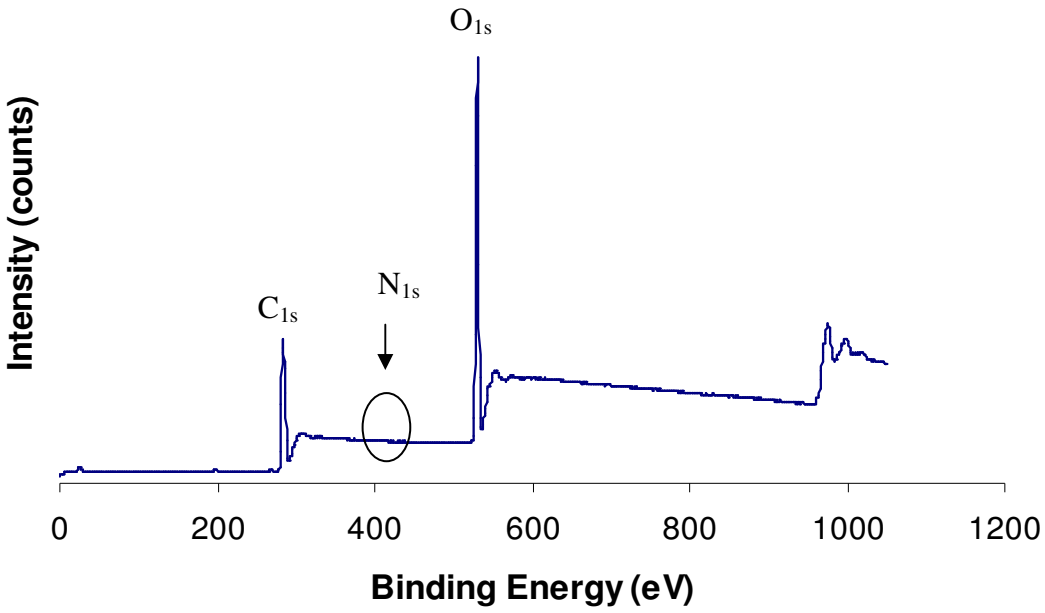

Figure 3. 15. General XPS survey scans of PEGylated nanoparticles with characteristic peaks for carbon and oxygen atoms and nitrogen at 400 eV.

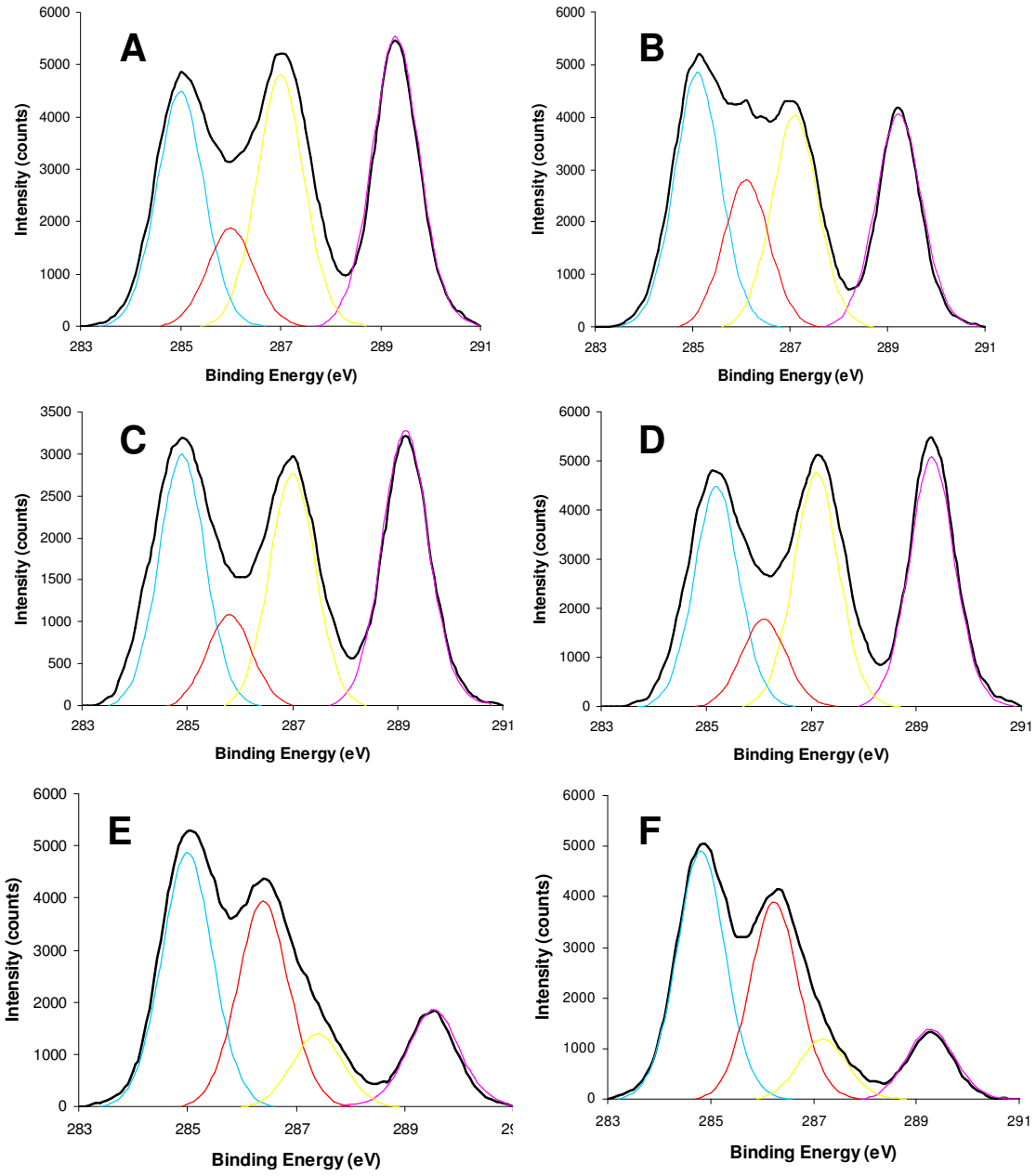

Figure 3. 16. Synthetic XPS peak fits for C_{1s} envelopes of PLGA (A), PEG-PLA (B), PLGA:PEG-PLA (7:1, wt/wt) (C), PLGA + KTpClPB (D), PLGA:PEG-PLA + KTpClPB (E), and PLGA:PEG-PLA + KTpClPB+doxorubicin (F) nanoparticles.

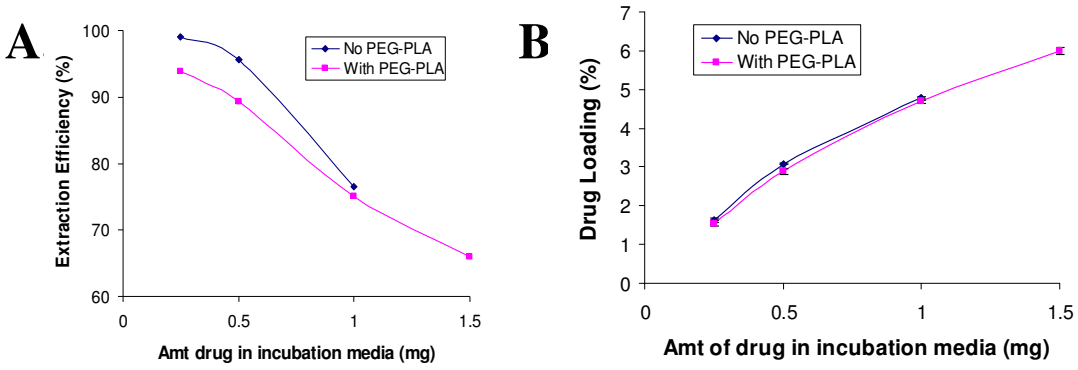

C.

DoxHCl in incubation media (mg)	Zeta potential (mV)		Particle size (nm)	
	Non-PEGylated	PEGylated	Non-PEGylated	PEGylated
0 (blank)	-35.4	-35.7	132.0	128.8
0.25	-24.5	-38.7	120.2	115.0
0.5	-26.6	-33.5	123.0	112.8
1	-22.1	-24.0	117.1	230.1
1.5	NA*	-26.4	NA*	322.1

*Aggregation of non-PEGylated nanoparticles

Figure 3. 17. DoxHCl extraction/absorption into regular or PEGylated nanoparticles at different ratios of doxHCl to 15 mg nanoparticles with extraction efficiency (A) and drug loading (B) and associated table of zeta potential and size of drug-loaded regular or PEGylated nanoparticles (C).

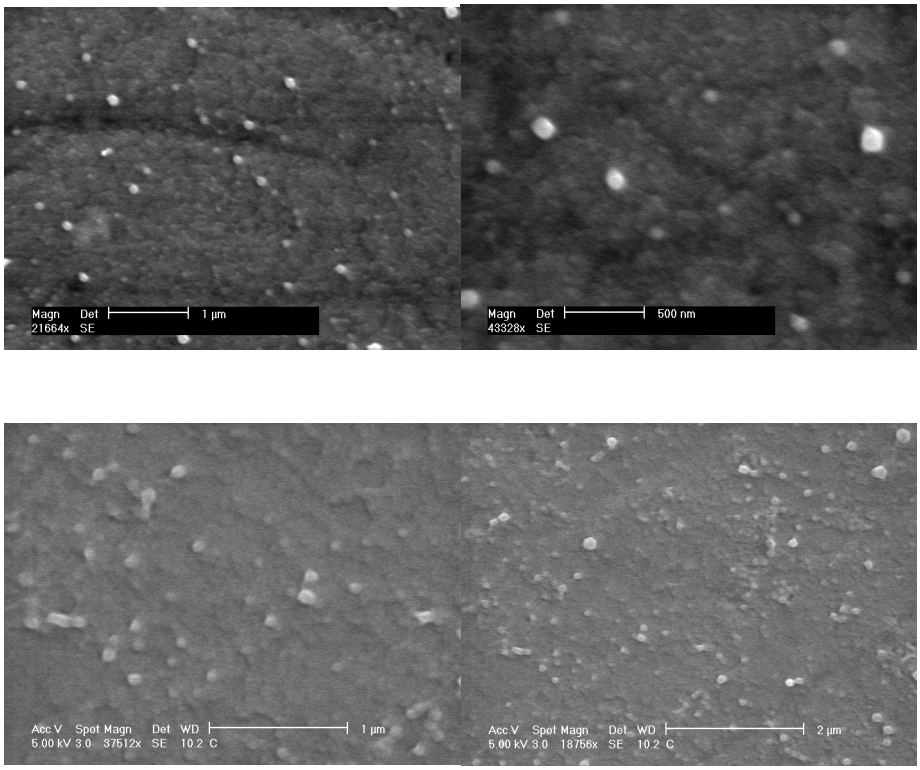

Figure 3. 18. SEM of non-PEGylated (top row) and PEGylated (bottom row) nanoparticles with KTpClPB and doxHCl loaded.

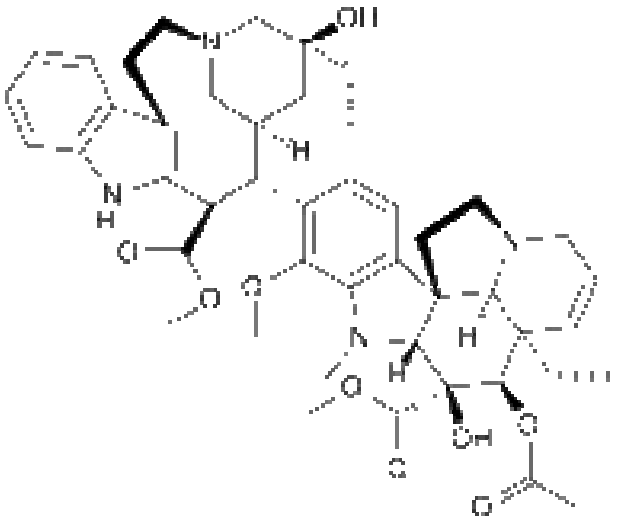

Figure 3. 19. Structure of vinblastine sulfate.

List of references:

Arias, J. L., F. Linares-Molinero, et al. (2008). "Study of carbonyl iron/poly(butylcyanoacrylate) (core/shell) particles as anticancer drug delivery systems - Loading and release properties." European Journal of Pharmaceutical Sciences **33**(3): 252-261.

Arias, J. L., M. A. Ruiz, et al. (2008). "Poly(alkylcyanoacrylate) colloidal particles as vehicles for antitumour drug delivery: A comparative study." Colloids and Surfaces B-Biointerfaces **62**(1): 64-70.

Asuri, P., S. S. Karajanagi, et al. (2007). "Enhanced stability of enzymes adsorbed onto nanoparticles." Journal of Nanoscience and Nanotechnology **7**(4-5): 1675-1678.

Blasi, P., S. S. D'Souza, et al. (2005). "Plasticizing effect of water on poly(lactide-co-glycolide)." Journal of Controlled Release **108**(1): 1-9.

Cai, C., U. Bakowsky, et al. (2008). "Charged nanoparticles as protein delivery systems: A feasibility study using lysozyme as model protein." Eur J Pharm Biopharm **69**(1): 31-42.

Dong, Y. C. and S. S. Feng (2004). "Methoxy poly(ethylene glycol)-poly(lactide) (MPEG-PLA) nanoparticles for controlled delivery of anticancer drugs." Biomaterials **25**(14): 2843-2849.

Gaertner, L. S., C. L. Murray, et al. (1998). "Transepithelial transport of nicotine and vinblastine in isolated malpighian tubules of the tobacco hornworm (Manduca sexta) suggests a P-glycoprotein-like mechanism." Journal of Experimental Biology **201**(18): 2637-2645.

Galindo-Rodriguez, S., E. Allemann, et al. (2004). "Physicochemical parameters associated with nanoparticle formation in the salting-out, emulsification-diffusion, and nanoprecipitation methods." Pharmaceutical Research **21**(8): 1428-1439.

Ganjali, M. R., P. Norouzi, et al. (2006). "Application of 8-amino-N-(2-hydroxybenzylidene)naphthyl amine as a neutral ionophore in the construction of a lanthanum ion-selective sensor." Analytica Chimica Acta **576**(2): 275-282.

Gou, M. L., M. J. Huang, et al. (2007). "Preparation of anionic poly(epsilon-caprolactone)-poly(ethylene glycol)poly(epsilon-caprolactone) copolymeric nanoparticles as basic protein antigen carrier." Growth Factors **25**: 202-208.

Gupta, V. K., A. K. Singh, et al. (2008). "Electroanalytical performance of a terbium(III)-selective sensor based on a neutral ionophore in environmental and medicinal samples." Analytical and Bioanalytical Chemistry **390**(8): 2171-2181.

Heald, C. R., S. Stolnik, et al. (2002). "Poly(lactic acid)-poly(ethylene oxide) (PLA-PEG) nanoparticles: NMR studies of the central solidlike PLA core and the liquid PEG corona." Langmuir **18**(9): 3669-3675.

Jung, T., A. Breitenbach, et al. (2000). "Sulfobutylated poly(vinyl alcohol)-graft-poly(lactide-co-glycolide)s facilitate the preparation of small negatively charged biodegradable nanospheres." Journal of Controlled Release **67**(2-3): 157-169.

Kang, J. C. and S. P. Schwendeman (2003). "Determination of diffusion coefficient of a small hydrophobic probe in poly(lactide-co-glycolide) microparticles by laser scanning confocal microscopy." Macromolecules **36**(4): 1324-1330.

Krauel, K., N. M. Davies, et al. (2005). "Using different structure types of microemulsions for the preparation of poly(alkylcyanoacrylate) nanoparticles by interfacial polymerization." Journal of Controlled Release **106**(1-2): 76-87.

Missirlis, D., R. Kawamura, et al. (2006). "Doxorubicin encapsulation and diffusional release from stable, polymeric, hydrogel nanoparticles." European Journal of Pharmaceutical Sciences **29**(2): 120-129.

Olivier, J. C., R. Huertas, et al. (2002). "Synthesis of pegylated immunonanoparticles." Pharmaceutical Research **19**(8): 1137-1143.

Park, K. (2007). "Nanotechnology: What it can do for drug delivery." Journal of Controlled Release **120**(1-2): 1-3.

Pourcelle, V., S. Devouge, et al. (2007). "PCL-PEG-Based nanoparticles grafted with GRGDS peptide: Preparation and surface analysis by XPS." Biomacromolecules **8**: 3977-3983.

Scholes, P. D., A. G. A. Coombes, et al. (1999). "Detection and determination of surface levels of poloxamer and PVA surfactant on biodegradable nanospheres using SSIMS and XPS." Journal of Controlled Release **59**(3): 261-278.

Shakesheff, K. M., C. Evora, et al. (1997). "The adsorption of poly(vinyl alcohol) to biodegradable microparticles studied by x-ray photoelectron spectroscopy (XPS)." Journal of Colloid and Interface Science **185**(2): 538-547.

Soma, C. E., C. Dubernet, et al. (2000). "Investigation of the role of macrophages on the cytotoxicity of doxorubicin and doxorubicin-loaded nanoparticles on M5076 cells in vitro." Journal of Controlled Release **68**(2): 283-289.

Soppimath, K. S., T. M. Aminabhavi, et al. (2001). "Biodegradable polymeric nanoparticles as drug delivery devices." Journal of Controlled Release **70**(1-2): 1-20.

Wong, H. L., R. Bendayan, et al. (2004). "Development of solid lipid nanoparticles containing lonically complexed chemotherapeutic drugs and chemosensitizers." Journal of Pharmaceutical Sciences **93**(8): 1993-2008.

Yang, Y. Y., Y. Wang, et al. (2006). "Polymeric core-shell nanoparticles for therapeutics." Clinical and Experimental Pharmacology and Physiology **33**(5-6): 557-562.

Yoo, H. S., J. E. Oh, et al. (1999). "Biodegradable nanoparticles containing doxorubicin-PLGA conjugate for sustained release." Pharmaceutical Research **16**(7): 1114-1118.

Zobel, H. P., A. Zimmer, et al. (1999). "Evaluation of aminoalkylmethacrylate nanoparticles as colloidal drug carrier systems. Part I: synthesis of monomers, dependence of the physical properties on the polymerization methods." European Journal of Pharmaceutics and Biopharmaceutics **47**(3): 203-213.

Chapter 4

Comparison of Reverse Loading with Common Emulsion-Based Loading Methods for Preparation of DoxHCl /PLGA Nanoparticles

4.1 Abstract

Traditional delivery of doxorubicin hydrochloride (doxHCl) by emulsion-based polymeric nanoparticles, where drug is entrapped into nanoparticles during its formation, have suffered from low drug loading and poor encapsulation efficiency as well as burst release. During this study, doxHCl was loaded with a novel reverse drug loading procedure, where drug was loaded into pre-formulated blank nanoparticles, and compared with traditional emulsion nanoparticles (water-in-oil-in-water (W/O/W) and oil-in-water (O/W)). A lipophilic borate-based anion, KTpClPB, was incorporated into the nanoparticles for optimized reverse drug loading and drug incorporation. Results showed traditional entrapment methods (W/O/W and O/W) were improved by incorporation of the lipophilic anion KTpClPB into polymeric nanoparticles, with drug loading increasing from 1.3% up to 3.3%. Comparatively, reverse drug loading, after optimization and using KTpClPB-loaded polymeric nanoparticles, reached doxHCl loading of up to 7% using a simple process. Release from reverse drug loaded nanoparticles showed an initial 30% drug release within 3 hours with close to 80% drug released in 2 days, however, there were no significant differences in drug release profiles between traditional or reverse loaded nanoparticles and presence of KTpClPB did not appear to improve drug release. Overall, the results showed the reverse loading strategy was superior to traditional drug loading strategies for drug delivery.

4.2 Introduction

Over the past several decades, interest in using biodegradable polymeric nanoparticles as drug delivery vehicles have intensified due to advantages such as small

size, ability to load and preserve the efficacy of different drugs, passive and active targeting and formulation using different polymers to confer different properties. In terms of size range, polymeric nanoparticles have diameters between 10 to 1000 nm, allowing them to freely circulate in the bloodstream without causing blockage (Yang, Wang et al. 2006). Different types of drugs may also be encapsulated into nanoparticles through entrapment, chemical conjugation, or adsorption methods; which can protect drugs against degradation, promote controlled and sustained drug release, and reduce side effects (Soppimath, Aminabhavi et al. 2001; Sahoo and Labhasetwar 2003). In addition, nanoparticles can improve drug accumulation at disease sites via passive or active targeting. Passive targeting takes advantage of a phenomenon called enhanced permeability and retention (EPR) effect, where nanoparticles accumulate in solid tumor regions with a more leaky and permeable vasculature and impaired lymphatic drainage. Active targeting can be achieved by conjugating ligands, such as antibodies, peptides, and sugars, which target antigens overexpressed on disease cells of interest, to the surface of nanoparticles (deVerdiere, Dubernet et al. 1997; Maeda, Wu et al. 2000; Abou-Jawde, Choueiri et al. 2003; Yang, Wang et al. 2006). Moreover, numerous polymers have been synthesized to study improved nanoparticle production and design, with the polyester family, including members such as poly(lactic acid) (PLA), poly(ε-caprolactone) (PCL), and poly(lactide-co-glycolide) (PLGA), receiving attention because of their biocompatibility and biodegradability (Astete and Sabliov 2006); PLGA, in particular, has been used in numerous FDA-approved medical devices.

One drug that has benefited from polymeric nanoparticle delivery is doxorubicin hydrochloride (doxHCl) (Fig. 4.1). This chemotherapeutic drug is effective against a range of tumor cells and kills cells by intercalating between DNA helix to prevent cell replication. It is made of hydrophobic fused rings covalently linked to a hydrophilic sugar moiety with an attached amine group with a pKa of 8.2. Despite their effectiveness, doxHCl has many side effects, including life-threatening cardiotoxicity, due to poor targeting ability and short plasma half-life.

DoxHCl efficacy has been improved using polymeric nanoparticles formulated through traditional emulsion-based methods where drug can be dissolved in the aqueous phase or first extracted into an organic phase to facilitate drug entrapment during

nanoparticle formation; although new problems that have arisen include low drug loading, low encapsulation efficiency and initial burst release (Soppimath, Aminabhavi et al. 2001; Galindo-Rodriguez, Allemann et al. 2004). Examples of these different emulsion formulations include oil-in-water (O/W) emulsion, where doxHCl is converted into hydrophobic doxorubicin and dissolved in the oil phase along with a polymer and emulsified to form nanoparticles, and water-in-oil-in-water (W/O/W) emulsion, where doxHCl is dissolved in an inner aqueous phase and emulsified into polymer-containing oil phase, and then this primary emulsion is again emulsified into an outer aqueous phase to form nanoparticles.

In recent years, another loading strategy, adsorption drug loading, where blank nanoparticles are incubated in a concentrated drug solution to facilitate drug uptake, has been applied more frequently and has proven to be effective for loading different drugs at relatively high loading (Asuri, Karajanagi et al. 2007; Arias, Linares-Molinero et al. 2008). More recently, this strategy has been combined with another technique, ion complexation, which takes advantage of electrostatic interactions between drug molecules and opposite charges embedded in nanoparticles to increase drug loading and encapsulation efficiency to further enhance drug uptake. Together, this created an active uptake mechanism that can "sucks" up drugs it comes into contact with, instead of solely relying on passive drug concentration gradient for drug to diffuse into nanoparticles. For this reason, this uptake procedure will be referred to as "reverse drug loading" during this study.

Various studies have demonstrated benefits of ion complexing nanoparticles for improved drug loading, encapsulation efficiency, release profile, and pharmacokinetic drug distribution (Janes, Fresneau et al. 2001; Cavalli, Gasco et al. 2002; Wong, Bendayan et al. 2004; Wong, Rauth et al. 2006; Cafaggi, Russo et al. 2007; Chavanpatil, Khdair et al. 2007; Tian, Bromberg et al. 2007). Currently, this strategy has been mainly used with anionic polymers or copolymers specially synthesized for uptake of protein/peptides due to their potential degradation under normal drug loading conditions. Examples of this include using sulfobutylated poly(vinyl alcohol)-graft-poly(lactide-*co*-glycolide) to incorporate tetanus toxoid (Jung, Breitenbach et al. 2000), poly(ε-caprolactone)-poly(ethylene glycol)-poly(ε-caprolactone) to enhance human basic

fibroblast growth factor incorporation and using poly(styrene-*co*-4-styrene-sulfonate) to enhance lysozyme loading (Cai, Bakowsky et al. 2008).

With all the potential advantages of ion complexing nanoparticles and reverse drug loading, this system will be applied to doxHCl to promote its loading relative to existing emulsion-based method. This study was designed as follows. First, a model lipophilic anion, KTpClPB, will be tested for its potential to be loaded into polymeric nanoparticles using O/W or W/O/W emulsion procedures. Then, various properties, such as drug loading, particle size, and *in vitro* release, will be compared for traditional O/W and W/O/W nanoparticles with entrapped doxHCl and ion-pairing nanoparticles with doxHCl taken up via reverse loading. Lastly, optimization of reverse loading procedure will be done to further improve drug uptake and loading.

4.3 Materials/Methods

4.3.1 Materials

Potassium tetrakis(4-chlorophenyl)borate (KTpClPB) was purchased from Sigma-Aldrich. Doxorubicin hydrochloride (doxHCl) (>99% purity, lyophilized powder) was purchased from Hisun Pharmaceuticals (China) and vinblastine sulfate (>99% purity) was generously donated by Hisun Pharmaceuticals (China). Poly(D,L-lactide-*co*-glycolide), 50/50, with inherent viscosity of 0.2 dL/g and MW_w of 15 kDa (resomer 502H) and 0.34 dL/g and MW_w of 38 kDa (resomer 503H), were purchased from Boehringer Ingelheim. Poly(vinyl alcohol) (PVA) of MW_w of 25,000 (88% hydrolyzed) was purchased from Polysciences Inc. L-lactide (>99% purity) was purchased from Sigma-Aldrich. Methoxy-poly(ethylene glycol) (mPEG-NH_2, MW_w = 5,000) was purchased from Nektar Therapeutics. Spectra/por 7 dialysis bags (MWCO: 10-12K or 50K, Spectrum) were purchased from Fisher Scientific. All other chemicals and solvents were of analytical grade and purchased from commercial suppliers.

All other chemicals and solvents were of analytical grade and purchased from commercial suppliers.

4.3.2 PEG-PLA copolymer synthesis

The methoxy-poly(ethylene glycol)-poly(lactic acid) (PEG-PLA) was synthesized by a standard ring opening polymerization. Briefly, L-lactide (Sigma, 98% purity) was pre-purified by recrystallization from ethyl acetate and the catalyst, stannous octoate (Tin(II) 2-ethylhexanoate, Sigma, 95% purity), was pre-purified by distillation. The desired molar ratio of L-lactide to mPEG-NH_2 was weighed out and added to the reaction flask followed by addition of stannous octoate at equivalent molar ratio to mPEG-NH_2. Dry toluene (10 mL / 1.5 g of reactants) was added to dissolve and mix the reagents. The reaction proceeded with stirring at 110^{o}C for 2 hours under moisture-free argon atmosphere. At the end of the polymerization step, copolymer was purified and recovered as follows. The copolymer crystallized upon cooling and was dissolved with cooled dichloromethane followed by ether addition to reprecipitate the copolymer. The previous procedure was repeated and the copolymer was collected by filtration on a Buchner funnel. They were then dried at 37^{o}C in a vacuum oven overnight.

PEG-PLA was analyzed by ^{1}H NMR spectroscopy using a Bruker DRX 500 spectrometer (Bruker Biospin Inc., Billerica, MA) operating at 500 MHz. Peak areas for different hydrogens were used for PEG-PLA molecular weight determination.

4.3.3. General nanoparticle preparation

Nanoparticles were formulated using either oil-in-water (O/W) or water-in-oil-in-water (W/O/W) emulsion procedure (Fig. 4.2). For O/W emulsion, different amounts of polymer were dissolved in 2 mL ethyl acetate (oil phase) and emulsified, by sonication (20 seconds) on ice using a probe sonicator (Sonics VibraCell) at 50% power, in 2 mL 3% PVA solution (aqueous phase). The O/W emulsion was diluted into 40 mL of 0.075% PVA solution under rapid magnetic stirring for 4-5 hours. Nanoparticle suspensions were collected and washed using an Amicon Stirred Cell with a 50 nm Millipore Nitrocellulose filter. W/O/W emulsion formulation was similar to O/W except that 0.3 mL of DIW (inner aqueous phase) was first emulsified, by sonication (30 seconds) on ice using a probe sonicator (Sonics VibraCell) at 50% power, in 2 mL ethyl acetate (oil phase)

containing dissolved polymer. This primary emulsion was further emulsified in 2.4 mL of 3% PVA solution (outer aqueous phase).

KTpClPB-loaded nanoparticles were formulated using the same O/W or W/O/W procedure above except that predetermined amounts of KTpClPB were dissolved in ethyl acetate before emulsification.

For doxHCl loading into O/W nanoparticles during formulation (emulsion procedures), the process remained the same except that ethyl acetate with known KTpClPB concentration was used to extract doxHCl from aqueous to the ethyl acetate phase and then used as the oil phase. DoxHCl concentration in the aqueous phase before and after extraction was determined using HPLC protocol (see below) to determine the amount of doxHCl in the ethyl acetate (oil) phase. For drug loading into W/O/W nanoparticles, all steps remained the same except that 2.5 mg doxHCl was first dissolved in the inner aqueous phase.

PEGylated nanoparticles were formulated using the same O/W procedure above with modifications. 502H PLGA and KTpClPB were dissolved in 2 mL ethyl acetate and mixed with PEG-PLA dissolved in 0.2 mL methylene chloride. This oil phase was emulsified in 2.2 mL of 3% PVA solution. All other steps were unchanged.

4.3.4 DoxHCl concentration determination methods

4.3.4.1 HPLC method

A Waters HPLC system (Waters, Milford, MA) was used for chromatographic separation of doxHCl. It consisted of a 1525 Binary HPLC pump, 717 plus autosampler, and 474 scanning fluorescence detector. Waters Breeze® chromatography software was used to acquire and process data. A Waters Nova-Pak® C_{18} column (3.9 x 150 mm I.D.) (Waters, Milford, MA) was used with a filtered and degassed ACN : 20 mM, pH 3 potassium phosphate : TFA (30:70:0.1, v/v/v) mobile phase. Chromatography was performed at a flow rate of 1 mL/min and fluorescence detection was set at $\lambda_{excitation}$ of 480 nm and $\lambda_{emission}$ of 590 nm at room temperature.

DoxHCl in the samples were analyzed using corresponding standards injected separately.

4.3.4.2 UV method

A Beckman DU650 spectrophotometer was used for UV analysis. Samples or standards containing doxHCl in methanol were analyzed using a quartz spectrophotometer cell (Starna Cells Inc.) at a scanning rate of 1200/min and scanning range of 400-750 nm. Absorbance wavelength was set at 480 nm and all sample had baseline reading set at 750 nm.

4.3.5 Nanoparticle physical characterization

4.3.5.1 Particle size/zeta potential determination

Nanoparticle suspensions were diluted to 0.5 mg/mL and transferred into fold capillary cells for both zeta potential and particle size determination. Samples were analyzed using a Malvern ZetaSizer Nano ZS (Malvern Instruments).

4.3.5.2 SEM morphological analysis

Nanoparticle suspensions were diluted to 50 µg/mL and dried overnight on viewing stubs. Morphology was observed, after coating with a layer of gold (2-5 nm), by scanning electron microscopy (Philips XL30 Field Emission Gun Scanning Electron Microscopy).

4.3.6 Reverse drug loading procedure

Drug was dissolved to desired concentrations in deionized water (DIW). Both the drug solution and a blank nanoparticle suspension (with known concentration) were added consecutively into DIW so that 1) drug and nanoparticle reach desired concentrations and relative weight ratio and 2) final suspension volume reached 4 mL. Mixtures were shaken (Ika KS130 instrument) for 1 hour at different temperatures.

After drug loading, mixtures were dialyzed in spectra/por 7 dialysis bag (MWCO: 50K, Spectrum) against 1 liter of DIW (replaced every hour during the first 3 hours) over

24 hours. Dialyzed suspensions were used for size, zeta potential, and drug loading determination.

4.3.7 Drug loading determination

Drug-loaded nanoparticle suspensions were lyophilized (in triplicate) and weighed into 2 mL polypropylene tubes. 0.1 mL methylene chloride was added to nanoparticles, followed by shaking for 10 minutes, then addition of 1.5 mL methanol and shaking for over 12 hours. These suspensions were spun down at 13,200 RPM for 8 min. Supernatant containing dissolved drug was diluted using methanol. Drug concentration was analyzed using UV doxHCl concentration determination procedure above.

4.3.8 *In vitro* drug release

Known amounts of drug-loaded nanoparticles or free doxorubicin hydrochloride were suspended or dissolved in 0.4 mL phosphate buffered saline (PBS) in a dialysis bag (spectra/por 7, MWCO: 50K). The dialysis bag was incubated in 15 mL PBS and shaken (Ika KS130) at 37^{o}C. Release media was collected and completely replaced at pre-determined time intervals with fresh incubation media. Drug concentration in the release media was analyzed using HPLC analysis procedure above.

4.4 Results/Discussion

4.4.1 Traditional nanoparticle formulation strategies

Drug loading, an essential property of nanoparticles, may be important for reducing total administered dose of a drug and administration time per dose as well as indirectly improving drug targeting and reduce side effects. For polymeric nanoparticles, a common formulation/drug loading strategy was emulsification/solvent evaporation, where drugs were encapsulated or entrapped during nanoparticle formation. Two of the most commonly utilized versions of this strategy include water-in-oil-in-water (W/O/W) and oil-in-water (O/W) emulsions (Verrecchia, Huve et al. 1993; Sjostrom, Kaplun et al. 1995; Zambaux, Bonneaux et al. 1998). Despite their effectiveness, improvements in

drug loading and encapsulation efficiency for hydrophilic small molecule drugs such as doxorubicin hydrochloride (doxHCl) may be possible. Here, ion pairing strategy, with incorporation of a model lipophilic anion, KTpClPB, was combined with emulsion formulation to test for improvements in drug loading and encapsulation efficiency of a model drug, doxorubicin hydrochloride (doxHCl).

Traditional W/O/W and O/W emulsion, with doxHCl and KTpClPB incorporation during nanoparticle formation, were formulated using a procedure outlined in Fig. 4.3. An earlier study (Chapter 3, Table 3.2) had proven KTpClPB encapsulation into polymeric nanoparticles although more than half of these molecules were lost during formulation. For all nanoparticle formulations, PLGA 502H, which has a high acid number (Table 4.1), was used. Acid number was directly correlated to the number of carboxylic acids present, thus higher acid number indicated increased binding potential to cationic hydrophilic small molecule drugs (Chapter 3, Fig 3.9).

In this study, to properly compare between the two traditional emulsion formulations, initial doxHCl addition were maximized; although because the drug was loaded into different phases for the two emulsions using different methods, the maximal amounts in both cases were different.

4.4.1.1 Comparison of traditional formulations

Previous data (Chapter 3, Fig 3.9) showed nanoparticles with smaller diameters had higher drug loading due to higher surface area/volume ratio and possibly higher charge density per particle. For this reason, KTpClPB-loaded W/O/W and O/W nanoparticles were each formulated at three different polymer concentrations (20, 30, or 40 mg/mL) in ethyl acetate to try to reduce particle size while KTpClPB-free W/O/W nanoparticles were used as controls.

4.4.1.1.1 SEM and particle sizing

SEM images of nanoparticles showed spherical morphology for the different nanoparticles with average size between 100-200 nm (Fig. 4.6). For KTpClPB-loaded samples, reducing polymer concentration decreased nanoparticle size from 123.8 nm to

109.7 nm for O/W nanoparticles and from 115.8 nm to 95.8 nm for W/O/W particles (Fig. 4.4C) with KTpClPB added. While not shown, W/O/W nanoparticles, without KTpClPB addition, were greater than 170 nm in diameter. This result proved KTpClPB incorporation could reduce particle size to a more desirable range of around 100 nm and reduced polymer concentration could also reduce particle size, although statistically, this might not be significant.

4.4.1.1.2 Drug loading and encapsulation efficiency

KTpClPB incorporation was important for drug loading as this increased from 1.3% to 3.3% with addition of KTpClPB into W/O/W nanoparticles (Fig. 4.4A). Comparison between KTpClPB-loaded O/W and W/O/W nanoparticles showed O/W nanoparticles had higher drug loading across all polymer concentrations although the difference was only around 0.5% - 1% (Fig. 4.4B). Higher drug loading values for O/W nanoparticles were also deceiving because 5 mg of doxHCl was initially present during O/W nanoparticle formulation through extraction into the oil phase while only 2.5 mg doxHCl was dissolved in the inner aqueous phase of W/O/W nanoparticles during formulation (PLGA and KTpClPB amounts equal for both emulsions). This meant encapsulation efficiency, or amount of original drug added that was retained, was better for W/O/W nanoparticles, ranging from 62-71%, than O/W nanoparticles, which ranged from 37-53% (Fig. 4.4C). Because higher drug loading represented a potentially more efficacious dose while higher encapsulation efficiency could mean less wasted drug, it was important to know which property was more desirable in order to select a suitable formulation unless an improved drug loading strategy, which could maximize both factors, can be proposed.

For both emulsion formulations with KTpClPB added, the highest loading was achieved at 20 mg/mL polymer concentration (3.3% for W/O/W and 3.8% for O/W nanoparticles), and both values were comparable to or better than previously published results for similar nanoparticles (Yoo, Oh et al. 1999; Yi, Kim et al. 2005; Chavanpatil, Khdair et al. 2007). Further increases in drug loading may be possible by increasing the theoretical drug loading (drug amount added/total material added, wt/wt) and this was the initial rationale behind reducing the polymer concentration while keeping initial drug

amount added constant. However, results from Fig. 4.4A and 4.4B suggested further reduction in polymer concentration might not achieve significant improvements. In addition, since the volume of the inner aqueous phase of W/O/W nanoparticles limited the amount of drug that could be initially added (due to solubility constraints) while doxHCl extraction into the oil phase of O/W nanoparticles was limited by KTpClPB solubility in the organic phase, the above drug loading values for these formulations appeared to be maximized and a new drug loading approach was required to dramatically improve drug loading.

4.4.1.1.3 *In vitro* release

Desirable drug release profile for nanoparticles should be zero-order and lasting over several weeks. However, currently, unless drug molecules were chemically conjugated to individual polymers within a nanoparticle, it was difficult to achieve this. Typical *in vitro* drug release profiles for many polymeric nanoparticles showed an initial burst of over 40% within the first 3 hours of release (Soma, Dubernet et al. 2000; Wong, Bendayan et al. 2004; Missirlis, Kawamura et al. 2006) with limited release afterwards. For the present systems, *in vitro* drug release profiles were also biphasic with a relatively fast initial release within the first 3-6 hours followed by very slow release afterwards until a plateau starts to develop after 12-24 hours of release (Fig. 4.5). KTpClPB-loaded W/O/W nanoparticles showed the smallest burst release after 3 hours with less than 20% drug released, while KTpClPB-loaded O/W nanoparticles had the largest burst release after 3 hours with around 40% drug released. Despite a higher burst release within the first 3 hours, KTpClPB-loaded O/W nanoparticles demonstrated a more complete release after 2 days with 87% of total drug released while KTpClPB-loaded W/O/W nanoparticles only released 55% of total loaded drug. For W/O/W nanoparticles with no KTpClPB, there was a higher initial burst release, but also more complete release by 2 days, relative to KTpClPB-loaded W/O/W nanoparticles.

Based on the *in vitro* release profiles, drug release appeared to be diffusion-controlled for all the formulations and KTpClPB did not offer obvious benefits for slowing down drug release. Other than that, it was hard to draw conclusions from this information given that KTpClPB-free W/O/W nanoparticles had less than half the drug

loading compared with KTpClPB-loaded W/O/W or O/W nanoparticles (Fig. 4.4) and due to random errors at different timepoints, it was also hard to conclude if any of the formulations demonstrated smaller burst release than the others. However, based on total drug release after two days, it was obvious O/W nanoparticles were more desirable for drug delivery than W/O/W nanoparticles.

4.4.2 Reverse drug loading

4.4.2.1 Description

Even though actual doxHCl loading into traditional W/O/W and O/W emulsion nanoparticles was relatively high according to previous results, an alternative strategy which might further increase drug loading and encapsulation efficiency was "reverse drug loading", where blank nanoparticles were incubated in a concentrated drug solution to facilitate drug uptake (Fig. 4.7). In this case, since nanoparticles contained a lipophilic anion, KTpClPB, active drug uptake was possible via electrostatic interactions and potentially hydrophobic interaction (pi-pi stacking).

Blank nanoparticles in this study were formulated using a blend of PLGA (502H) and PEG-PLA (7:1, wt/wt) polymers with maximal KTpClPB addition. This system offered several advantages over existing systems in that 1) nanoparticle formulation was a simple O/W emulsion procedure with a simple washing process, 2) PEG polymer presence on nanoparticle surface created a hydrophilic shell to prevent protein adsorption and particle-particle aggregation, 3) KTpClPB promoted electrostatic interactions with cationic drug molecule such as doxHCl, 4) aromatic rings of KTpClPB provided additional hydrophobic interactions (pi-pi stacking) with aromatic rings on drug molecules such as doxHCl, and 5) higher acid number of PLGA (502H) led to more free carboxylic acids for additional charge-charge interactions with cationic drugs.

Several factors were further evaluated to optimize the reverse loading procedure before comparing this formulation with traditional emulsion formulations.

4.4.2.2 Optimization: incubation time

Drug absorption kinetics, or the rate at which drug molecules bind to nanoparticles, could be important because nanoparticle systems that take up drug quickly could offer time-saving advantages during manufacturing as well as potential applications for drug uptake in human body, where contact time between nanoparticles and dissolved drugs could be very short. For this study, a 12 hour incubation period was chosen and drug loading and encapsulation efficiency were determined after different incubation periods. Results showed there were no significant changes for either drug loading or encapsulation efficiency during this time (Fig. 4.8A). Drug loading varied from 3.8% to 4.1% while encapsulation efficiency ranged from 61% to 67%. More interestingly, these values were reached instantly upon mixing (T = 0) and suggested KTpClPB-loaded PEGylated nanoparticles, unlike those KTpClPB-free nanoparticles that depended upon passive drug concentration gradient for loading, actively took up and retained drug molecules it came into contact with. Because incubation time did not appear to be significant with the present system, previous incubation time of 1 hour was kept for future studies.

Even though particle size did not change with incubation time, an unexpected result from this study was that zeta potential values became more positive with longer incubation time (Fig. 4.8B), changing from -30.8 mV to -18.3 mV after 12 hours, even though drug loading did not change significantly. A possible explanation for this phenomenon could be polymer rearrangement over time that either promoted KTpClPB intercalation into the core regions of nanoparticles or perhaps hydrophobic dox/KTpClPB ion pairs gradually changed the surface layer salt composition of nanoparticles over time. Another possible explanation could simply be instrument error. However, if these measurements were correct, then it suggested nanoparticles may aggregate after long incubation periods (not seen here as particle size remained the same) due to surface charge neutralization and suggested shorter incubation periods (less than 2-3 hours) were desirable.

4.4.2.3 Optimization: polymer concentration

Studies with traditional W/O/W and O/W formulations, where doxHCl was encapsulated during particle formation, showed that reducing total polymer concentration

improved drug loading. With that in mind, the total polymer concentration of blank KTpClPB-loaded PEGylated nanoparticles were also decreased from 40 mg/mL in ethyl acetate to 20 mg/mL while the weight ratio between PLGA and PEG-PLA used was held constant.

4.4.2.3.1 Characterization: SEM, sizing and zeta potential

SEM images of PEGylated nanoparticles (Fig. 4.11) with different polymer concentrations showed spherical particles with average size between 100-150 nm, matching readings from the particle sizing instrument (Table 4.2). An interesting observation here was that particle size decreased after reverse drug loading for all the different nanoparticles. This was likely due to formation of hydrophobic ion pairs between doxHCl and KTpClPB that created a more hydrophobic environment and drove more water out of nanoparticles, thus decreasing the hydrodynamic radius of nanoparticles recognized by the particle sizing instrument. Zeta potential of nanoparticles made with the smallest polymer concentration appeared to be the most negative (Table 4.3), suggesting higher density of either PLGA polymer or KTpClPB or both per particle. For all three batches, there was initially a sharp increase in zeta potential (more positive) when increasing amounts of doxHCl was added into the incubation media, suggesting drug uptake and neutralization of surface charges. However, zeta potential values eventually reached a plateau and did not increase with addition of more doxHCl, suggesting any additional drug that was loaded into these nanoparticles localized into the inner core (or at least below the surface layer).

4.4.2.3.2 Drug loading

The different PEGylated nanoparticles were incubated with different amounts of doxHCl up to 2 mg. Results showed drug loading increased with increasing amounts of doxHCl in the incubation media for all three batches of nanoparticles (Fig. 4.9). No more doxHCl was studied after 2 mg doxHCl because according to Fig. 4.9, there was no significant improvement in drug loading between addition of 1.5 mg and 2 mg doxHCl into the incubation media. The three batches of nanoparticles had the same trend as

traditional W/O/W and O/W emulsion formulations, as nanoparticles formulated at the smallest polymer concentration, 20 mg/mL, had the highest drug loading across the different drug amounts incubated. In fact, drug loading increased up to 7% when 2 mg of doxHCl was present in the incubation media for nanoparticles made at 20 mg/mL polymer concentration. However, one of the problems here was that even though drug loading increased dramatically, encapsulation efficiency decreased even more dramatically. Here again, a tradeoff between drug loading and encapsulation efficiency took place and it was important to see which one of the two factors were more important before deciding the initial amount of drug that should be added into the incubation media.

4.4.2.3.3 *In vitro* release

Unlike drug loading results, doxHCl release profiles of all the PEGylated nanoparticles were similar (Fig. 4.10). Drug release was biphasic with an initial burst release of around 30% within the first three hours, followed by slower release afterwards until no more drug could be released after two days. Release was relatively complete with 70% to 80% of total encapsulated drug released in the first 2 days for the different nanoparticles. Considering that drug loading in these particles were approximately 7%, 6% and 6% for 20 mg/mL, 30 mg/mL and 40 mg/mL PEGylated nanoparticles, respectively, a significant amount of drug could be delivered using these systems to potentially enhance cancer cell cytotoxicity.

Based on similar release profiles for PEGylated nanoparticles and traditional W/O/W and O/W formulations with and without KTpClPB, this result again showed that KTpClPB incorporation was not beneficial for slowing down burst release even though electrostatic interactions between KTpClPB and doxHCl helped drug uptake and retention in nanoparticles. A likely hypothesis for this was that significant amounts of dissolved salts in the release media (phosphate-buffered saline) could compete with doxorubicin molecules for KTpClPB binding sites while the presence of sink release conditions, or virtually no drug in the release media, provided a reverse drug concentration gradient facilitating quick doxHCl release.

4.4.3 Comparison between traditional and reverse drug loading strategies

Despite excellent results obtained using both drug loading strategies, it was obvious that in terms of drug loading, reverse drug loading was a much superior method as 7% drug loading was almost twice that for drug loading values obtained using traditional emulsion formulations. This high drug loading, though, was reached by sacrificing encapsulation efficiency as this value decreased from 61-67% (3.8-4.1% drug loading) when 0.5 mg doxHCl was in the incubation media to ~33% (~7% drug loading) when 2 mg drug was present (all other conditions constant, data not shown). However, these values were still comparable to those for traditionally formulated emulsion nanoparticles, where encapsulation efficiency was 61.9% (3.2% drug loading) for KTpClPB-loaded W/O/W nanoparticles and 37.4% (3.8% drug loading) for KTpClPB-loaded O/W nanoparticles. The above data showed that at similar drug loading levels, encapsulation efficiency for reverse loading nanoparticles was comparable to or better than traditional drug loaded formulations. In addition, with similar drug release profiles and similar release rates, reverse loaded nanoparticles, with much higher drug loading, would be expected to release more absolute amounts of drug at different timepoints and promote efficacy.

With the above information in mind, it was clear that reverse drug loading was a more powerful drug loading and drug delivery tool compared to more commonly used strategies and it would also be interesting to see how well reverse loaded nanoparticles work as delivery vehicles.

4.5 Conclusion

Results showed that ion pairing strategy, using KTpClPB, could be used to improve drug loading and encapsulation efficiency of doxorubicin hydrochloride into either traditionally formulated nanoparticles or reverse loaded nanoparticles. Comparatively, traditional formulations, where drug was encapsulated during nanoparticle formation, was a more cumbersome process relative to the more flexible reverse loading procedure and produced larger sized nanoparticles. With KTpClPB incorporation, reverse drug loading, or incubation of doxHCl with preformulated blank

nanoparticles, produced the best results and obtained twice the drug loading after optimization, at 7%, compared with traditional formulation where doxHCl was encapsulated during nanoparticle formation. Unlike previous reports suggesting ion complexation strategy could obtain zero-order drug release, here, using KTpClPB as ion pairing agent, doxHCl release profile was not improved and burst release did not show significant reduction. These results showed reverse drug loading strategy was a more powerful tool for making drug delivery vehicles and these systems could potentially be more efficacious relative to more commonly used drug loading techniques.

Table 4. 1. Properties of PLGA tested

PLGA polymer	Molecular Weight (g/mol)	Viscosity	Acid number
Resomer® RG 502H	~15,000	0.2 dl/g	min. 6 mg KOH/g

Table 4. 2. Size and zeta potential of PEGylated nanoparticles before and after reverse drug loading (all 3 batches of nanoparticles had similar sizes before and after drug loading regardless of initial drug added) as a function of polymer concentration used during nanoparticle preparation

Polymer Concentration	**Representative particle size (nm)**	
	Before drug loading	**After drug loading**
20 mg/ml	128.8	99.1
30 mg/ml	138.2	113.2
40 mg/ml	146.1	124.7

Table 4. 3. Zeta potential of PEGylated nanoparticles before and after reverse drug loading as a function of doxHCl loading concentration

DoxHCl in incubation media (mg)	**Zeta potential of different nanoparticle formulations (mV)**		
	20 mg/ml	**30 mg/ml**	**40 mg/ml**
0 (blank)	-35.7	-38.3	-41.9
0.5	-20.0	-30.9	-31.4
1	-30.2	-28.1	-30.2
1.5	-26.9	-25.6	-30.9
2	-29.6	-25.3	-26.7

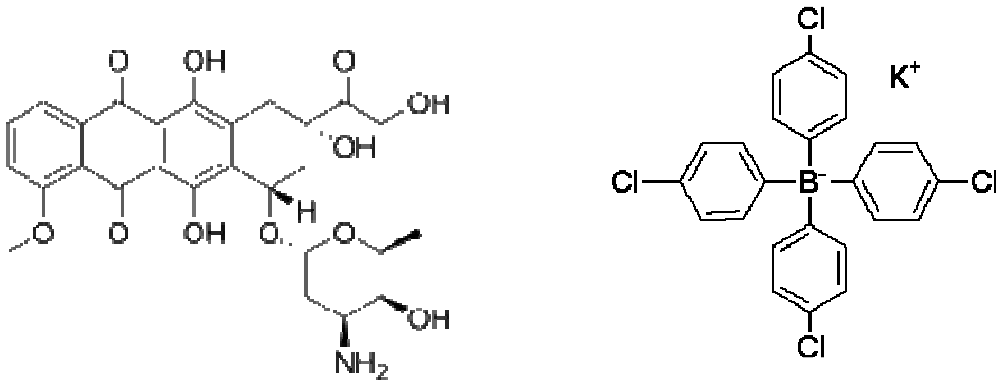

Figure 4. 1. Structure of doxorubicin hydrochloride (doxHCl), right, and potassium tetrakis(4-chlorophenyl)borate (KTpClPB), left.

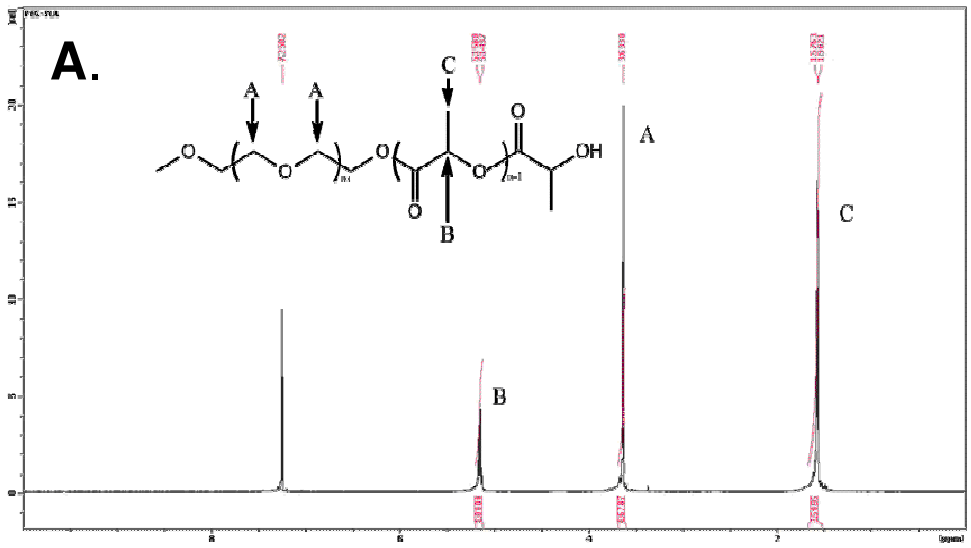

B.

PEG MW (g/mol)	PEG-PLA theoretical MW [1] (g/mol)	PEG-PLA calculated MW [2] (g/mol)	PEG-PLA calculated MW [3] (g/mol)
5,000	25,000	19408.54	22689.8

[1] Calculated based on wt ratios of PEG and l-lactide added during PEG-PLA synthesis
[2] Calculated based on area ratios of peaks A and B
[3] Caclulated based on area ratios of peaks A and C

Figure 4. 2. (A) ^{1}H-NMR spectrum of methoxyPEG-PLA copolymer in deuterochloroform and (B) associated table with theoretical and calculated molecular weights of the copolymer based on peak area ratios.

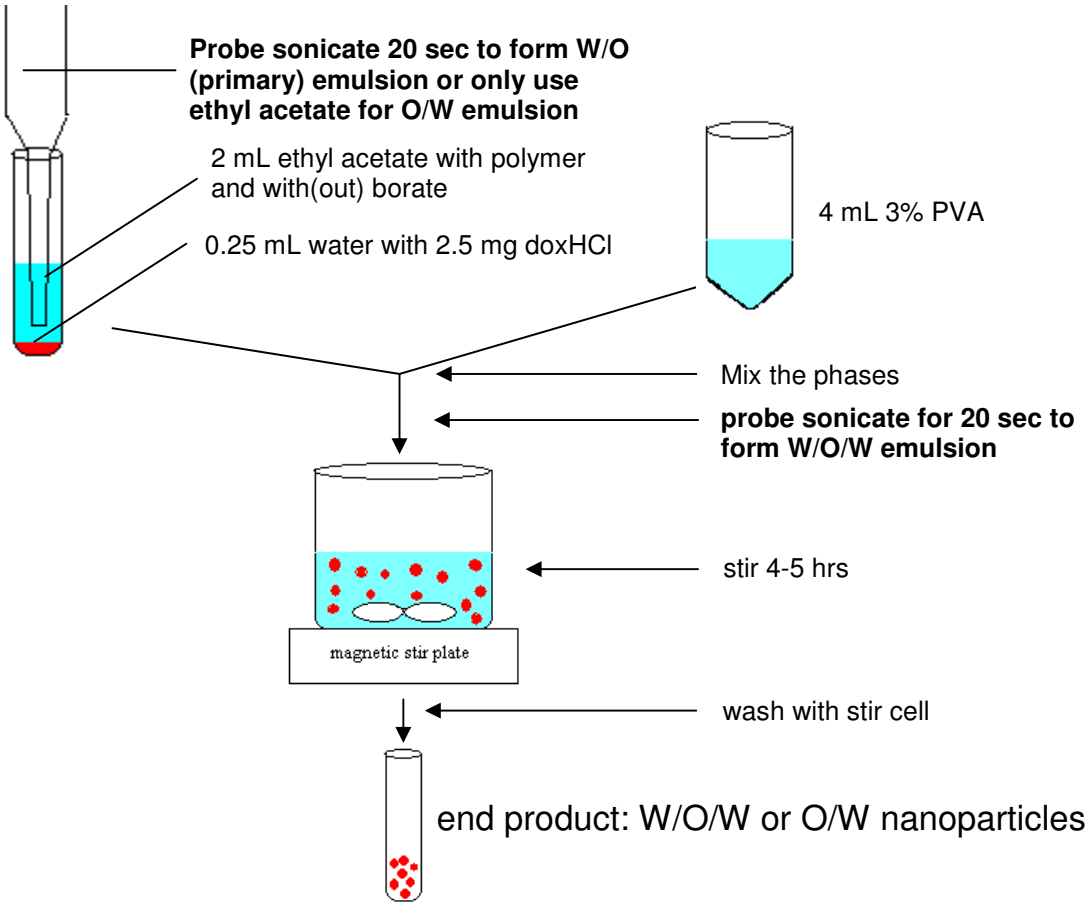

Figure 4. 3. General formulation procedure for drug-loaded W/O/W and O/W emulsion.

A

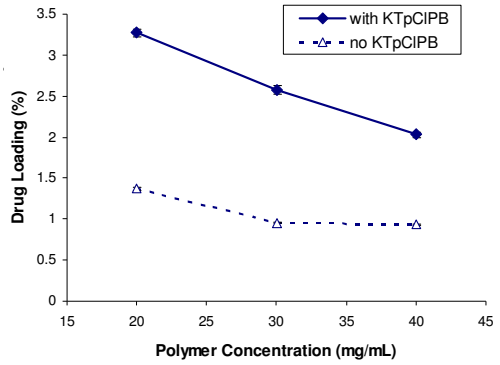

B.

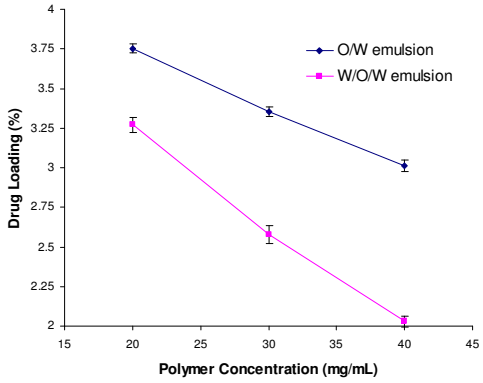

C.

Nanoparticle sample *	Encapsulation efficiency (%)		Particle size (nm)	
	W/O/W-KTpClPB	O/W-KTpClPB	W/O/W	O/W
20 mg/ml	61.9	37.4	95.8	109.7
30 mg/ml	69.5	46.0	107.0	112.3
40 mg/ml	70.9	53.0	115.8	123.8

* Nanoparticle sample denoted by polymer concentration used for nanoparticle preparation

Figure 4. 4. Drug loading comparison between W/O/W nanoparticles with and without KTpClPB encapsulation (A) and comparison between KTpClpB loaded W/O/W and O/W nanoparticles (B). Associated table of encapsulation efficiencies and size (C) for KTpClPB-loaded nanoparticles.

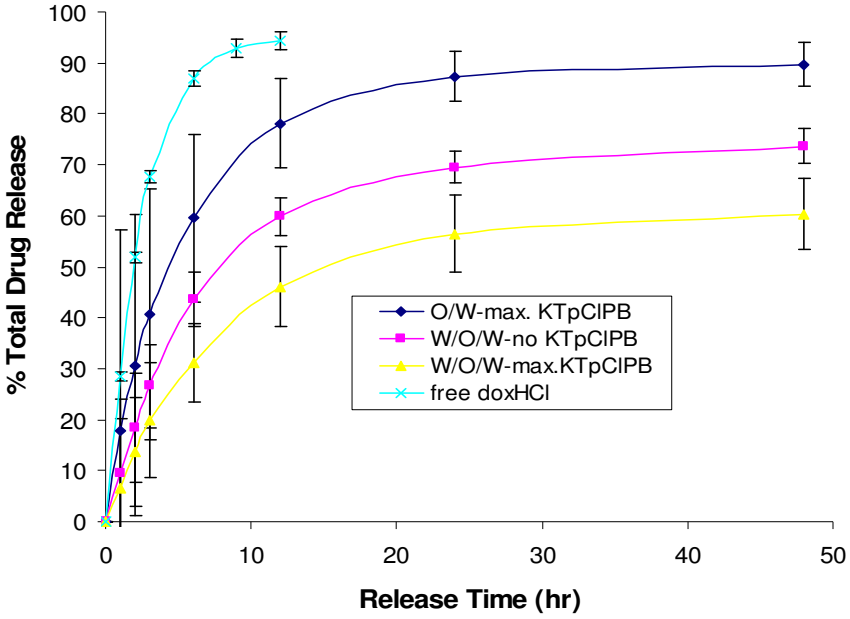

Figure 4. 5. *In vitro* doxHCl release curve for drug-loaded W/O/W nanoparticles (with and without KTpClPB) and O/W nanoparticles (with KTpClpB) versus free doxHCl.

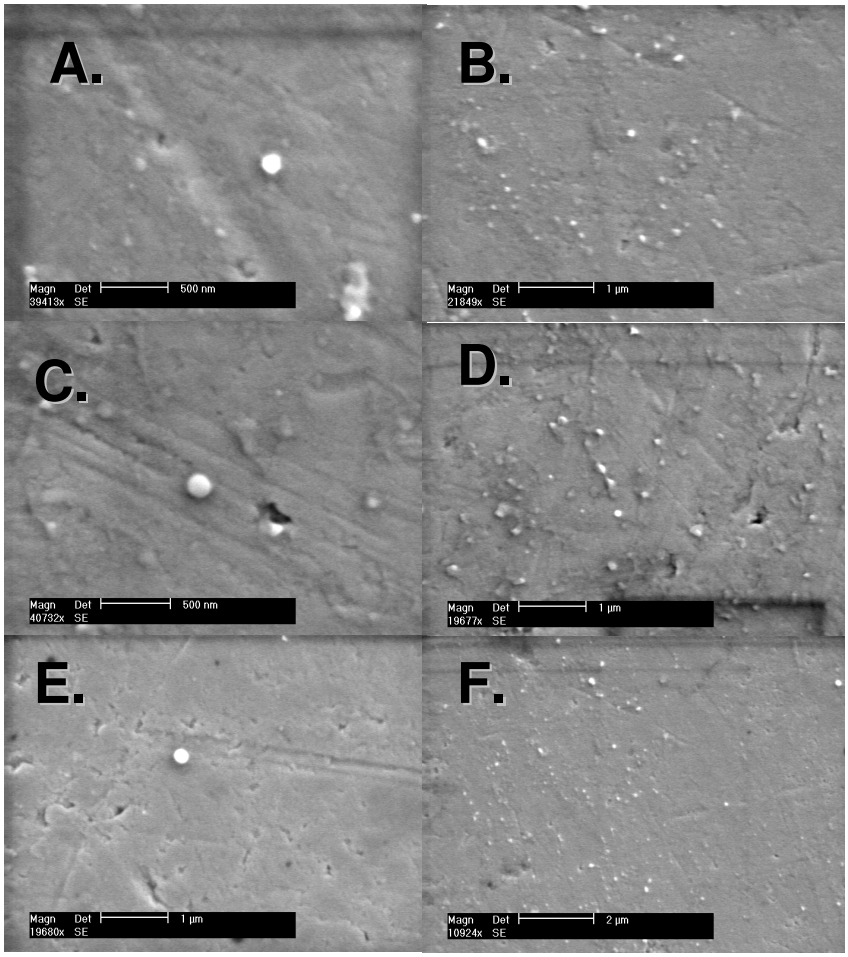

Figure 4. 6. SEM images of drug-loaded W/O/W nanoparticles (A and B), drug and KTpClPB-loaded W/O/W nanoparticles (C and D) and drug and KTpClPB-loaded O/W nanoparticles (E and F).

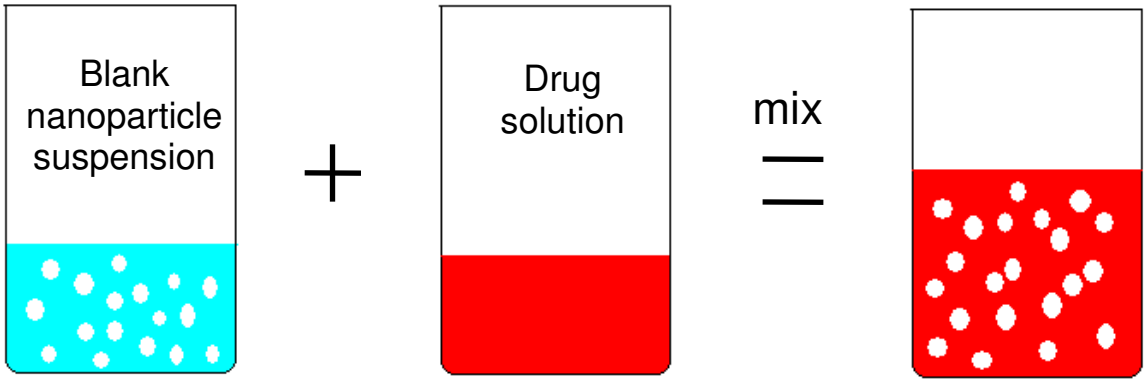

Figure 4. 7. Schematic of reverse drug loading into specially formulated nanoparticles.

A.

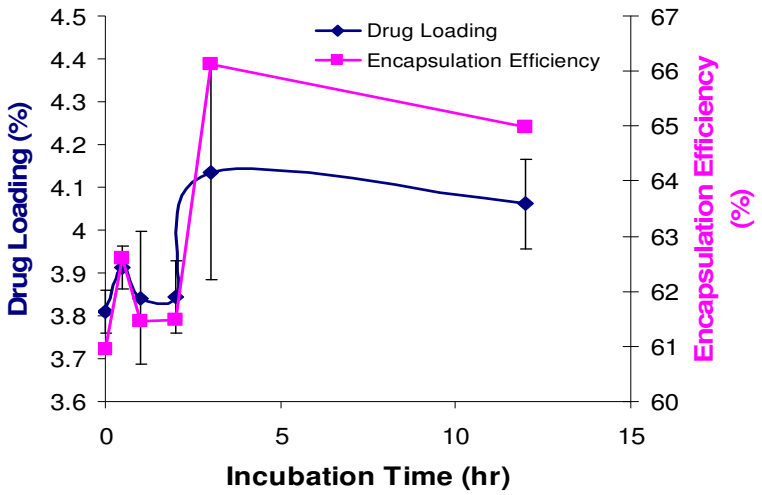

B.

Incubation time (hr)	Zeta potential (mV)	Particle size (nm)
0	-30.8	125.1
0.5	-30.1	122.5
1	-29.7	124.2
2	-29.9	124.7
3	-26.7	123.3
12	-18.3	123.3

Figure 4. 8. Drug loading, encapsulation efficiency (A) and associated particle zeta potential and size (B) for PEGylated nanoparticles over time via reverse drug loading process.

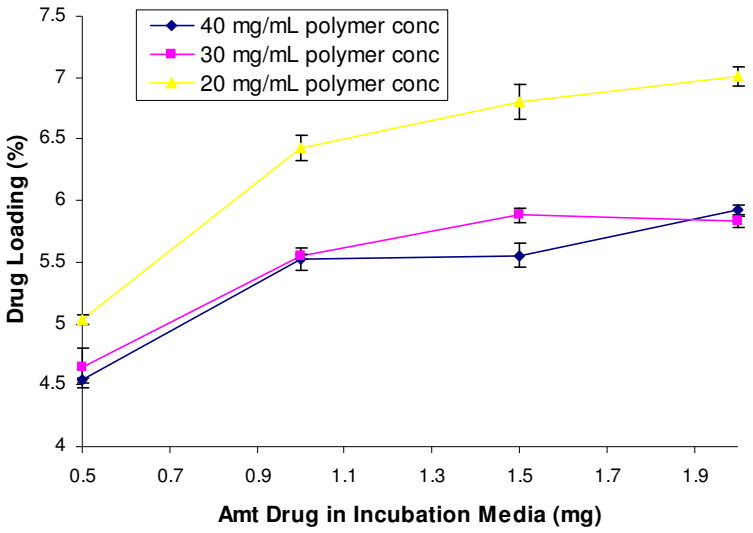

Figure 4. 9. Reverse doxHCl loading into PEGylated nanoparticles formulated at 20, 30, or 40 mg/ml total polymer concentration at different doxHCl to nanoparticle weight ratio after one hour incubation in DIW.

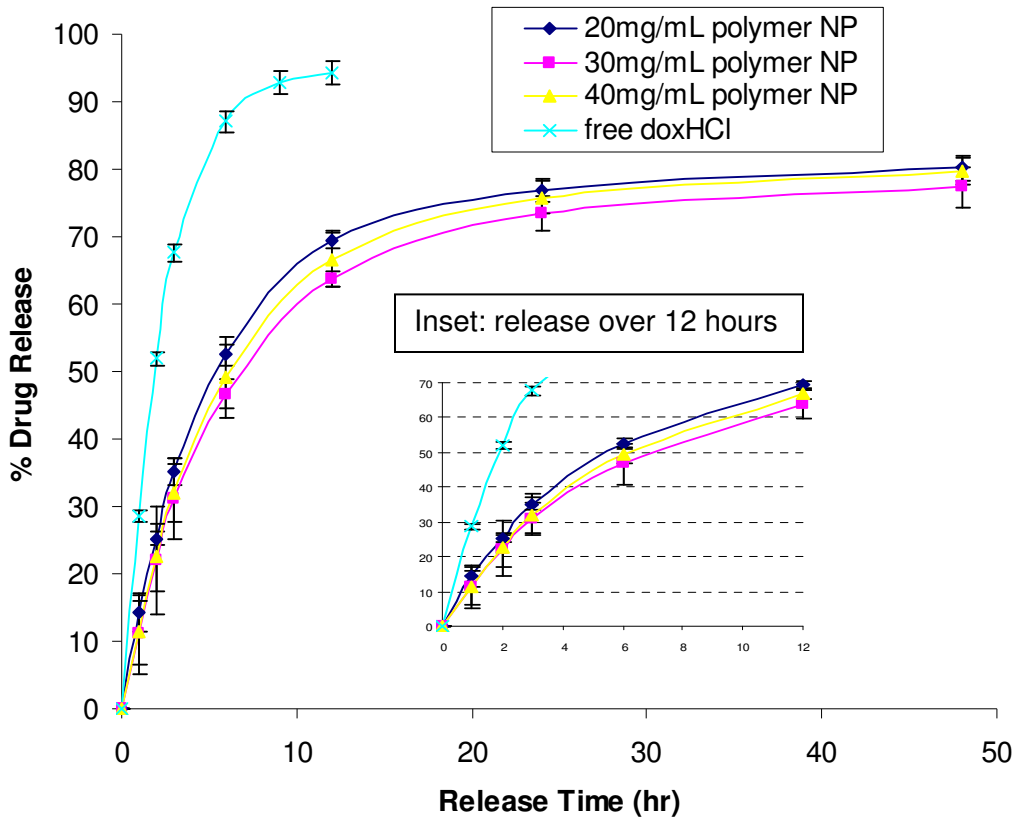

Figure 4. 10. *In vitro* doxHCl release from PEGylated nanoparticles formulated at different total polymer concentrations relative to free doxHCl.

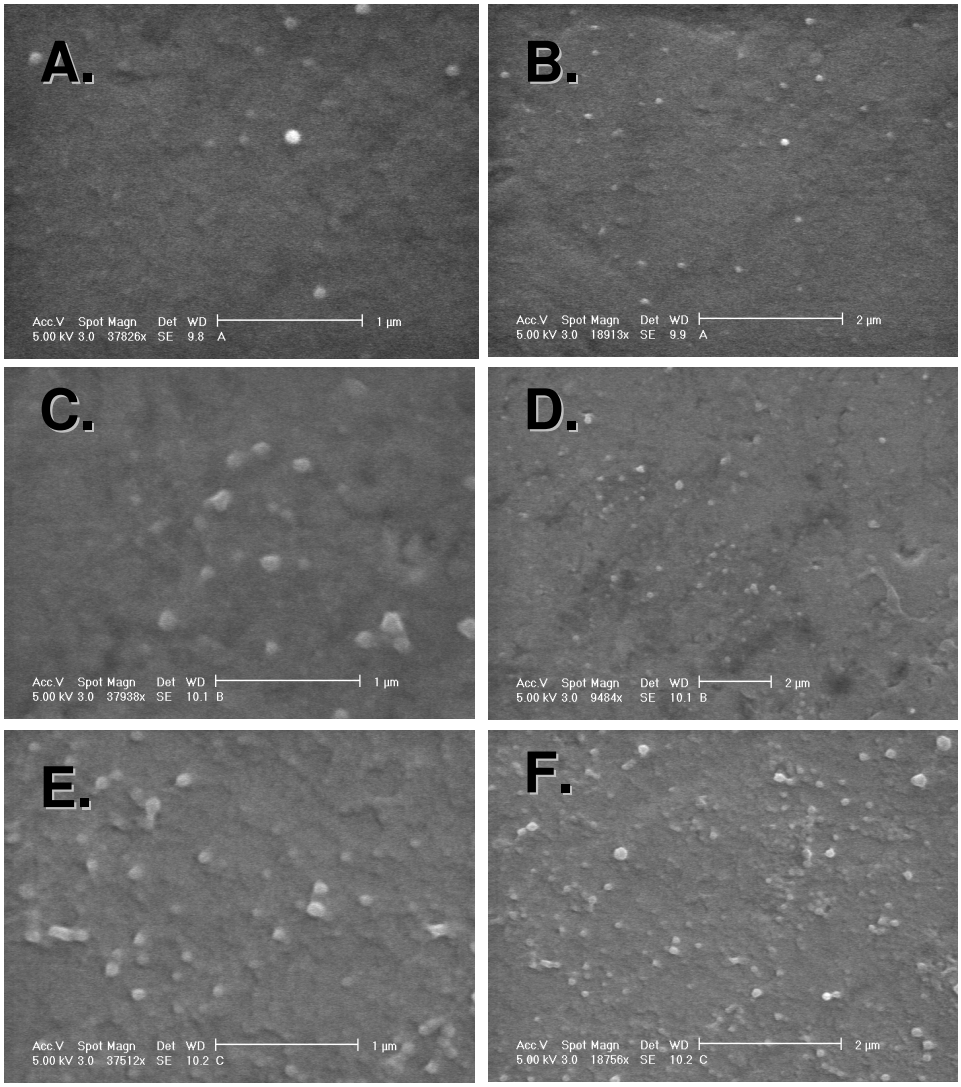

Figure 4. 11. SEM images of drug-loaded PEGylated nanoparticles formulated at 20 mg/ml (A and B), 30 mg/ml (C and D), and 40 mg/ml (E and F) total polymer concentration with maximal KTpClPB loading.

List of references:

Abou-Jawde, R., T. Choueiri, et al. (2003). "An overview of targeted treatments in cancer." Clinical Therapeutics **25**(8): 2121-2137.

Arias, J. L., F. Linares-Molinero, et al. (2008). "Study of carbonyl iron/poly(butylcyanoacrylate) (core/shell) particles as anticancer drug delivery systems - Loading and release properties." European Journal of Pharmaceutical Sciences **33**(3): 252-261.

Astete, C. E. and C. M. Sabliov (2006). "Synthesis and characterization of PLGA nanoparticles." Journal of Biomaterials Science-Polymer Edition **17**(3): 247-289.

Asuri, P., S. S. Karajanagi, et al. (2007). "Enhanced stability of enzymes adsorbed onto nanoparticles." Journal of Nanoscience and Nanotechnology **7**(4-5): 1675-1678.

Cafaggi, S., E. Russo, et al. (2007). "Preparation and evaluation of nanoparticles made of chitosan or N-trimethyl chitosan and a cisplatin-alginate complex." Journal of Controlled Release **121**(1-2): 110-123.

Cai, C., U. Bakowsky, et al. (2008). "Charged nanoparticles as protein delivery systems: A feasibility study using lysozyme as model protein." Eur J Pharm Biopharm **69**(1): 31-42.

Cavalli, R., M. R. Gasco, et al. (2002). "Solid lipid nanoparticles (SLN) as ocular delivery system for tobramycin." International Journal of Pharmaceutics **238**(1-2): 241-245.

Chavanpatil, M. D., A. Khdair, et al. (2007). "Surfactant-polymer nanoparticles: A novel platform for sustained and enhanced cellular delivery of water-soluble molecules." Pharmaceutical Research **24**(4): 803-810.

Chavanpatil, M. D., A. Khdair, et al. (2007). "Polymer-surfactant nanoparticles for sustained release of water-soluble drugs." Journal of Pharmaceutical Sciences **96**: 3379-3389.

deVerdiere, A. C., C. Dubernet, et al. (1997). "Reversion of multidrug resistance with polyalkylcyanoacrylate nanoparticles: Towards a mechanism of action." British Journal of Cancer **76**(2): 198-205.

Galindo-Rodriguez, S., E. Allemann, et al. (2004). "Physicochemical parameters associated with nanoparticle formation in the salting-out, emulsification-diffusion, and nanoprecipitation methods." Pharmaceutical Research **21**(8): 1428-1439.

Janes, K. A., M. P. Fresneau, et al. (2001). "Chitosan nanoparticles as delivery systems for doxorubicin." Journal of Controlled Release **73**(2-3): 255-267.

Jung, T., A. Breitenbach, et al. (2000). "Sulfobutylated poly(vinyl alcohol)-graft-poly(lactide-co-glycolide)s facilitate the preparation of small negatively charged biodegradable nanospheres." Journal of Controlled Release **67**(2-3): 157-169.

Maeda, H., J. Wu, et al. (2000). "Tumor vascular permeability and the EPR effect in macromolecular therapeutics: a review." Journal of Controlled Release **65**(1-2): 271-284.

Missirlis, D., R. Kawamura, et al. (2006). "Doxorubicin encapsulation and diffusional release from stable, polymeric, hydrogel nanoparticles." European Journal of Pharmaceutical Sciences **29**(2): 120-129.

Sahoo, S. K. and V. Labhasetwar (2003). "Nanotech approaches to delivery and imaging drug." Drug Discovery Today **8**(24): 1112-1120.

Sjostrom, B., A. Kaplun, et al. (1995). "Structures of Nanoparticles Prepared from Oil-in-Water Emulsions." Pharmaceutical Research **12**(1): 39-48.

Soma, C. E., C. Dubernet, et al. (2000). "Investigation of the role of macrophages on the cytotoxicity of doxorubicin and doxorubicin-loaded nanoparticles on M5076 cells in vitro." Journal of Controlled Release **68**(2): 283-289.

Soppimath, K. S., T. M. Aminabhavi, et al. (2001). "Biodegradable polymeric nanoparticles as drug delivery devices." Journal of Controlled Release **70**(1-2): 1-20.

Tian, Y., L. Bromberg, et al. (2007). "Complexation and release of doxorubicin from its complexes with pluronic P85-b-poly(acrylic acid) block copolymers." Journal of Controlled Release **121**: 137-145.

Verrecchia, T., P. Huve, et al. (1993). "Adsorption-Desorption of Human Serum-Albumin at the Surface of Poly(Lactic Acid) Nanoparticles Prepared by a Solvent Evaporation Process." Journal of Biomedical Materials Research **27**(8): 1019-1028.

Wong, H. L., R. Bendayan, et al. (2004). "Development of solid lipid nanoparticles containing lonically complexed chemotherapeutic drugs and chemosensitizers." Journal of Pharmaceutical Sciences **93**(8): 1993-2008.

Wong, H. L., A. M. Rauth, et al. (2006). "A new polymer-lipid hybrid nanoparticle system increases cytotoxicity of doxorubicin against multidrug-resistant human breast cancer cells." Pharmaceutical Research **23**(7): 1574-1585.

Yang, Y. Y., Y. Wang, et al. (2006). "Polymeric core-shell nanoparticles for therapeutics." Clinical and Experimental Pharmacology and Physiology **33**(5-6): 557-562.

Yi, Y. W., J. H. Kim, et al. (2005). "A polymeric nanoparticle consisting of mPEG-PLA-Toco and PLMA-COONa as a drug carrier: Improvements in cellular uptake and biodistribution." Pharmaceutical Research **22**(2): 200-208.

Yoo, H. S., J. E. Oh, et al. (1999). "Biodegradable nanoparticles containing doxorubicin-PLGA conjugate for sustained release." Pharmaceutical Research **16**(7): 1114-1118.

Zambaux, M. F., F. Bonneaux, et al. (1998). "Influence of experimental parameters on the characteristics of poly(lactic acid) nanoparticles prepared by a double emulsion method." Journal of Controlled Release **50**(1-3): 31-40.

Chapter 5

Conclusions

5.1 Ion Pairing

Ion pairing has been an important strategy widely applied in the last several decades. Starting as a strategy where an excipient was used to preserve protein integrity and stability, it has been adapted to small molecule drugs, such as anticancer drugs (e.g. cisplatin), to change their hydrophilic-lipophilic balance (HLB) and obtain desirable solubility properties. More recently, although not specifically mentioned, this strategy has contributed to improved drug encapsulation into nanoparticles. An area that has yet to be investigated, though, was whether small molecule lipophilic anions could be coupled to small molecule hydrophilic cationic drugs to form new complexes with increased hydrophobicity and achieve their encapsulation into hydrophobic cores of polymeric nanoparticles. This strategy could be advantageous for improving drug loading and encapsulation efficiency, slowing down drug release, providing treatment for drug overdoses, and domestic applications such as water treatment.

5.1.1 Alkyl sulfates

Alkyl sulfates, such as sodium dodecyl sulfate (SDS), represent a class of potentially useful lipophilic anions; they are amphiphilic molecules with hydrophobic carbon chains and hydrophilic, anionic sulfate groups (Fig. 2.1). Ion complexation of these compounds with amine groups on doxorubicin hydrochloride (doxHCl) could form hydrophobic ion pairs with hydrophobicity that increases with increasing carbon chain length of alkyl sulfates. In the first part of this study, doxorubicin complexes were successfully formed in water using sulfates such as sodium octyl sulfate (SOS), sodium dodecyl sulfate (SDS), sodium tetradecyl sulfate (STS), and sodium octadecyl sulfate (SODS), indicating presence of new classes of doxorubicin drug that maintained the

integrity of doxorubicin hydrochloride but changed its solubility. As expected, aqueous solubility decreased significantly with increasing alkyl chain length (from 17.24 mM for doxHCl to 0.011 mM for doxSODS) and increasing methylene chloride/PBS partition coefficient (from 0.33 for doxSOS to 2.49 for doxSODS), while similar EC_{50} values for doxHCl and various doxorubicin complexes showed that cell cytotoxicity was primarily caused by doxorubicin itself, with the complex dissociating before doxorubicin can exert its effect. Even though these novel drug complexes were hydrophobic with low aqueous solubility, beneficial for slowing drug release in aqueous media, a critical problem with these complexes was that they did not dissolve at high concentrations in organic solvents commonly used for nanoparticle formulation, such as methylene chloride, chloroform, and ethyl acetate; nor do they dissolve well in solvents miscible with organic solvents such as methanol, acetone, and acetonitrile. Because of the solubility issue, emulsion formulations specially tailored for the complexes, solid-in-oil-in-water (S/O/W) and water-in-oil-in-water (W/O/W), achieved minimal drug loading.

5.1.2 Alkyl borates

Although alkyl sulfate studies failed in its final goal of significantly improving drug loading in nanoparticles, this was significant because it was the first time such small molecules had been ion paired with a drug like doxorubicin hydrochloride. More importantly, this study showed ion pairing for drugs like doxorubicin could form new entities and this overall strategy should be pursued while the ion pairing agent, alkyl sulfate, should be exchanged for lipophilic anions with proven solubility in organic solvent commonly used for nanoparticle formulation. After rigorous search, borate-based lipophilic anions were selected as model lipophilic anions for further studies (Fig. 3.2).

Borate-based anions have negatively charged borates for ion pairing as well as four aromatic rings connected to the central boron for potential hydrophobic interactions (pi-pi stacking) with drug molecules such as doxorubicin. Solubility studies for different borates in this study showed poor solubility in methylene chloride and chloroform, but solubility in ethyl acetate reached 2.5 mg/mL, which was significant because ethyl acetate was commonly used to formulate emulsion-based nanoparticles. Extraction in ethyl acetate showed dissolved borate molecules could take up doxorubicin and there was

an approximately 1:1 molar extraction of doxHCl by NaTPB, KTpClPB, and KTBTFMPB, proving that 1) hydrophilic doxHCl could be easily and quickly extracted into a hydrophobic phase at high concentrations, 2) charge-charge interactions dominated, and 3) borate compounds, if incorporated into nanoparticles, could extract doxHCl in case of drug overdose to reduce toxicity. Because of leaching concerns with NaTPB and price of KTBTFMPB, KTpClPB was ultimately chosen for nanoparticle incorporation.

5.2 Nanoparticle formulation

5.2.1 Blank nanoparticle formation

Knowing KTpClPB could extract the model hydrophilic drug, doxHCl, from the aqueous to ethyl acetate phase and that the KTpClPB/doxorubicin complex had relatively high solubility in ethyl acetate, it was important to determine two things. First, whether KTpClPB-loaded polymeric nanoparticles could be formulation; second, if these nanoparticles, when suspended in a doxHCl solution, could take up drug to reach high loading (reverse drug loading) and factors that influence this process; and third, how reverse drug loading compare to traditional drug loading procedures such as water-in-oil-in-water (W/O/W) and oil-in-water (O/W) where drug is loaded during nanoparticle formation.

Formulation of KTpClPB-loaded polymeric nanoparticles via O/W procedure and reverse loading of doxHCl were very simple and scaling up should present minimal difficulty although this was not studied. KTpClPB incorporation into nanoparticles was proven through extraction and with theoretically maximal KTpClPB loading, less than half of the KTpClPB present was actually encapsulated into nanoparticles. This demonstrated an upper limit on the weight percent of KTpClPB encapsulation into nanoparticles and that improving drug loading had to rely on more than simply KTpClPB co-incorporation into nanoparticles.

5.2.2 Optimized drug uptake

Some important variables tested for improving drug uptake were selected based on the components of the reverse loading procedure and results showed that 1) maximizing the acid number of polymers introduced more free acid groups (via carboxylic acids) available for ion complexing with doxHCl and higher loading and encapsulation efficiency , 2) maximizing KTpClPB incorporation continuously increased doxHCl loading, presumably due to charge interactions although hydrophobic interactions may also play a small role, 3) increasing drug:nanoparticles (wt/wt) ratio increased the concentration gradient to drive drug into the nanoparticles, 4) formulating PEGylated instead of regular nanoparticles reduced nanoparticle aggregation caused by surface charge neutralization, 5) making smaller nanoparticles by decreasing polymer concentration to boost the surface area/volume ratio and potentially increase KTpClPB percent loading, and 6) in an observation previously reported by Kang et al., increasing incubation temperature from room temperature to 37^{o} C increases drug loading and encapsulation efficiency through increasing polymer rearrangement within nanoparticles.

Altogether, the improvements above increased loading for two model drugs, doxHCl and vinblastine sulfate (VS), in KTpClPB-loaded polymeric nanoparticles to as high as 7% and 9%, respectively, while nanoparticles averaged between 100-160 nm in diameter with spherical morphology. This demonstrated broad applicability of this reverse loading procedure and specially formulated nanoparticles toward this entire class of drugs as well as the effectiveness of ion complexation strategy using KTpClPB. An area requiring further improvement was the poor drug release profile, which showed up to 30% total drug release within the first three hours, 70-80% by 24 hours and essentially no release afterwards. This result was different from results shown by Chavanpatil et al, where AOT-based nanoparticles provided sustained release of water-soluble drugs. However, in their study, AOT, a lipophilic anion, was chemically conjugated to nanoparticles as opposed to simple physical incorporation of KTpClPB into polymeric nanoparticles in this study. More importantly, the result showed that adsorption loading, although simple and effective and widely used for protein loading, could result in particle aggregation if charges on nanoparticle surfaces are neutralized in the absence of surface hydrophilic moieties such as PEG. However, in certain cases where drug removal in non-

physiological settings is required, this aggregation/sedimentation could prove to be a useful mechanism.

5.3 Traditional versus incubation drug loading

Comparison between traditional drug entrapment (O/W and W/O/W), where drug loaded into nanoparticles during its formation, was compared with the optimized reverse drug loading procedure, or drug loading after nanoparticle formation. Traditional entrapment strategies (O/W and W/O/W) showed dramatically improved drug loading and encapsulation efficiency with KTpClPB incorporation, as doxHCl loading increased from 1.3% for W/O/W nanoparticles with no KTpClPB to more than 3.3% with KTpClPB added; and encapsulation efficiency increased from a high of 22% for W/O/W nanoparticles with no KTpClPB, to more than 62% for O/W and more than 38% for W/O/W nanoparticles with KTpClPB addition. As promising as these improvements were, they dimmed in contrast to the ~7% drug loading obtained through reverse drug loading although encapsulation efficiency was sacrificed for high drug loading for reverse loading method. Furthermore, drug release profiles for traditional drug loading and reverse loading nanoparticles showed no significant difference. With these comparisons in mind, reverse drug loading was not only a simpler, but also a more effective strategy for optimizing drug loading; this study was also important as it demonstrated that KTpClPB presence in nanoparticles enhanced drug loading, regardless of when drugs were actually added to nanoparticles.

5.4 Plasma drug uptake

As mentioned before, one of the new areas of research was use of nanoparticulate materials to take up drug and promote detoxification. Despite demonstrating detoxification potential *in vitro* (in deionized water), almost none of the studies showed how well their systems might work *in vivo*, where numerous substances present in blood, such as competing salts and plasma proteins, may interfere with drug uptake. Since KTpClPB-loaded polymeric nanoparticles demonstrated excellent drug uptake properties, it was interesting to see if they could do the same when in plasma. Because a large-scale

and expensive *in vivo* study is unwarranted if these nanoparticles cannot take up significant amounts of drug under physiological conditions, doxHCl uptake in plasma was examined. Results of the plasma drug uptake study was very interesting as low doxHCl concentrations (those at or near normal therapeutic concentrations) showed minimal drug uptake, while at three or four times the normal therapeutic concentration, drug uptake efficiency and nanoparticle drug loading increased dramatically. This type of result, which had not been shown before, supported the applicability of this nanoparticle system as not only a high loading drug carrier, but a potentially useful drug detoxification system which does not reduce drug efficacy when a normal dose is administered but can reduce toxicity when toxic levels are reached.

5.5 Use of Borate-Based Compounds for Ion Pairing

Despite significant improvements in doxorubicin and vinblastine loading into the specially formulated ion-complexing nanoparticles in this study, one of the main concerns in this study was the use of potassium tetrakis(4-chlorophenyl)borate (KTpClPB) as the ion pairing agent.

By itself, boron is actually present in the human diet and up to 2 mg of boron may be ingested daily (Sahelian). However, KTpClPB is a compound which is known to be harmful when ingested . Because there have been no studies of KTpClPB toxicity in animals or humans, the safety of using KTpClPB-loaded nanoparticles, even at very small amounts such as those in this study, still presents an obstacle for therapeutic use.

With the above precaution in mind, one of the alleviating factors could be that they are incorporated into nanoparticles and do not appear to leach. Nanoparticles in the human body may be cleared by various organs, especially those of the reticuloendothelial system (liver and spleen) and kidneys. This means that within a few days of nanoparticle administration, those that do not concentrate at tumor sites should be removed by body organs as long as KTpClPB does not cause toxicity to those organs at low concentrations.

5.6 Conclusions

Results from reverse loading experiments using KTpClPB-loaded nanoparticles presented some interesting possibilities. In addition to their potential as detoxifiers, these nanoparticles, with rapid uptake of cationic small molecule drugs or peptides/proteins, may be applied to extraction of other cationic molecules. In addition, reverse loading, in combination with ion complexation using KTpClPB, may be applied to carriers such as microspheres to create effective drug depots. With a larger diameter and potential for increased KTpClPB loading, drug loading in microspheres could be significantly improved while the smaller surface area-to-volume ratio of microspheres may promote sustained drug release over many months. Another interesting application for KTpClPB-loaded nanoparticles may be water purification where cationic metals such as calcium and magnesium are removed to reduced water hardness. Here, aggregation and sedimentation of drug loaded, non-PEGylated nanoparticles may actually be desirable as a mechanism for its removal from purified water.